Some gravitational aspects of scalar field dark matter

P. Valageas

IPhT - CEA Saclay

Collaboration with Ph. Brax, A. Boudon, R. Galazo-Garcia, J. Cembranos, C. Burrage

arXiv: 2204.09401, 2304.10221, 2305.18540, 2307.15391

Annecy - October 1st, 2024

Dark Matter

I- Evidence

II- Ultra-Light Dark Matter

III- Scalar-Field Dark Matter models (SFDM)

IV- Quartic self-interaction

Galaxy-scale dynamics: Formation of SFDM halos with a flat core

I- Non-relativistic regime

II- Soliton

III- Soliton formation

Black Hole dynamics inside DM solitons / Accretion and Dynamical friction

I- Radial infall onto a BH

II- BH moving inside a SFDM cloud (soliton)

III- Subsonic regime

IV- Supersonic regime

Gravitational Waves emitted by a BH binary inside a SFDM soliton

I- Additional forces on the BHs due to the dark matter environment

II- Decay of the orbital orbit

III- Phase of the GW waveform

IV- Fisher matrix analysis

V- Region in the parameter space that can be detected

Impact of the time-dependent DM gravitational potential on GW

I- DARK MATTER

Rich evidence for Dark Matter through its gravitational effects, from galactic to cosmological scales.

- 1933, Zwicky: motion of galaxies in the Coma cluster
- 1970s, Bosma, Rubin: rotation curves of spiral galaxies
- 1970s, Ostriker, Peebles: stability of disks in spiral galaxies
- 1980s, Peebles, Primack, Bond, White, …: Cosmic Microwave Background, Gravitational lensing, mass in X-ray clusters, …

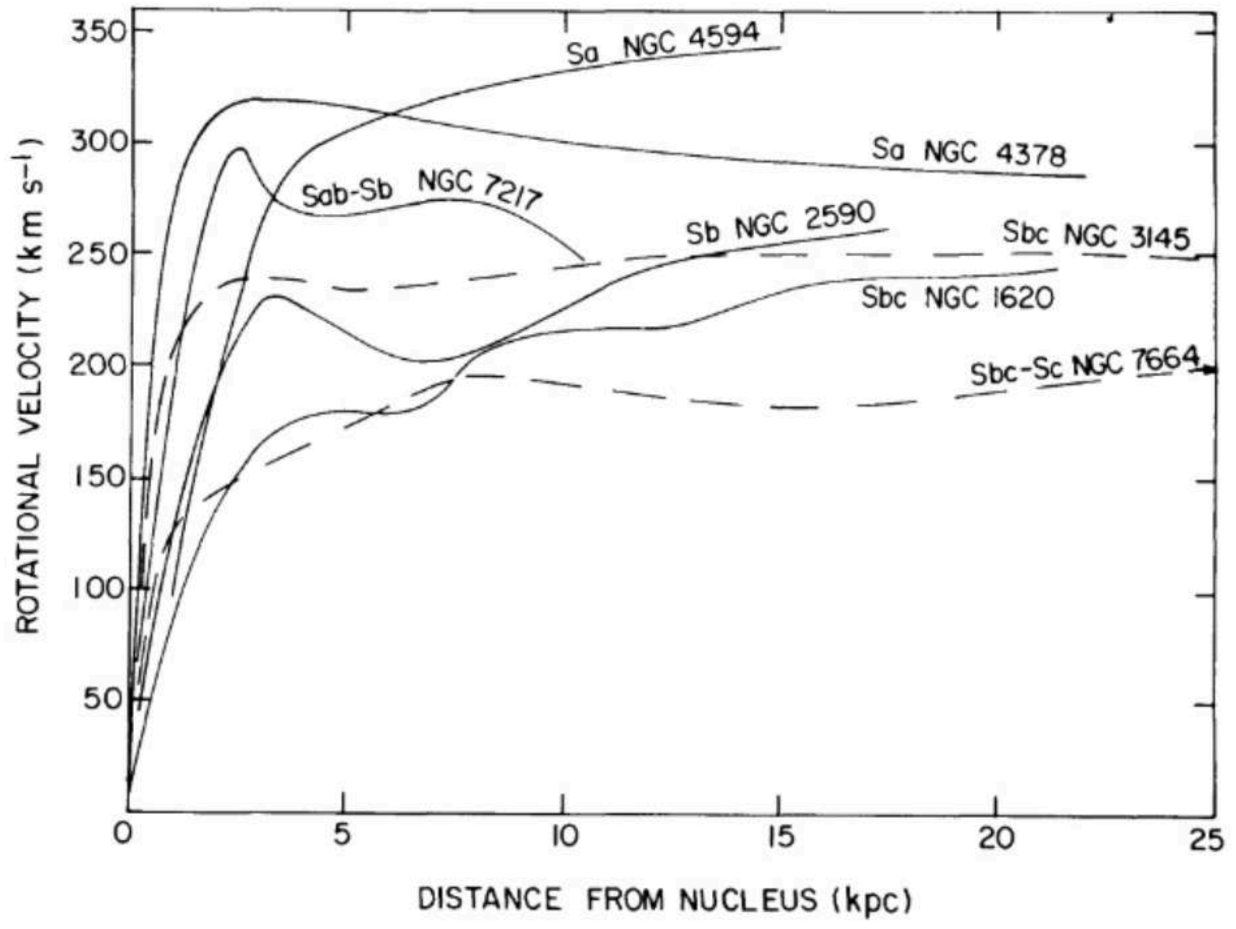

Rotational velocities for seven galaxies as a function of distance from nucleus.
Rubin et al. (1978).

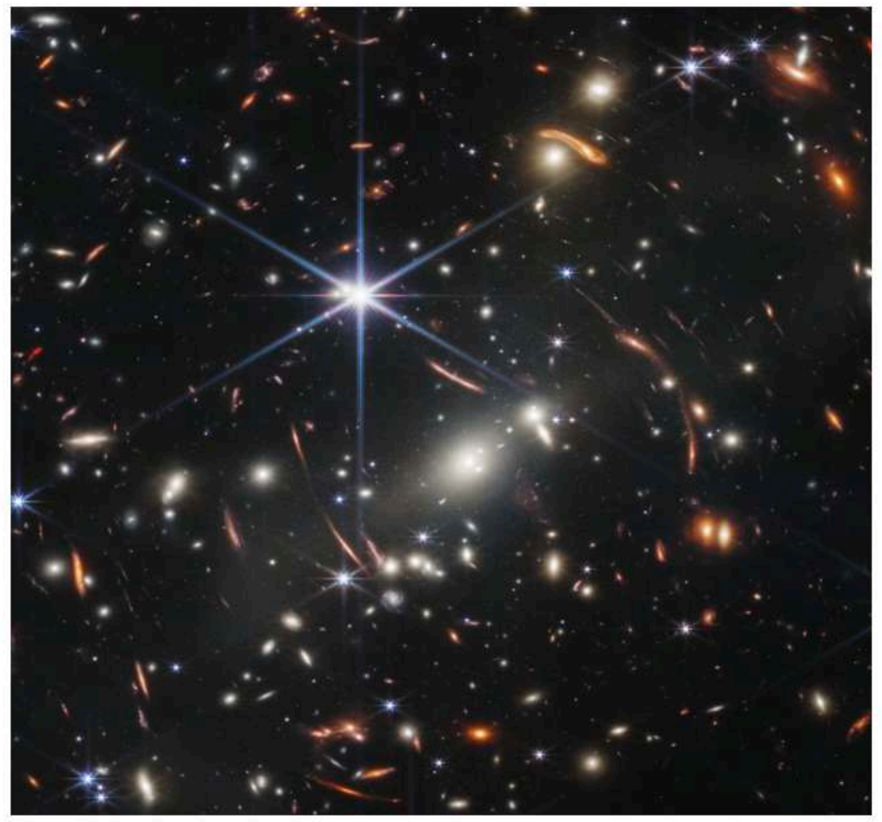

Gravitational lensing in Webb's First Deep Field taken by JWST (2022).
Galaxy cluster SMACS 0723
Credit edit: NASA, ESA, CSA, and STScI

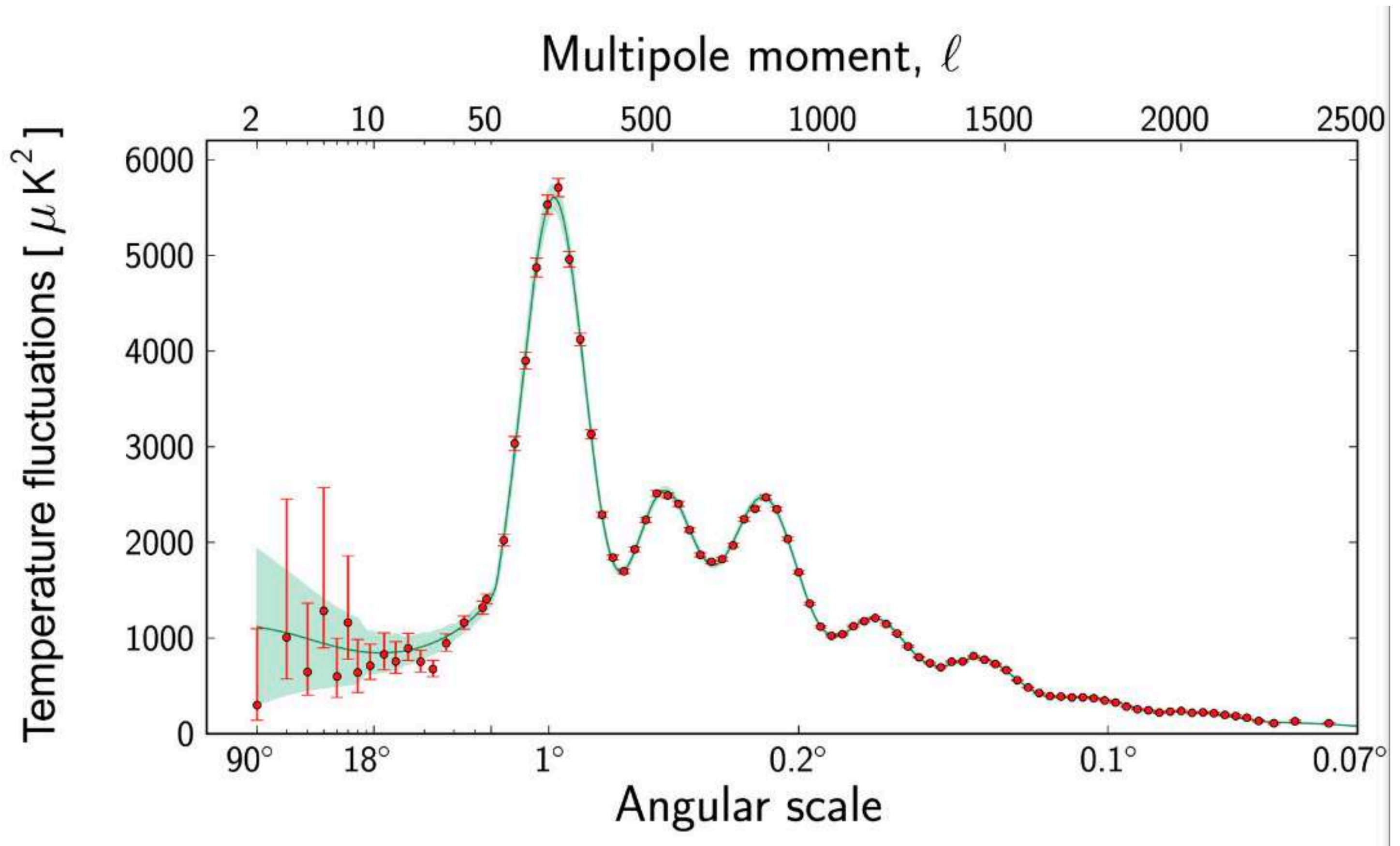

CMB temperature fluctuations at different angular scales on the sky.
Credit: ESA and the Planck Collaboration

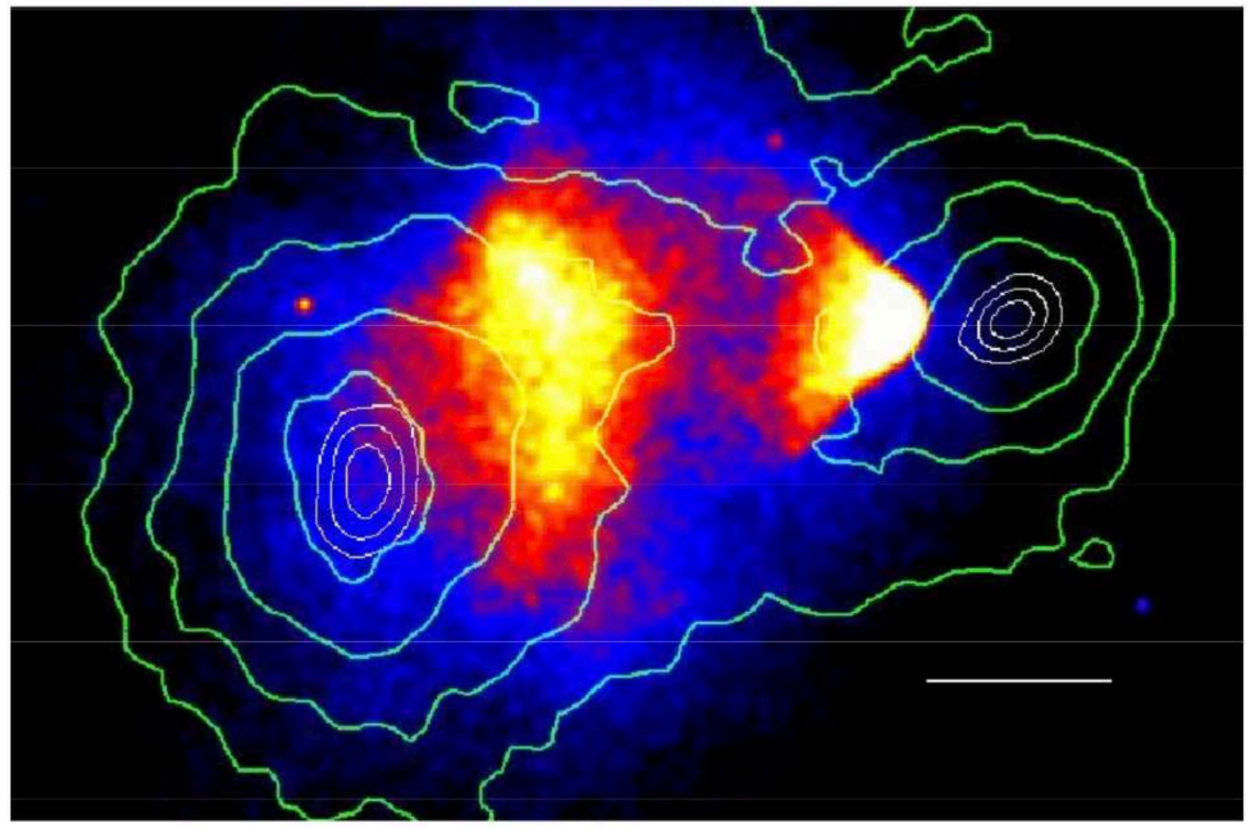

Bullet cluster (Clown et al. 2006): colors=X-ray gas, green isocontours=projected density measured by gravitational lensing

Known properties of DM

- 27% of the energy density of the universe
- Cold (non-relativistic)
- Dark: small electromagnetic interactions
- Collisionless / pressureless: small self-interactions or interactions with baryons

Energy content of the Universe

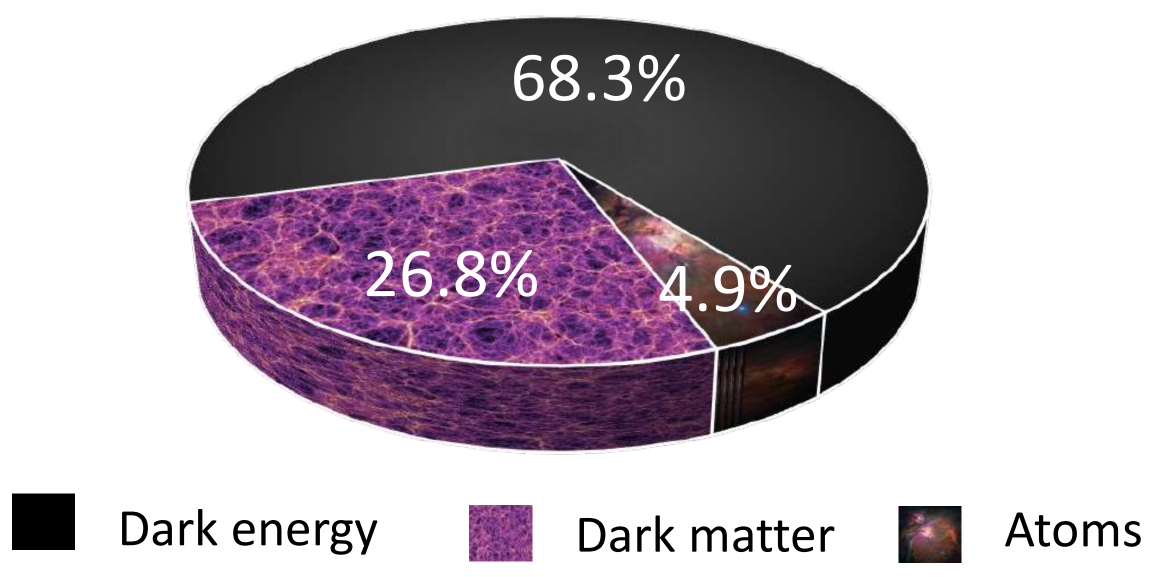

However there remains a huge uncertainty on its mass and many scenarios exist, from elementary particles to macroscopic objects:

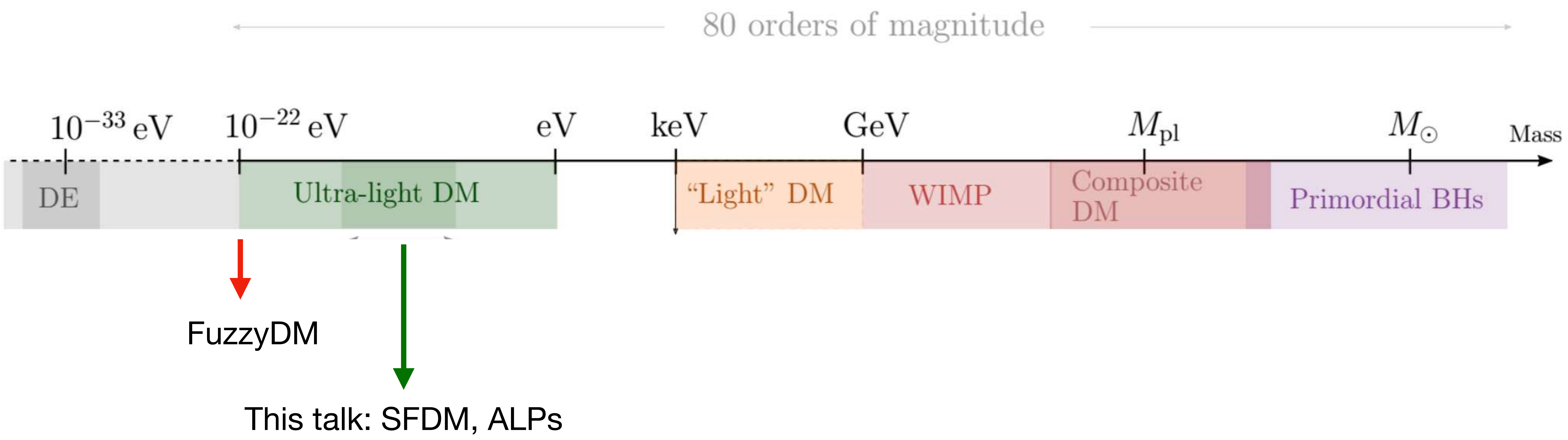

Many DM candidates

scalar / axions / ALP

neutrinos

modified gravity

WIMPs

PBH

other

Bertone and Tait, 1810.01668

II- Ultra-Light Dark Matter

Renewed interest in recent years (Hui, Ostriker, Tremaine, Witten 2017), especially since WIMPs have not been detected yet and ULDM might alleviate some small-scale tensions of LCDM.

Missing satellite problem

Predicted ΛCDM substructure

Simulation by V. Robles and T. Kelley and collaborators.

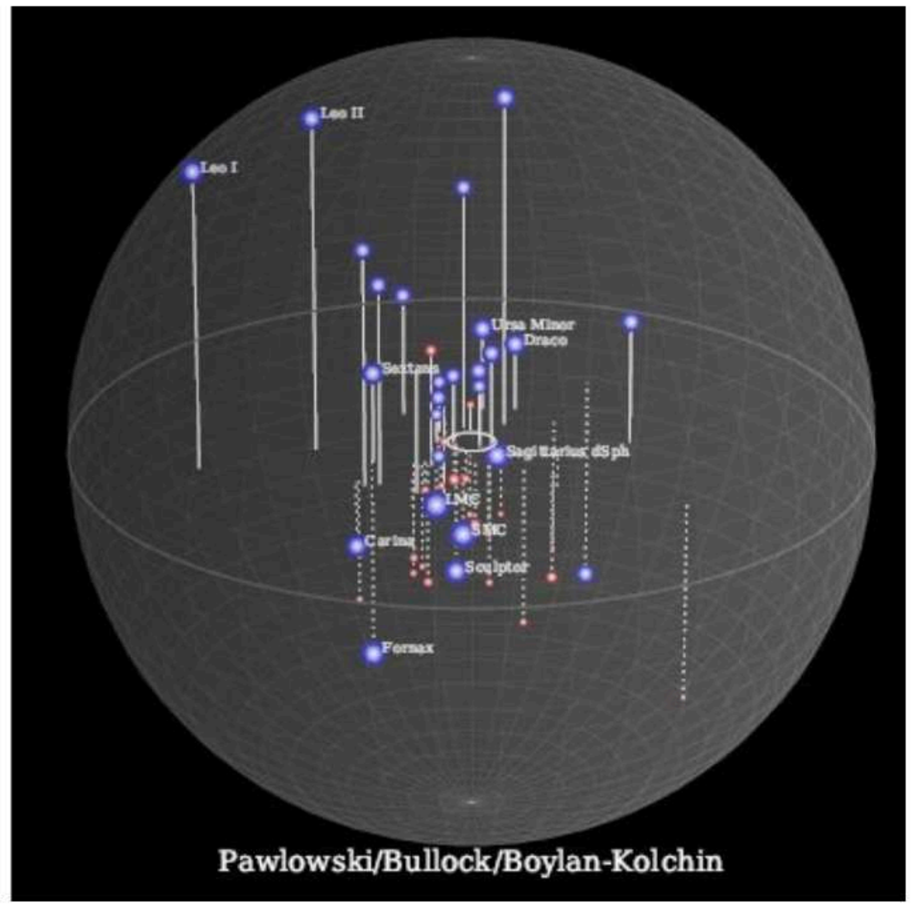

Known Milky Way satellites

James S. Bullock, M. Boylan-Kolchin, M. Pawlowski

Core/cusp problem

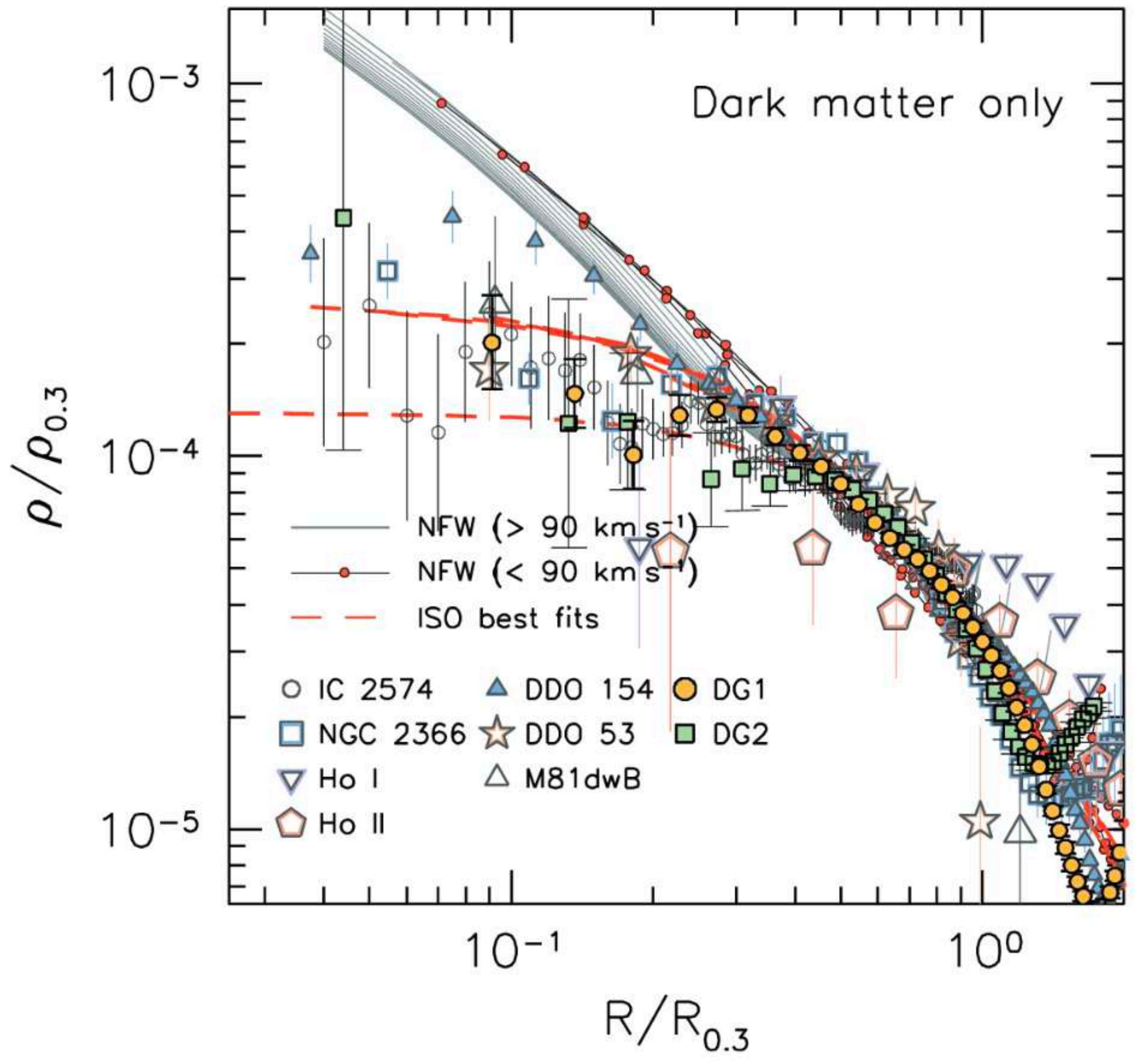

Density profiles observations and simulations

Antonino Popolo, Morgan Le Delliou (2017)

These problems may be solved by a proper account of baryonic physics (feedback from Supernovae and AGN), but ULDM remains an interesting candidate on its own.

Fuzzy Dark Matter

De Broglie wavelength: $$\lambda_{\rm dB} = 2\pi/(mv) \simeq \left(\frac{m}{10^{-22}\,{\rm eV}}\right)^{-1} \left(\frac{v}{100\,{\rm km/s}}\right)^{-1} {\rm kpc}$$

The DM density field behaves like CDM on large scales but structures are suppressed below $\lambda_{\rm dB}$

In particular, hydrostatic flat cores (« solitons ») can form at the center of DM halos.

For Fuzzy Dark Matter: $m \sim 10^{-22}{\rm eV}$ $\lambda_{\rm dB} \sim 1\,{\rm kpc}$

However, this model already seems ruled out by Lyman-alpha forest power spectra (because of this suppression of small-scale power).

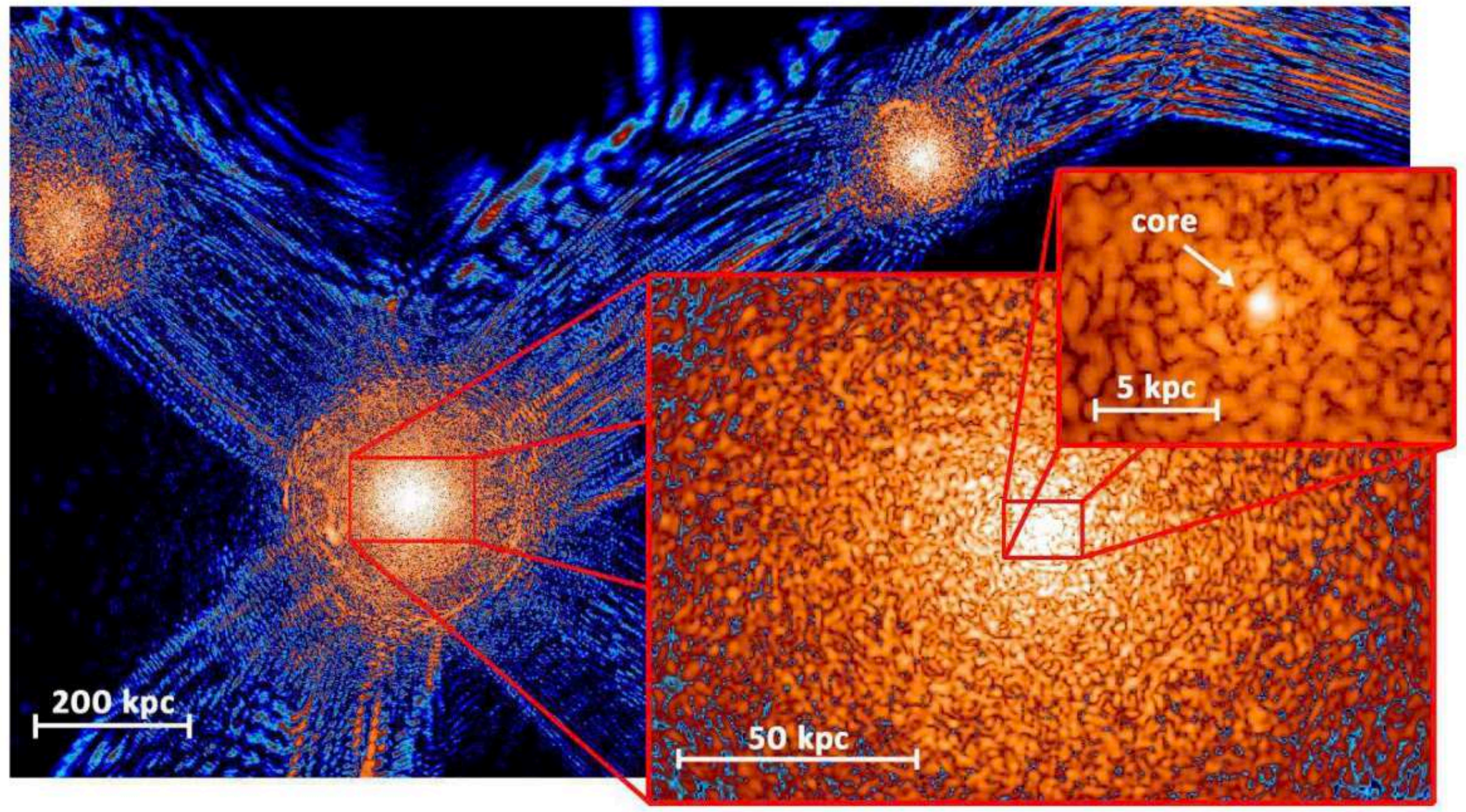

A slice of density field of ψDM simulation on various scales at z=0.1

Schive, Chiueh, and Broadhurst (2014)

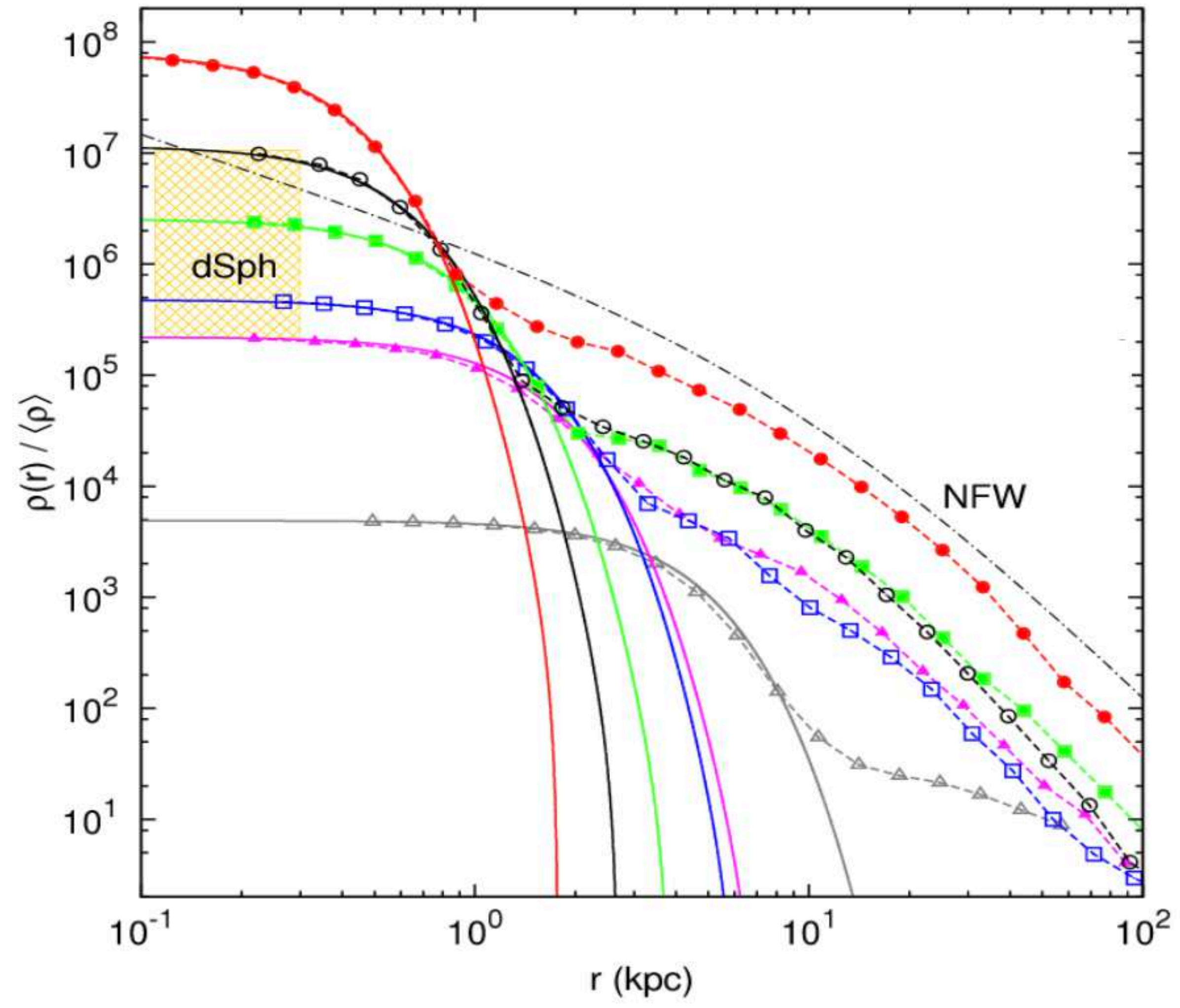

Radial density profiles of haloes formed in the ψDM model

In the FDM model, the wavelike dynamics below $\lambda_{\rm dB}$, which leads to the suppression of small-scale power, appears as an effective « quantum pressure » in the hydrodynamical regime.

Scalar field Dark Matter with self-interactions

Instead of relying on this quantum pressure (large $\lambda_{\rm dB}$), we can also suppress small-scale structures through self-interactions.

This also generates an effective pressure, which is now due to the self-interactions.

III- Scalar-field models

$$S_\phi = \int d^4x\sqrt{-g}\left[-\frac{1}{2}g^{\mu\nu}\partial_\mu\phi\partial_\nu\phi - V(\phi)\right].$$

Background:

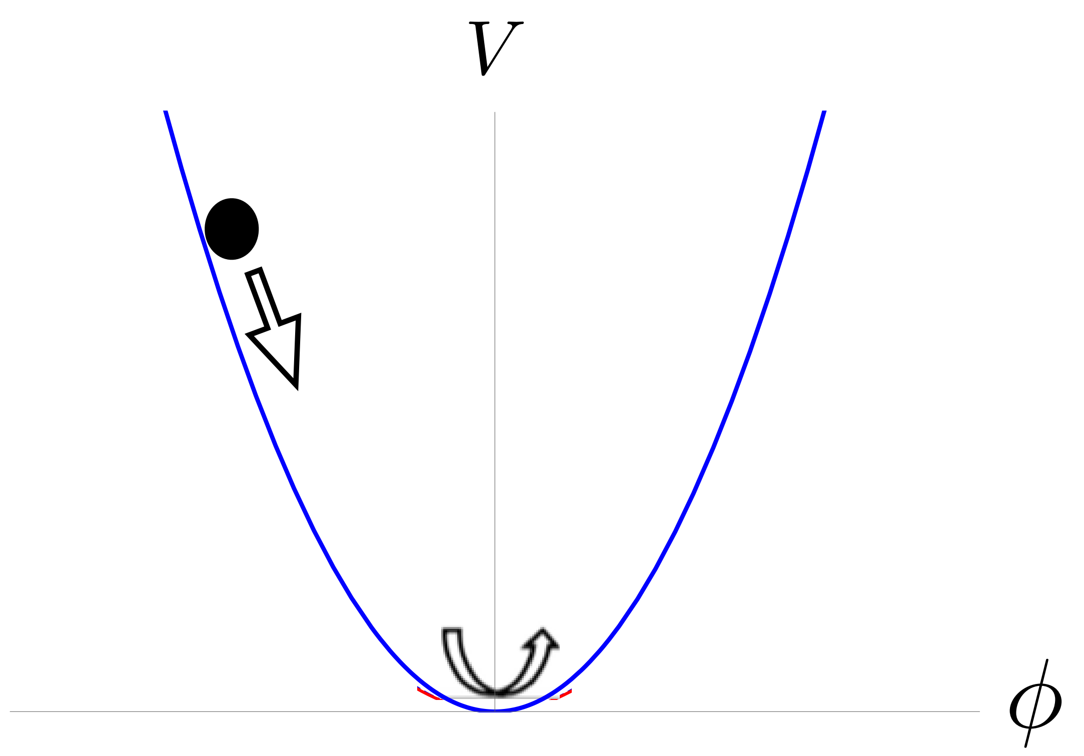

Klein-Gordon . eq.: $$\ddot{\phi} + 3H\dot{\phi} + \frac{dV}{d\phi} = 0$$

e.g., no self-interactions: $$V = \frac{1}{2}m^2\phi^2$$

$H \ll m$ the scalar field oscillates with frequency m, and a slow decay of the amplitude:

$$\phi = \phi_0(a/a_0)^{-3/2}\cos(mt)$$

→ behaves like dark matter: $\rho \propto a^{-3}$

$$V \propto \phi^n \rightarrow w = \frac{\langle p_\phi\rangle}{\langle \rho_\phi\rangle} = \frac{n-2}{n+2}$$

Brax et al. 2019

→ For a mostly quadratic potential with small self-interactions:

$$V(\phi) = \frac{1}{2}m^2\phi^2 + V_{\rm I}(\phi) \qquad V_{\rm I} \ll \frac{1}{2}m^2\phi^2$$

$$\bar{\phi}(t) = \bar{\varphi}(t)\cos(mt - \bar{S}(t)) \qquad \bar{\varphi} = \bar{\varphi}_0 a^{-3/2} \qquad \bar{S}(t) = \bar{S}_0 - \int_{t_0}^{t} dt m \Phi_{\rm I}\left(\frac{m^2\bar{\varphi}_0^2}{2a^3}\right)$$

IV- Quartic self-interaction

Fuzzy Dark Matter (FDM) + self-interactions

$$S_\phi = \int d^4x\sqrt{-g}\left[-\frac{1}{2}g^{\mu\nu}\partial_\mu\phi\partial_\nu\phi - V(\phi)\right]$$

$$V(\phi) = \frac{m^2}{2}\phi^2 + V_{\rm I}(\phi) \;\; \text{with} \;\; V_{\rm I}(\phi) = \frac{\lambda_4}{4}\phi^4, \quad \lambda_4 > 0$$

$\rho \propto a^{-3}$

Repulsive self-interaction $\longrightarrow$ Effective pressure

One characteristic density / length-scale:

$$\boxed{\rho_a = \frac{4m^4}{3\lambda_4}, \quad r_a = \frac{1}{\sqrt{4\pi\mathcal{G}\rho_a}}}$$

Relativistic regime - strong self-interaction

Jeans length - Radius of solitons

Very large occupation numbers: $N \sim \dfrac{\rho}{mp^3} \gg 1$ $\qquad m \ll 1 \text{ eV}$

De Broglie wavelength: $\lambda_{\rm dB} = \dfrac{2\pi}{mv} \lesssim 1 \text{ kpc}$ $\qquad m \gtrsim 10^{-22} \text{ eV}$

Also, k-essence models: $S_\phi = \int d^4x\sqrt{-g}\left[\Lambda^4 K(X) - \frac{m^2}{2}\phi^2\right]$ $\qquad X = -\dfrac{1}{2\Lambda^4}g^{\mu\nu}\partial_\mu\phi\partial_\nu\phi$ $\qquad K(X) = X + K_{\rm I}(X)$

Parameter Space

$$\rho_a = \frac{4m^4}{3\lambda_4}$$

$$r_a = \frac{1}{\sqrt{4\pi \mathcal{G} \rho_a}}$$

$$r_s = 2\mathcal{G} M_{\text{BH}}$$

Only white area allowed

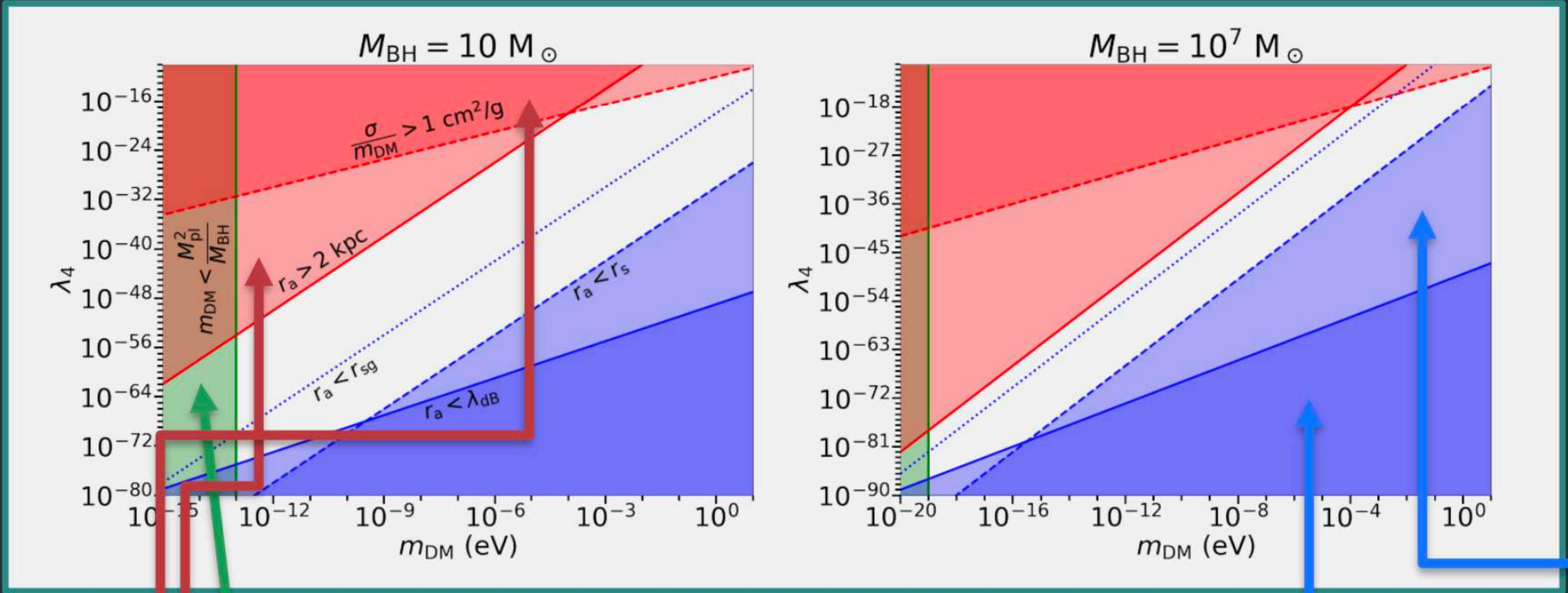

Boundaries

- Quantum pressure dominating over self-interactions
- Soliton larger than galatic scales
- Bound on cross-section due to observations of cluster mergers
- Leaving the Thomas-Fermi regime, considering $v = 10^{-3}$
- The black hole extends beyond the dark matter cloud

Galaxy-scale dynamics:

Formation of DM halos with a flat core

I- NON-RELATIVISTIC REGIME

On the scale of the galactic halo we are in the nonrelativistic regime: the frequencies and wave numbers of interest are much smaller than m and the metric fluctuations are small.

A) From Klein-Gordon eq. to Schrödinger eq.:

Decompose the real scalar field ϕ in terms of the complex scalar field ψ

$$\phi = \frac{1}{\sqrt{2m}}\left(e^{-imt}\psi + e^{imt}\psi^\star\right)$$

factorizes (removes) the fast oscillations of frequency m

$$\dot{\psi} \ll m\psi, \quad \nabla\psi \ll m\psi$$

$\psi(x,t)$ evolves slowly, on astrophysical or cosmological scales.

Instead of the Klein-Gordon eq., it obeys a (non-linear) Schrödinger eq.:

$$i\left(\dot{\psi} + \frac{3}{2}H\psi\right) = -\frac{\nabla^2\psi}{2ma^2} + m\Phi_{\rm N}\psi + \frac{\partial\mathcal{V}_{\rm I}}{\partial\psi^\star}$$

Newtonian gravitational potential

self-interactions

$$V_{\rm I}(\phi) = \Lambda^4 \sum_{p\geq 3} \frac{\lambda_p}{p}\left(\frac{\phi}{\Lambda}\right)^p$$

$$\Downarrow$$

$$\mathcal{V}_{\rm I}(\psi,\psi^\star) = \Lambda^4 \sum_{p\geq 2} \frac{\lambda_{2p}}{2p}\frac{(2p)!}{(p!)^2}\left(\frac{\psi\psi^\star}{2m\Lambda^2}\right)^p$$

(keep only even terms)

Inside galactic halos, we neglect the Hubble expansion:

Newtonian gravity

Self-interactions

$$i\dot{\psi} = -\frac{\nabla^2\psi}{2m} + m(\Phi_{\rm N} + \Phi_{\rm I})\psi$$

$$V_{\rm I}(\phi) = \frac{\lambda_4}{4}\phi^4$$

$$\Phi_{\rm I} = \frac{m|\psi|^2}{\rho_a}$$

$$\nabla^2\Phi_{\rm N} = 4\pi\mathcal{G}\rho \qquad \rho = m|\psi|^2$$

B) From Schrödinger eq. to Hydrodynamical eqs (Madelung transformation):

Madelung 1927, Chavanis 2012, ...

One can map the Schrödinger eq. to hydrodynamical eqs.: $\psi = \sqrt{\frac{\rho}{m}}e^{is}$ $\quad \vec{v} = \frac{\nabla s}{m}$

The real and imaginary parts of the Schrödinger eq. lead to the continuity and Euler eqs.:

$$\dot{\rho} + \nabla\cdot(\rho\vec{v}) = 0$$

conservation of probability for ψ $\Rightarrow$ conservation of matter for ρ

$$\dot{\vec{v}} + (\vec{v}\cdot\nabla)\vec{v} = -\nabla(\Phi_{\rm Q} + \Phi_{\rm N} + \Phi_{\rm I})$$

Self-interactions

$$\Phi_{\rm I} = \frac{\rho}{\rho_a}$$

effective pressure $\quad P_{\rm eff} \propto \rho^2$

$$\gamma = 2$$

« quantum pressure » $\quad \Phi_{\rm Q} = -\frac{\nabla^2\sqrt{\rho}}{2m^2\sqrt{\rho}}$

comes from part of the kinetic terms in ψ

In the following, we neglect the « quantum pressure » (which dominates for FDM) $\qquad$ large-m limit

II- SOLITON (ground state): HYDROSTATIC EQUILIBRIUM

As compared with CDM, the self-interactions allow the formation of hydrostatic equilibrium solutions, with a balance between gravity and the effective pressure:

$$\cancel{\dot{\vec{v}}} + (\vec{v} \cdot \cancel{\nabla})\vec{v} = -\nabla(\cancel{\Phi_{\rm Q}} + \Phi_{\rm N} + \Phi_{\rm I}) \rightarrow \nabla(\Phi_{\rm N} + \Phi_{\rm I}) = 0 \rightarrow \boxed{\rho(r) = \rho_0 \frac{\sin(r/r_a)}{(r/r_a)}}$$

$$R_{\rm sol} \simeq \pi r_a$$

$$\rho_a = \frac{4m^4}{3\lambda_4}, \quad r_a = \frac{1}{\sqrt{4\pi\mathcal{G}\rho_a}}$$

→ Finite-size halo, called « soliton » or « boson star »

P. Brax, J. Cembranos, PV, 1906.00730

Ruffini and Bonazolla 1969,
Chavanis 2011,
Schiappacasse and Hertzberg 2018, ...

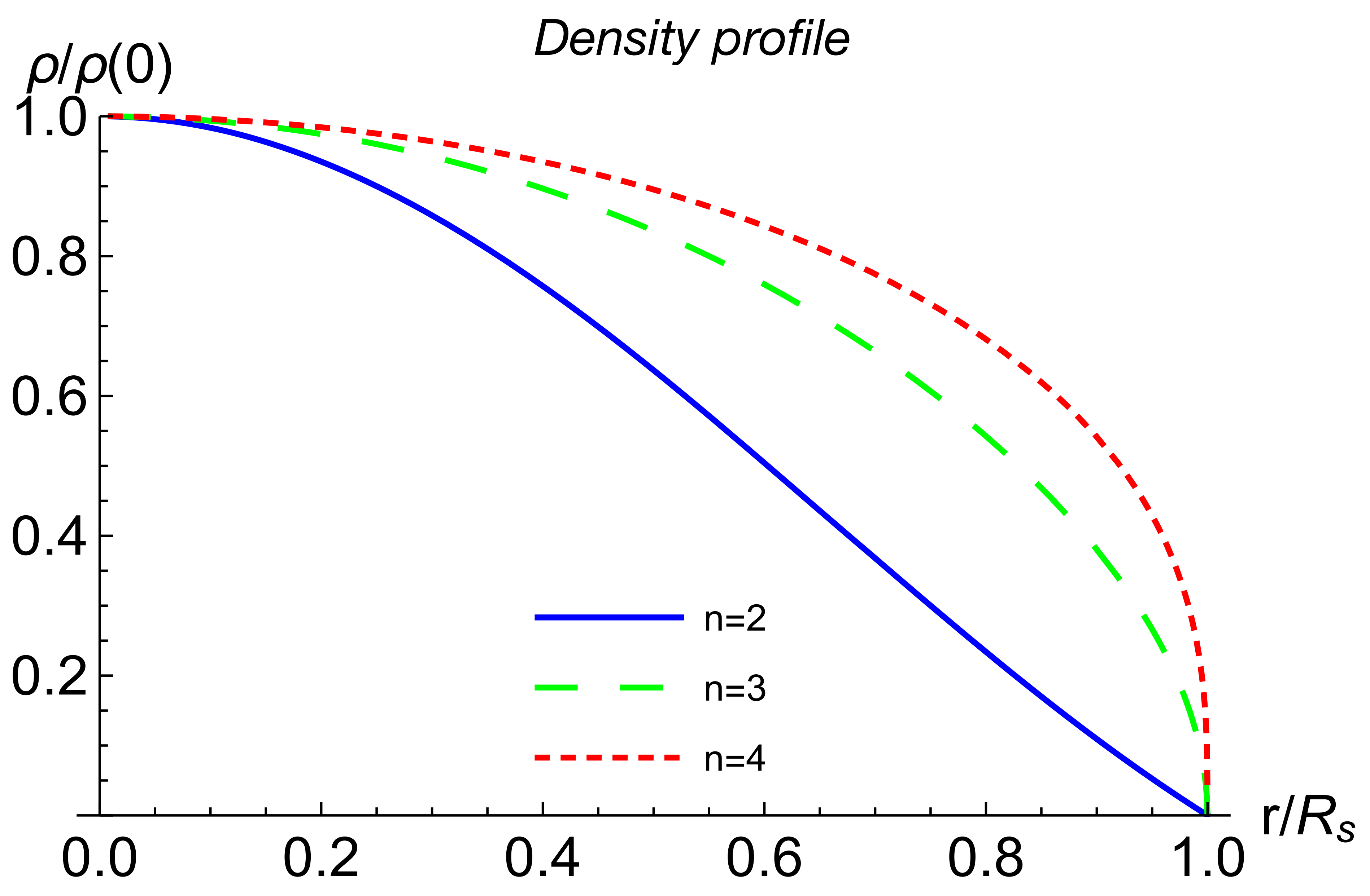

$$V_{\rm I}(\phi) = \Lambda^4 \frac{\lambda_{2n}}{2n} \frac{\phi^{2n}}{\Lambda^{2n}}$$

$m \gg 10^{-18}\mathrm{eV}$: galactic soliton governed by the balance between the repulsive self-interaction and self-gravity.

$m \sim 10^{-21}\mathrm{eV}$: Fuzzy Dark Matter (de Broglie wavelength of galactic size): galactic soliton governed by the balance between the quantum pressure and self-gravity.

Numerical simulations of FDM indeed find that solitons form, from gravitational collapse, within an extended NFW-like out-of-equilibrium halo.

Chen et al. 2020

Schive et al. 2014,
Veltmaat et al. 2018,
Mocz et al. 2019,
Amin and Mocz 2019, ...

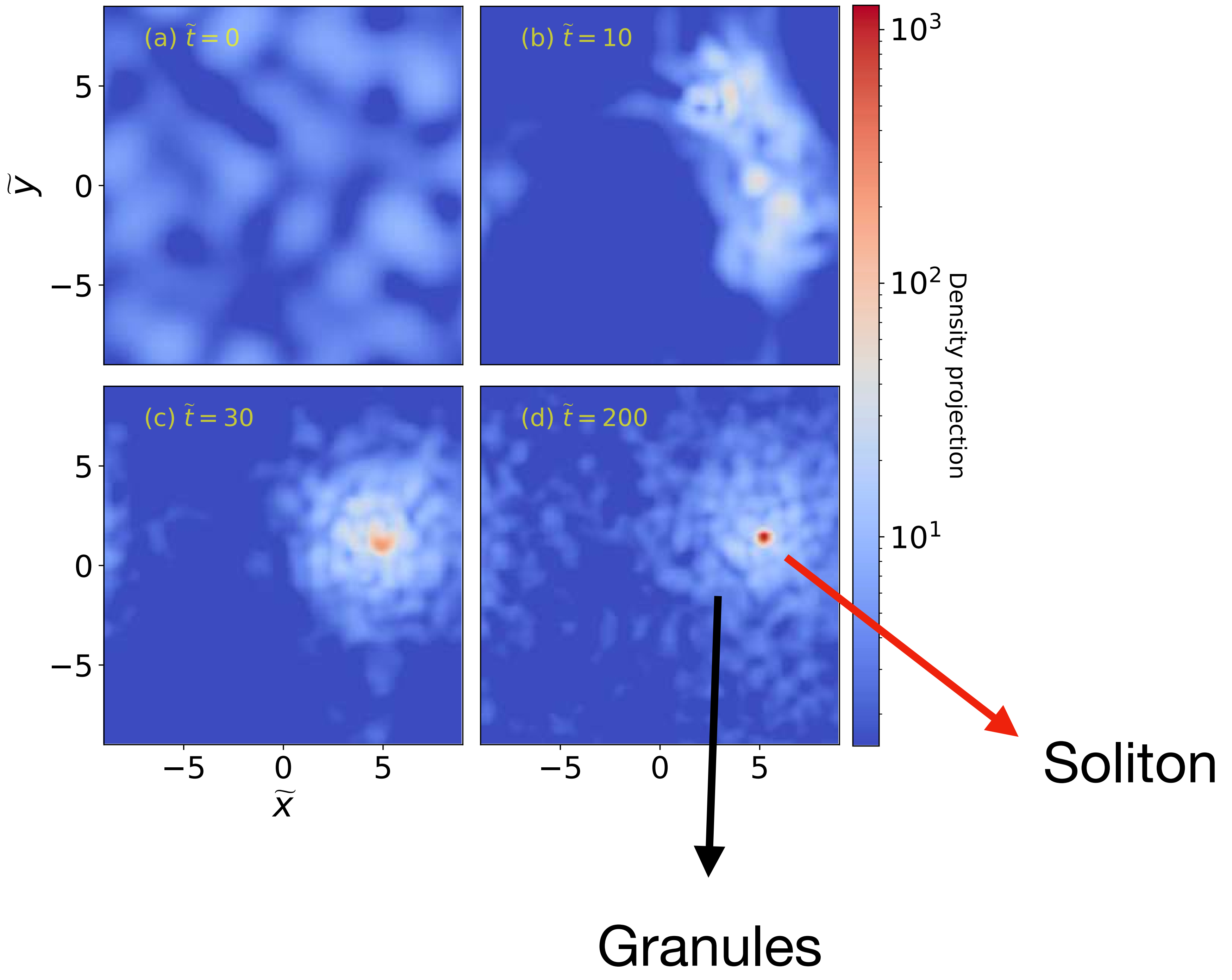

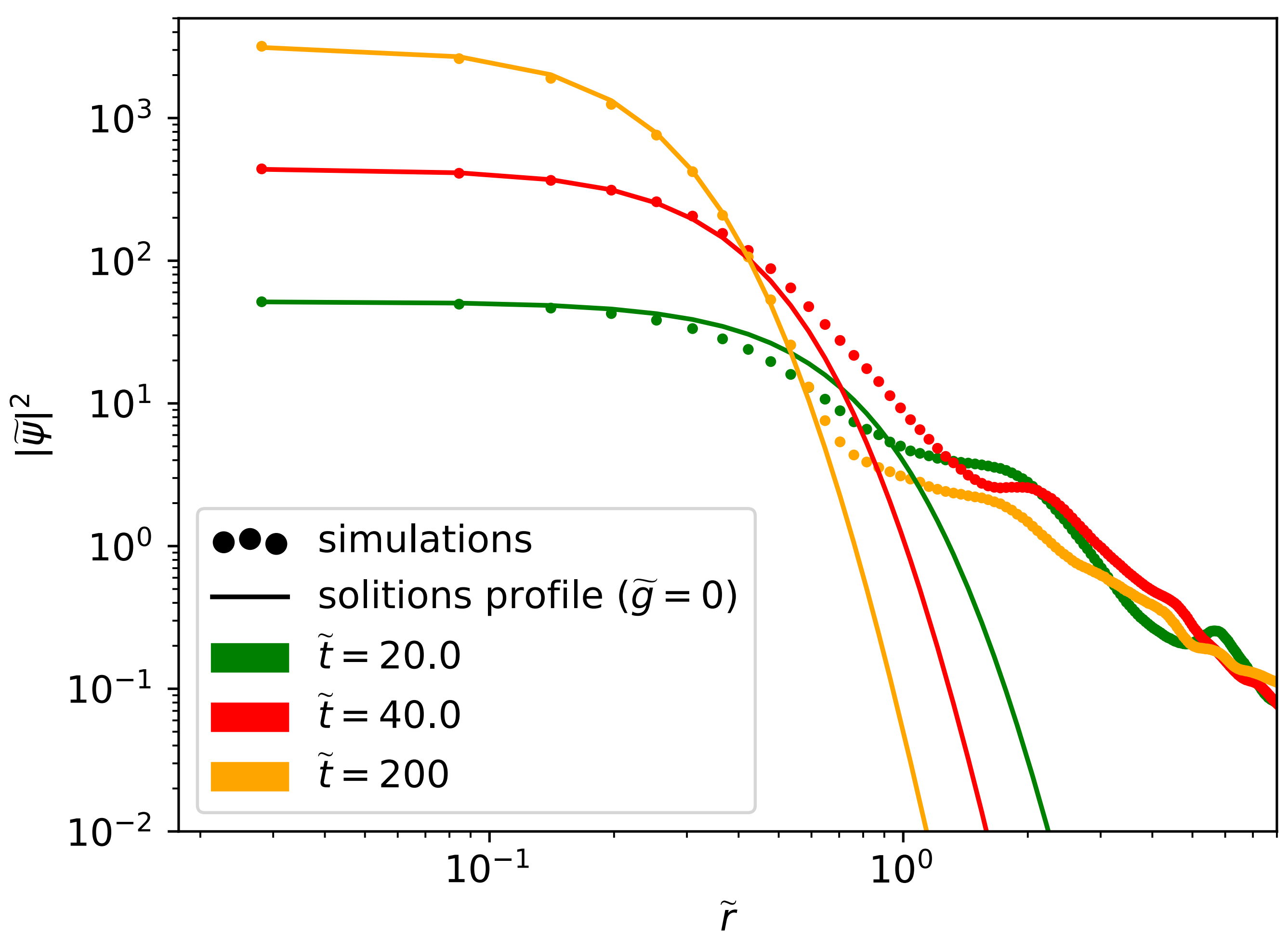

III- SOLITON FORMATION IN THE THOMAS-FERMI REGIME

(Self-interactions dominate over the quantum pressure in the soliton)

A) Numerical simulations

Initial conditions: halo (+ central soliton):

$$\psi_{\text{initial}} = \psi_{\text{sol}} + \psi_{\text{halo}}$$

$$\rho_{\text{sol}}(r) = \rho_{0\text{sol}} \frac{\sin(\pi r / R_{\text{sol}})}{\pi r / R_{\text{sol}}}, \quad \hat{\psi}_{\text{sol}}(r) = \sqrt{\rho_{\text{sol}}(r)}.$$

Stochastic halo: sum over eigenmodes of the target gravitational potential with random coefficients

$$\psi_{\text{halo}}(\vec{x}, t) = \sum_{n\ell m} a_{n\ell m} \hat{\psi}_{n\ell m}(\vec{x}) e^{-iE_{n\ell}t/\epsilon}$$

$$-\frac{\epsilon^2}{2}\nabla^2 \hat{\psi}_E + \bar{\Phi}\hat{\psi}_E = E\hat{\psi}_E$$

$$a_{n\ell m} = a(E_{n\ell}) e^{i\Theta_{n\ell m}}$$

random phase

$$\bar{\Phi}(r) = \bar{\Phi}_N(r), \quad \nabla^2 \bar{\Phi}_N = 4\pi\bar{\rho}$$

$$\langle \rho_{\text{halo}} \rangle = \sum_{n\ell m} a(E_{n\ell})^2 |\hat{\psi}_{n\ell m}|^2$$

sets $a(E)$

$$a(E)^2 = (2\pi\epsilon)^3 f(E) \qquad f(E) = \frac{1}{2\sqrt{2}\pi^2} \frac{d}{dE} \int_E^0 \frac{d\Phi_N}{\sqrt{\Phi_N - E}} \frac{d\rho_{\text{classical}}}{d\Phi_N}$$

(Eddington formula)

1) Soliton radius of the same order as the halo size

Initial 1D density plot

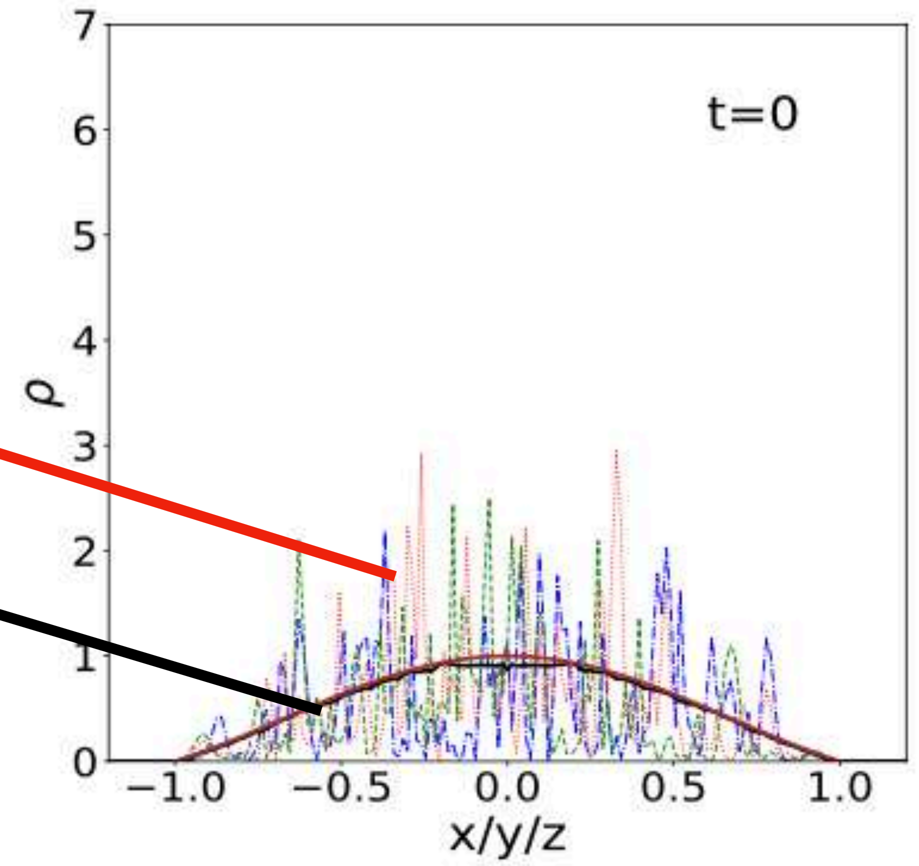

Initial 2D density plot

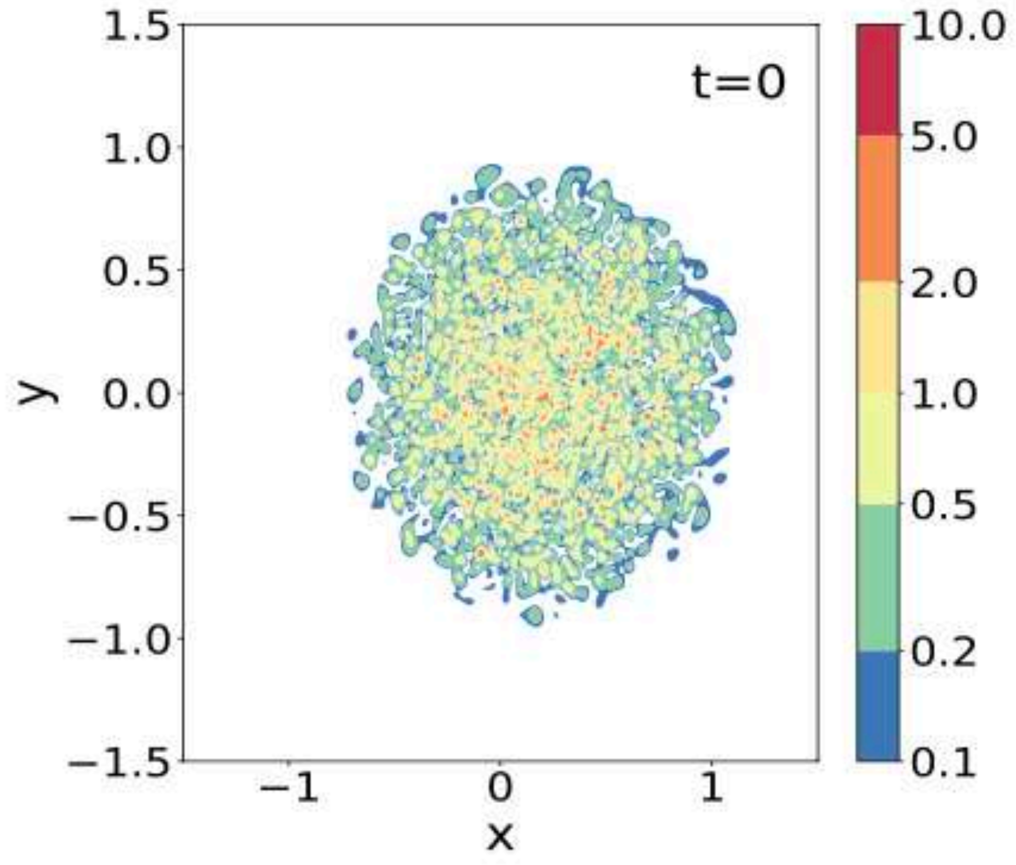

Final 1D density plot

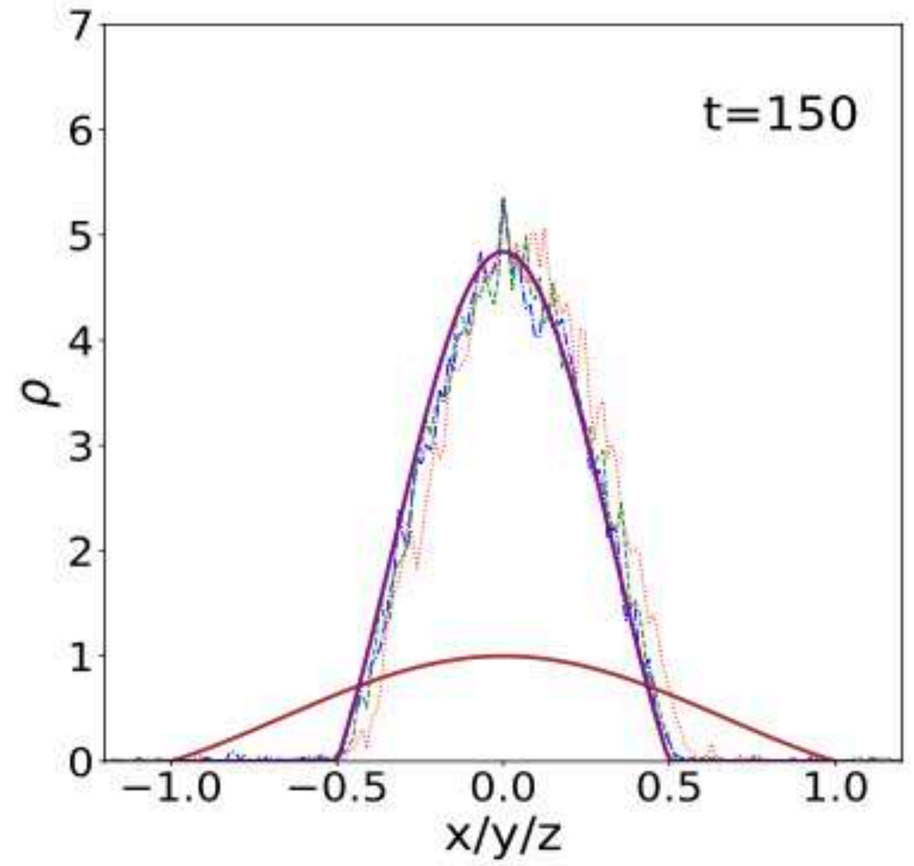

Final 2D density plot

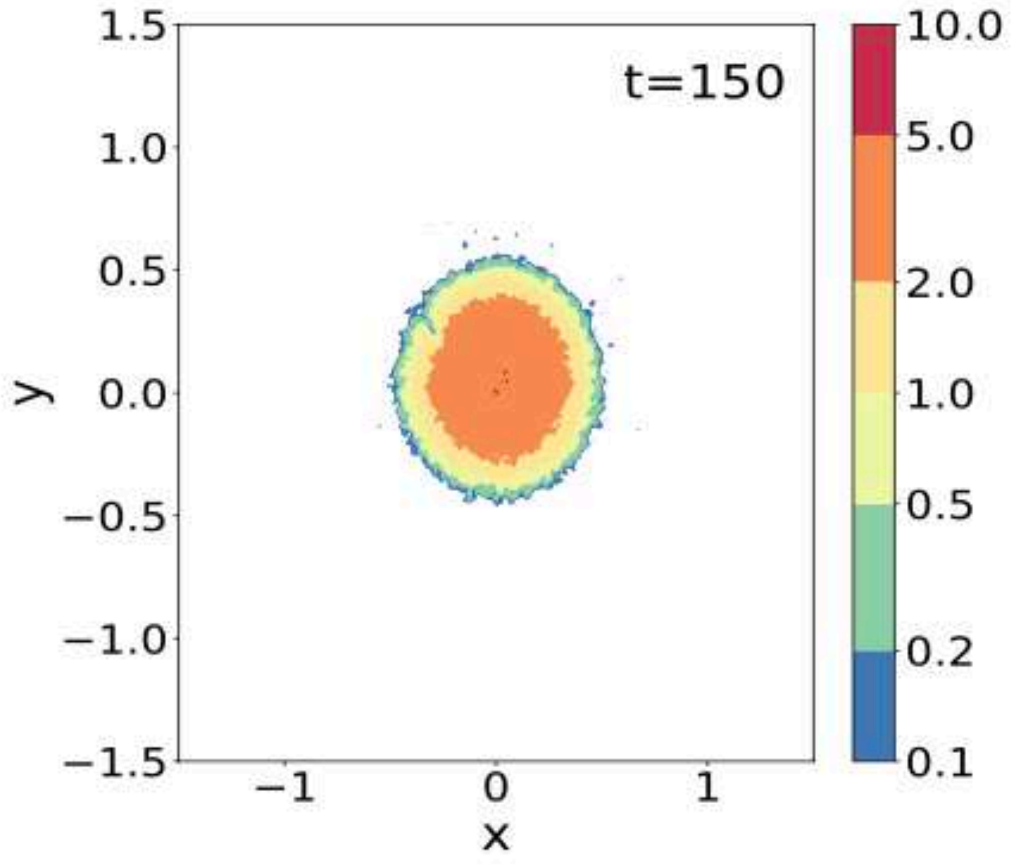

Initial stochastic halo

with a fixed mean

density profile

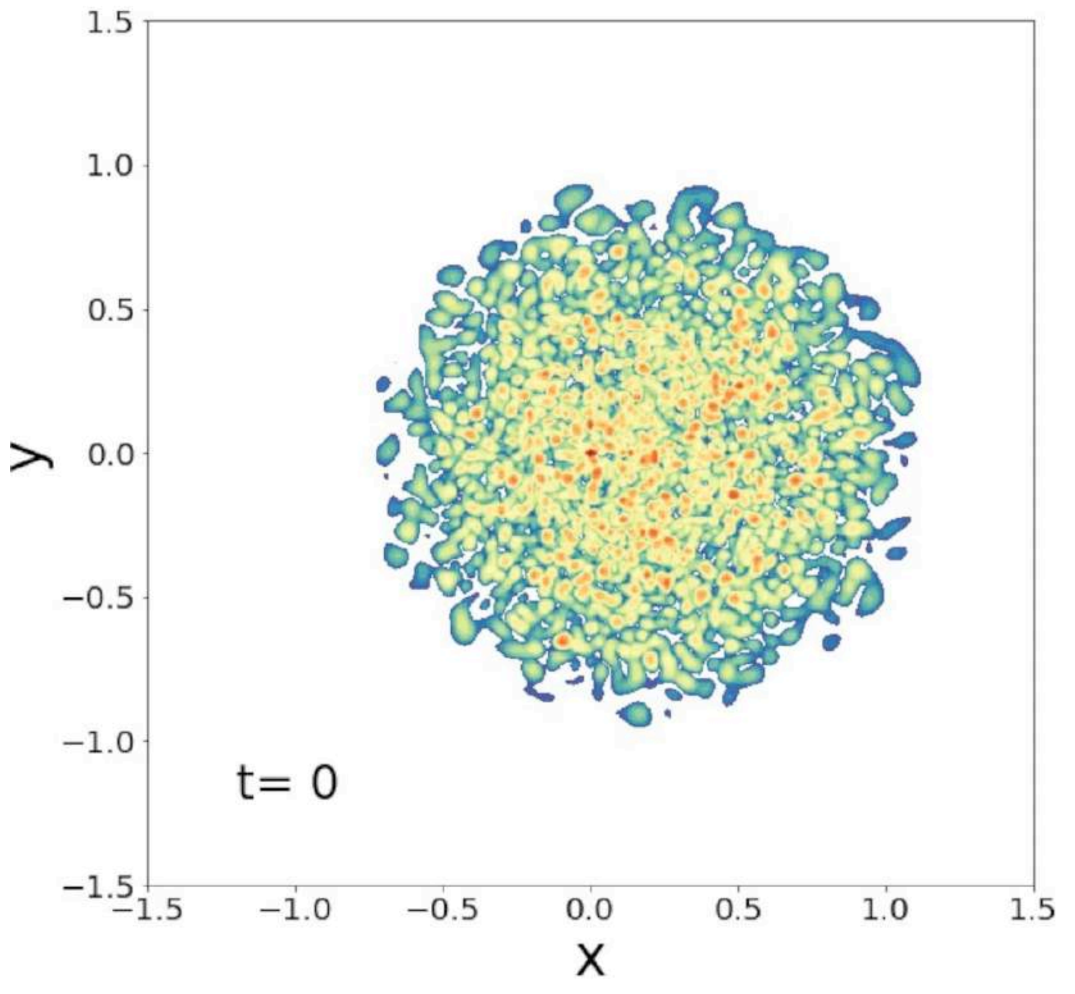

1D potential plot

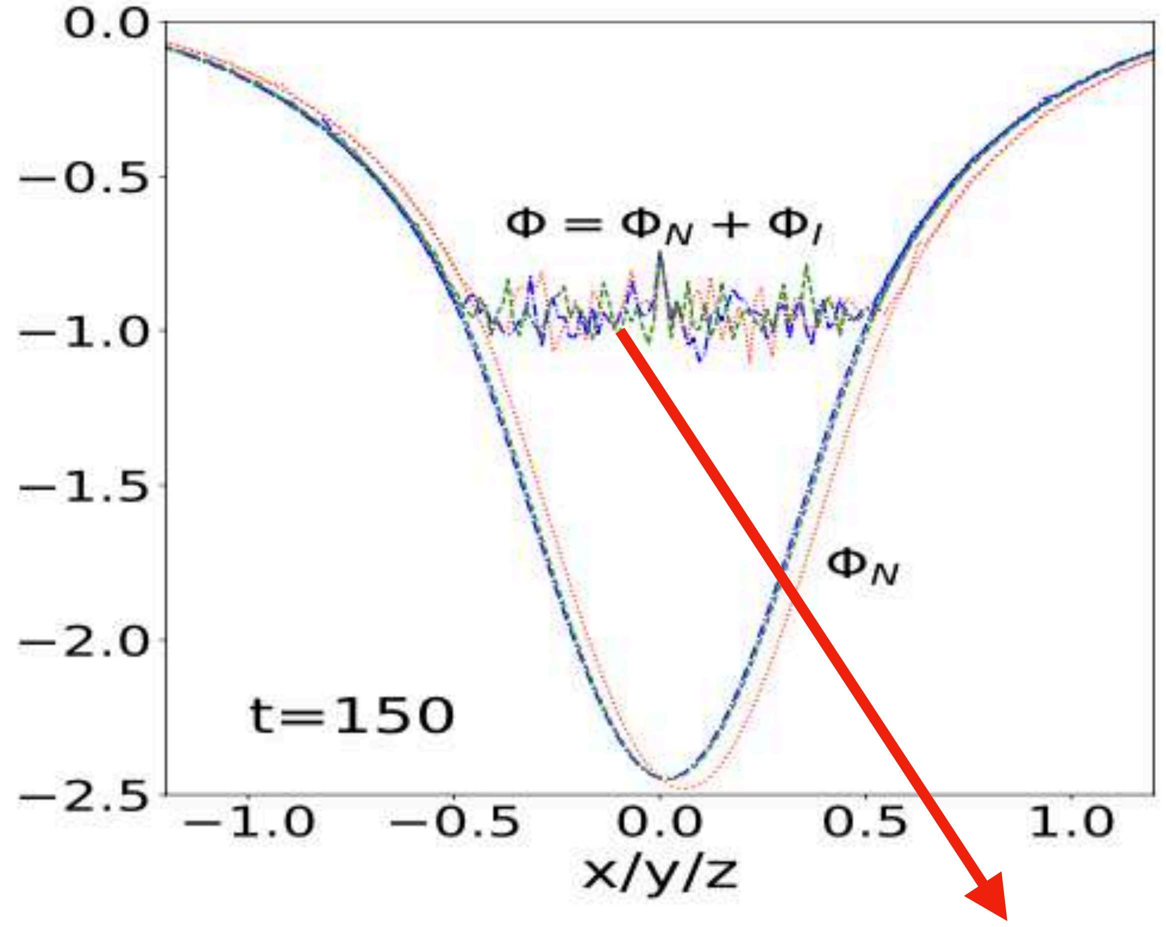

flat=soliton (hydrostatic eq.)

Evolution of total and soliton mass

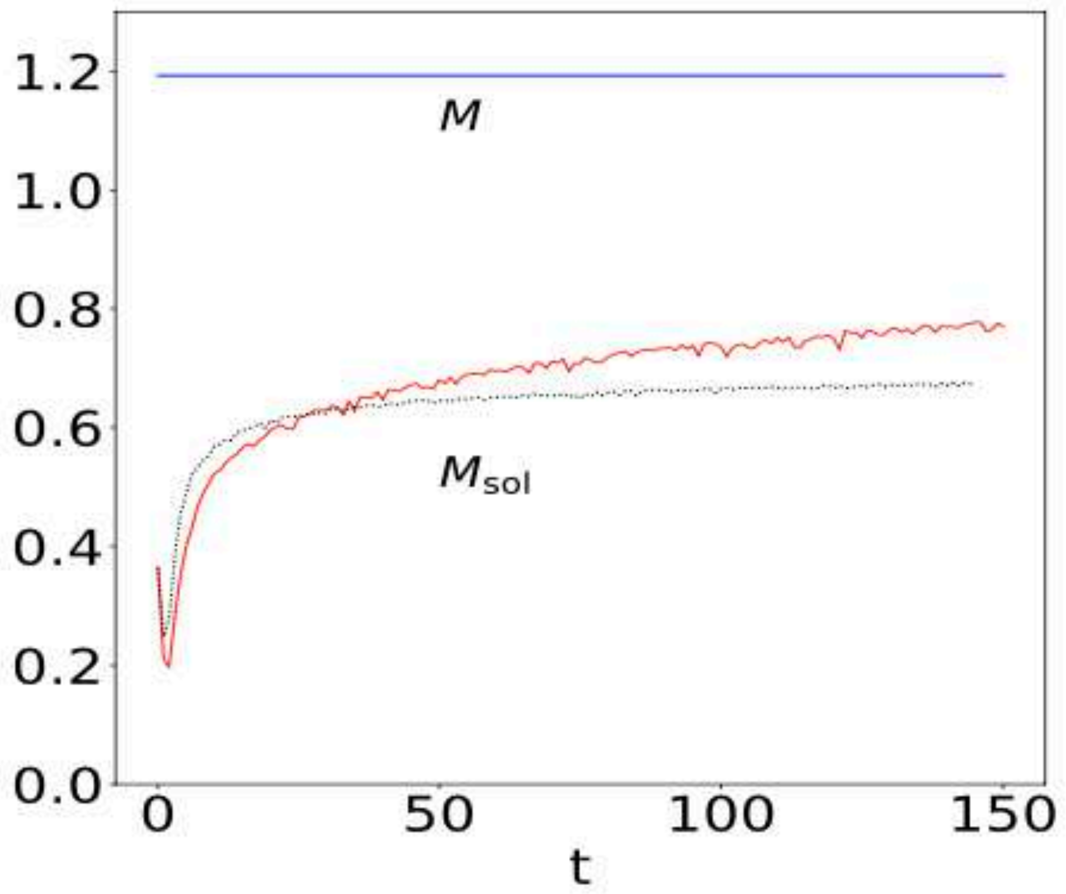

Evolution of energy components

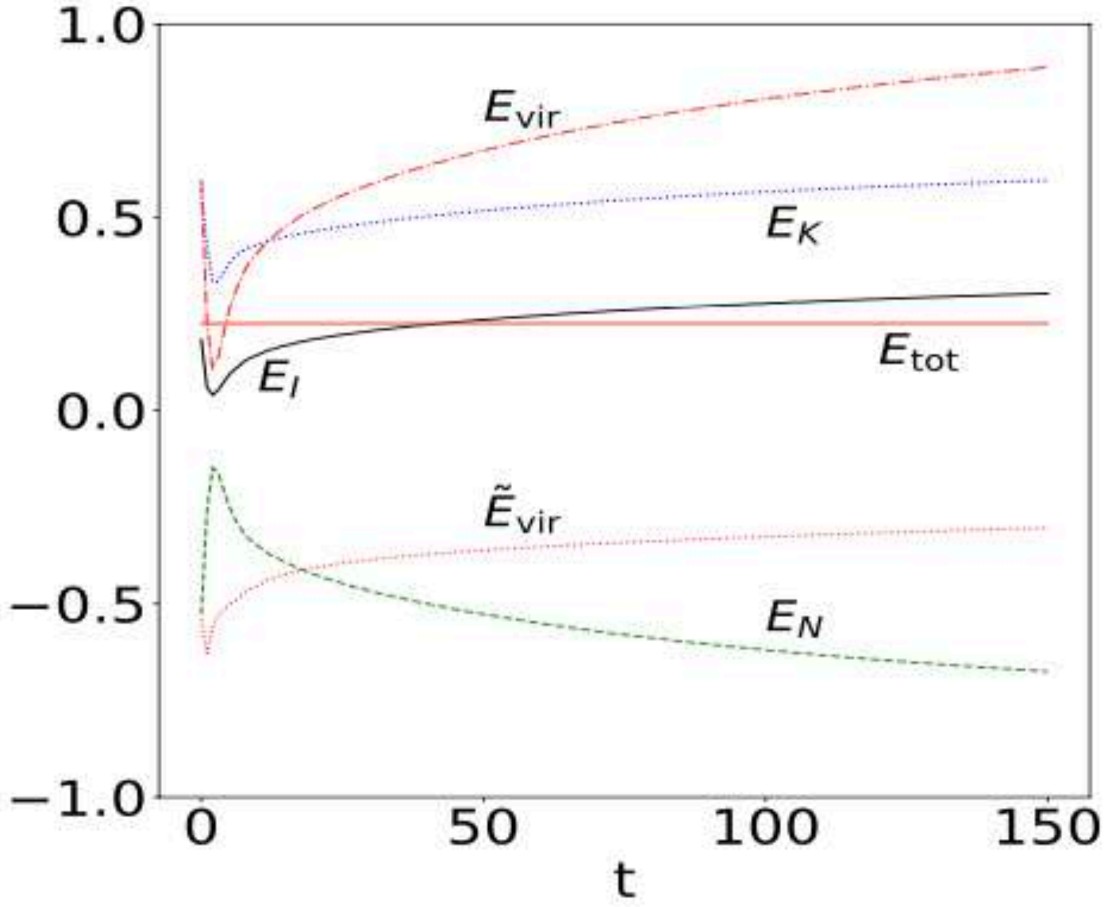

- At t ~ 8, the soliton is formed with Rsol ~ 0.5 and it contains ~ 50% of the total mass.
- The system reaches a quasi-stationary state.
- Afterwards, the soliton slowly grows.

2) Soliton radius much smaller than the halo size

1D density plots

2D density plots

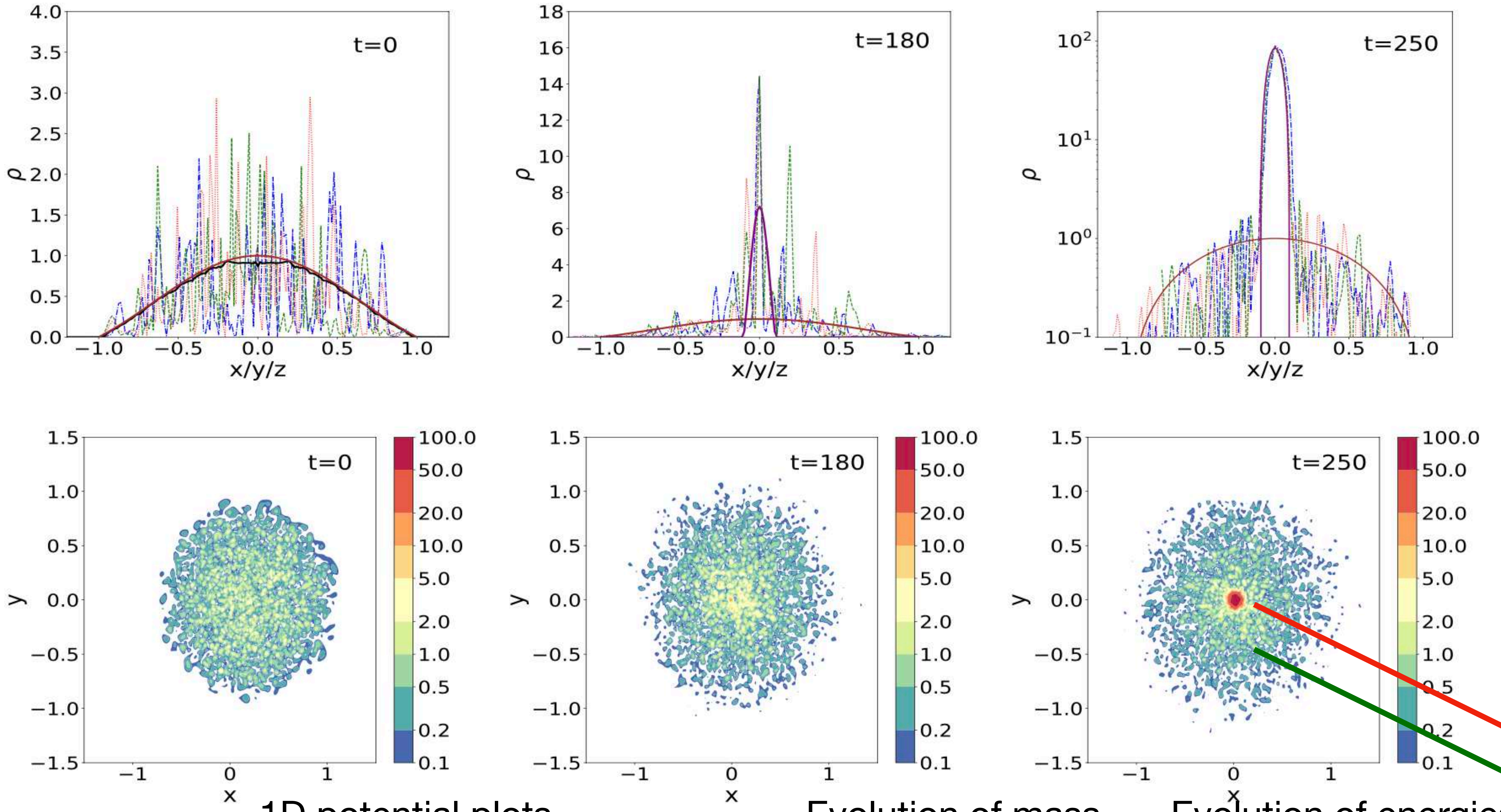

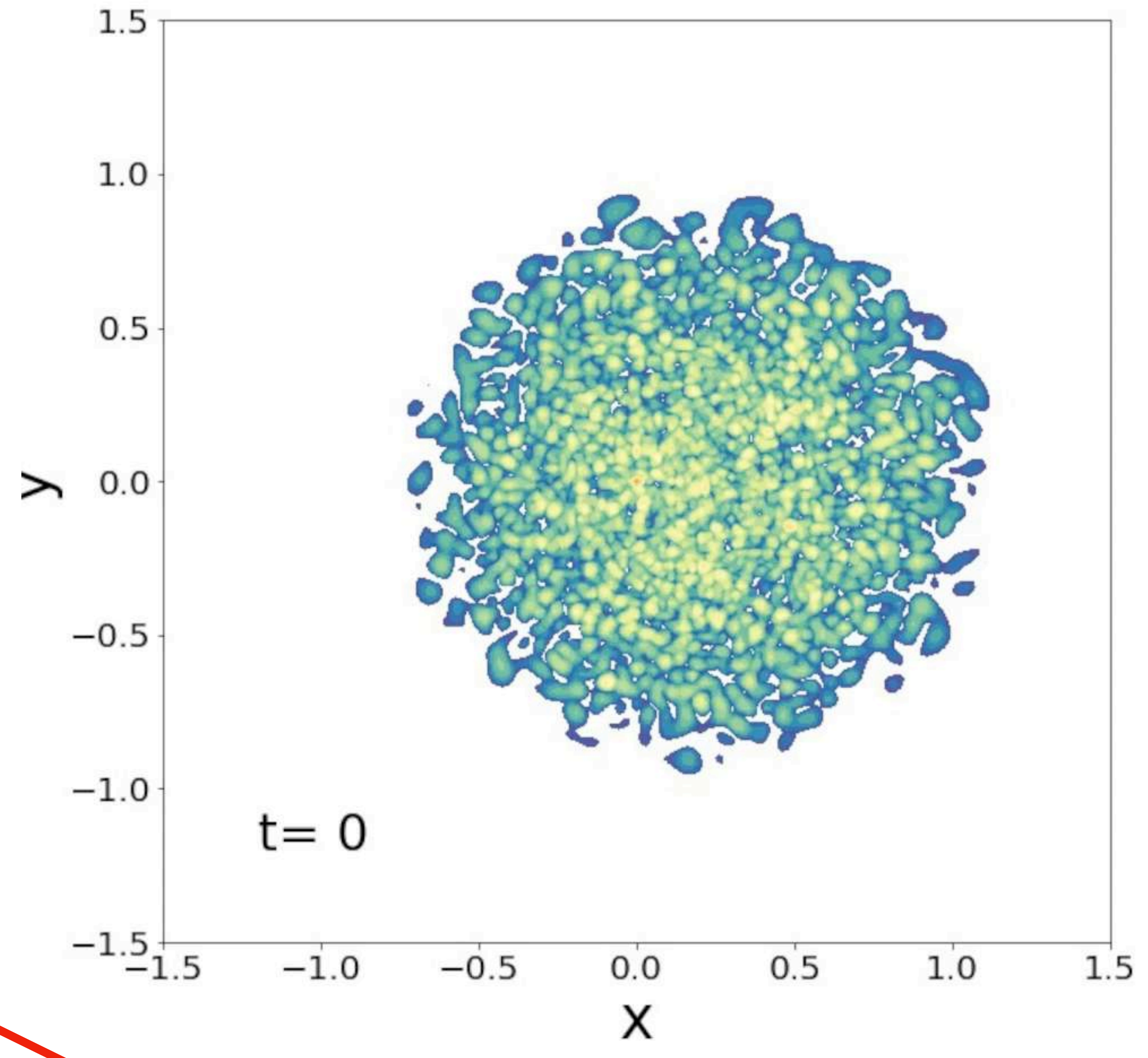

1D potential plots

Evolution of mass

Evolution of energies

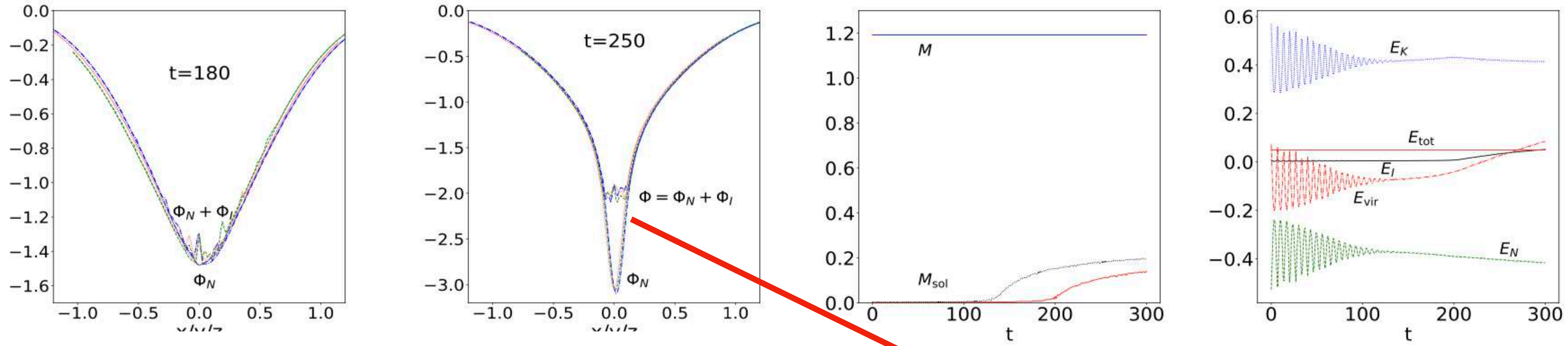

Central soliton

Stochastic halo (negligible self-interactions) dominated by kinetic terms and gravity (CDM - NFW)

flat=soliton

- By t ~ 100, the halo relaxes to a quasi-stationary state.
- At t ~180, FDM peak.
- At t ~ 200, self-interacting soliton forms, R_{sol} = 0.1 .

Transition from a FDM phase to a self-interacting phase.

3) Dependence of the soliton mass on the formation history

Growth with time of the soliton mass

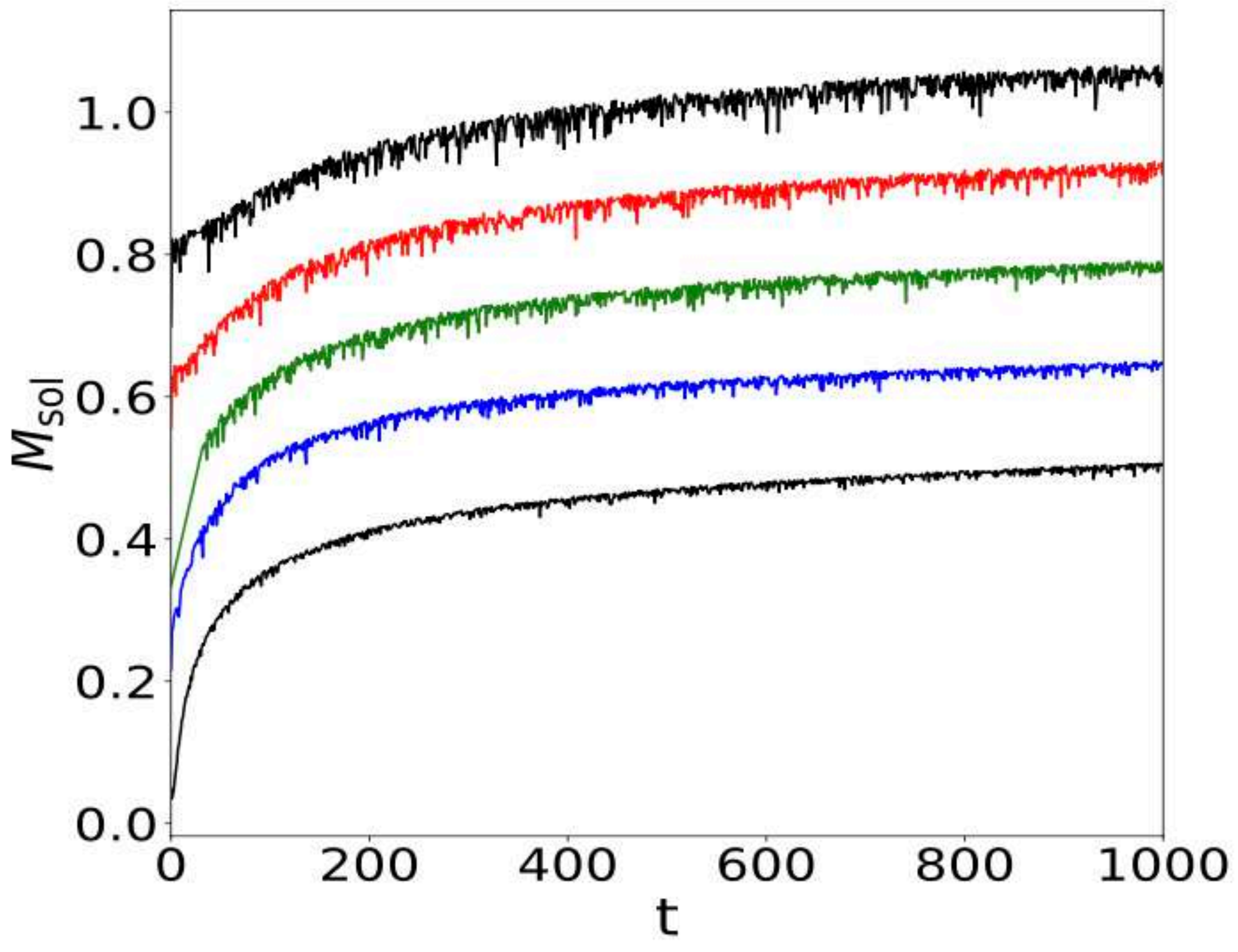

Growth rate as a function of the soliton mass, for several initial conditions

$$\Gamma_{\rm sol} = \frac{\dot{M}_0}{M_0}$$

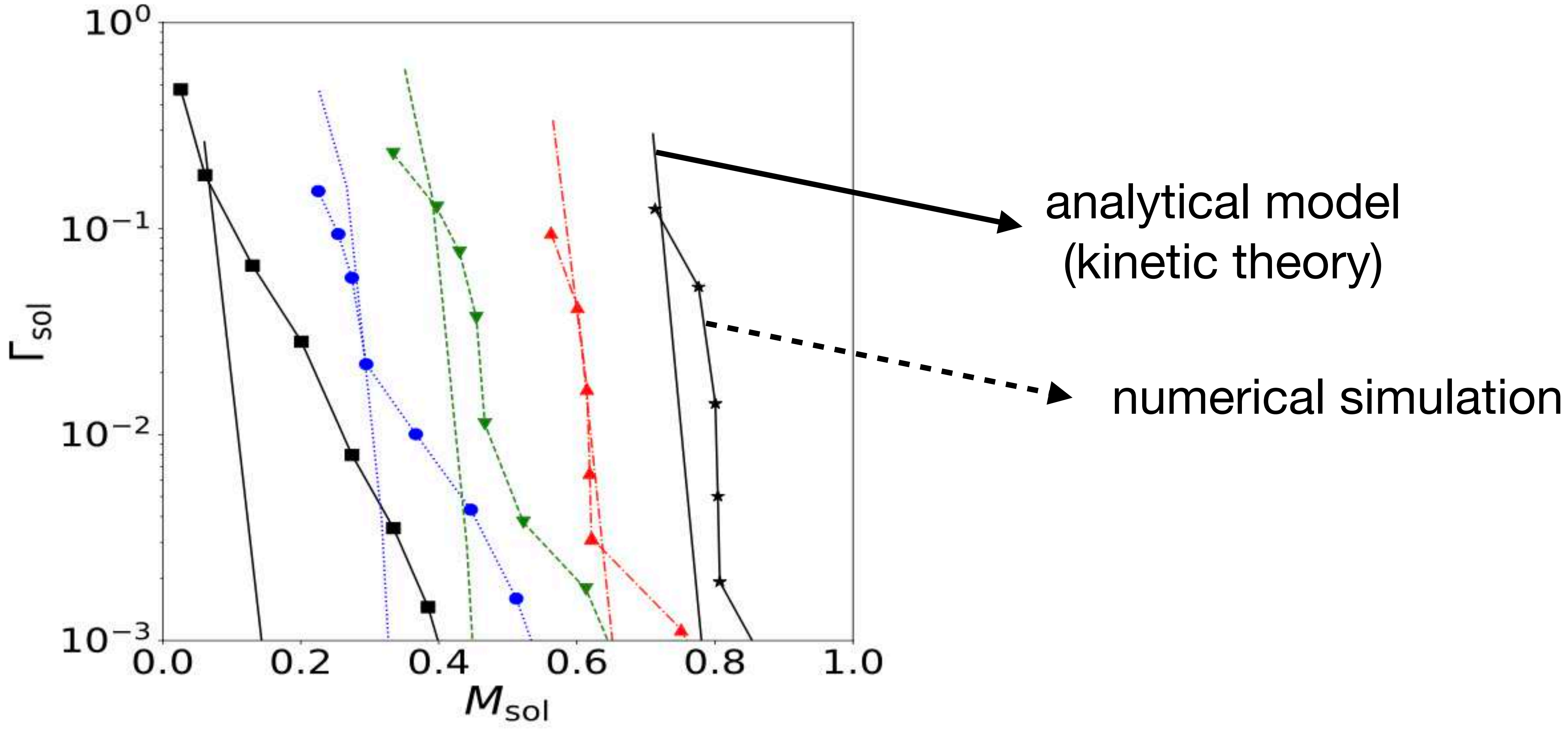

- The soliton always forms and grows, with a growth rate that decreases with time.
- Its mass can reach 50% of the total mass of the system.
- There is no sign of a scaling regime, where the growth rate would be independent of initial conditions.

→ Probably no well-defined halo-mass/soliton mass relation

B) Kinetic theory

To understand the growth of the soliton, we develop a kinetic theory:

Instead of following the wave function, we try to follow the evolution of the occupation numbers of the various eigenmodes of the Schrödinger eq. in a reference potential

Non-linear Schrödinger eq. (Gross-Pitaevskii):

$$i\epsilon\frac{\partial\psi}{\partial t} = -\frac{\epsilon^2}{2}\nabla^2\psi + \Phi\psi \qquad \Phi = (4\pi\nabla^{-2} + \lambda)\psi\psi^\star \qquad \epsilon = \frac{\lambda_{\rm dB}}{2\pi L_\star} \ll 1$$

If Φ is fixed, ψ can be decomposed over the eigenmodes with the simple time dependence $e^{-iE_n t/\epsilon}$

and there is no secular growth or evolution of the system.

However the fluctuations (or interference terms) induce a time-dependent potential and drive the evolution of the system.

Chan et al. (2022) considered the case of FDM over a flat background, expanding over plane waves.

Here we consider a non-flat background (self-gravity of the halo), with possibly a soliton in the initial conditions.

→ We cannot use Fourier analysis → We follow the evolution of the occupation numbers of the eigenmodes in the reference potential

- We write the potential as: $\Phi(\vec{x},t) = \bar{\Phi}(r) + \delta\Phi(\vec{x},t)$

average spherically symmetric part

fluctuating part

- We expand over the eigenmodes: $\psi(\vec{x},t) = \sum_j \sqrt{M_j(t)} e^{-i\theta_j(t)/\epsilon} \hat{\psi}_j(\vec{x})$

real-values eigenmode *j*

mass contained in the eigenmode *j*

Initial mass M_j is fixed, initial phase θ_j is random

- We substitute into the Schrödinger eq.: $i\epsilon\dot{M}_j + 2M_j\dot{\theta}_j = 2M_jE_j + \sum_{j'} 2\sqrt{M_jM_{j'}} e^{i(\theta_j-\theta_{j'})/\epsilon} \int d\vec{x}\, \hat{\psi}_j \delta\Phi \hat{\psi}_{j'}$

- We define the reference potential as the sum of the diagonal terms: $\bar{\Phi} = (4\pi\nabla^{-2} + \lambda) \sum_j M_j \hat{\psi}_j^2$ initially deterministic

and the remainder is given by the off-diagonal terms: $\delta\Phi = (4\pi\nabla^{-2} + \lambda) \sum_{j\neq j'} \sqrt{M_jM_{j'}} e^{i(\theta_j-\theta_{j'})/\epsilon} \hat{\psi}_j \hat{\psi}_{j'}$ initially random

- We perform a perturbative expansion (over powers of $\delta\Phi$): $M_j = M_j^{(0)} + M_j^{(1)} + M_j^{(2)} + \dots$

and we average over the random initial phases $\theta_j^{(0)}$

4-leg vertices: $V_{13;24} = \int d\vec{x}\, \hat{\psi}_1 \hat{\psi}_3 (4\pi\nabla^{-2} + \lambda) \hat{\psi}_2 \hat{\psi}_4$

- Zeroth order: $M_j^{(0)}(t) = \bar{M}_j, \quad \theta_j^{(0)}(t) = \bar{\theta}_j + \bar{\omega}_j t$

$\bar{\omega}_j = E_j + \sum_{j'}^{j'\neq j} M_{j'} V_{jj';j'j}$ renormalised frequency

$\omega_{12}^{34} = \omega_1 + \omega_2 - \omega_3 - \omega_4$

- First order: $\langle \dot{M}_j^{(1)} \rangle = 0$

- Second order:

$$\langle \dot{M}_1^{(2)} \rangle = \frac{2}{\epsilon} \sum_{234} \bar{M}_1 \bar{M}_2 \bar{M}_3 \bar{M}_4 \left\{ \frac{\sin(\bar{\omega}_{12}^{34} t/\epsilon)}{\bar{\omega}_{12}^{34}} \hat{V}_{13;24} \left[\frac{\hat{V}_{13;24} + \hat{V}_{14;23}}{\bar{M}_1} + \frac{\hat{V}_{23;14} + \hat{V}_{24;13}}{\bar{M}_2} - \frac{\hat{V}_{31;42} + \hat{V}_{32;41}}{\bar{M}_3} - \frac{\hat{V}_{41;32} + \hat{V}_{42;31}}{\bar{M}_4} \right] + \frac{\sin(\bar{\omega}_1^3 t/\epsilon)}{\bar{\omega}_1^3} \hat{V}_{12;23} \left[\frac{\hat{V}_{14;43}}{\bar{M}_1} - \frac{\hat{V}_{34;41}}{\bar{M}_3} \right] + \frac{\sin(\bar{\omega}_2^4 t/\epsilon)}{\bar{\omega}_2^4} \hat{V}_{23;34} \frac{\hat{V}_{14;21} - \hat{V}_{12;41}}{\bar{M}_2} \right\},$$

This is somewhat similar to four-wave systems (e.g., weak wave turbulence) over an homogeneous background, where we would have:

$$\langle \dot{M}_1^{(2)} \rangle = \frac{2}{\epsilon} \sum_{234} \bar{M}_1 \bar{M}_2 \bar{M}_3 \bar{M}_4 \frac{\sin(\bar{\omega}_{12}^{34} t/\epsilon)}{\bar{\omega}_{12}^{34}} 2\hat{V}_{1234}^2 \left[\frac{1}{\bar{M}_1} + \frac{1}{\bar{M}_2} - \frac{1}{\bar{M}_3} - \frac{1}{\bar{M}_4} \right]$$

For the soliton, ground state j=0, some of the Dirac factors (resonances) vanish and the equation simplifies: $j \neq 0: \quad \omega_j > \omega_0$

$$\dot{M}_0 = \frac{\pi}{\epsilon} \sum_{123} M_0 M_1 M_2 M_3 \, \delta_D(\omega_{01}^{23}) \, (V_{02;13} + V_{03;12})^2 \left(\frac{1}{M_0} + \frac{1}{M_1} - \frac{1}{M_2} - \frac{1}{M_3} \right).$$

Small solitons grow: $M_0 \to 0: \quad \dot{M}_0 = \frac{2\pi}{\epsilon} \sum_{123} M_1 M_2 M_3 \, \delta_D(\omega_{01}^{23}) \, (V_{02;13} + V_{03;12})^2 > 0$

We make a simple approximation for the occupation numbers of the excited modes:

we assume that the increase of mass of the soliton comes from the lowest energy modes, which are depleted up to some energy threshold while the occupation numbers of higher energy levels are not modified

$$\sum_j^{E_j < E_{\mathrm{coll}}} (2\ell + 1) M_{n\ell}(0) = M_{\mathrm{sol}} - M_{\mathrm{sol}}(0)$$

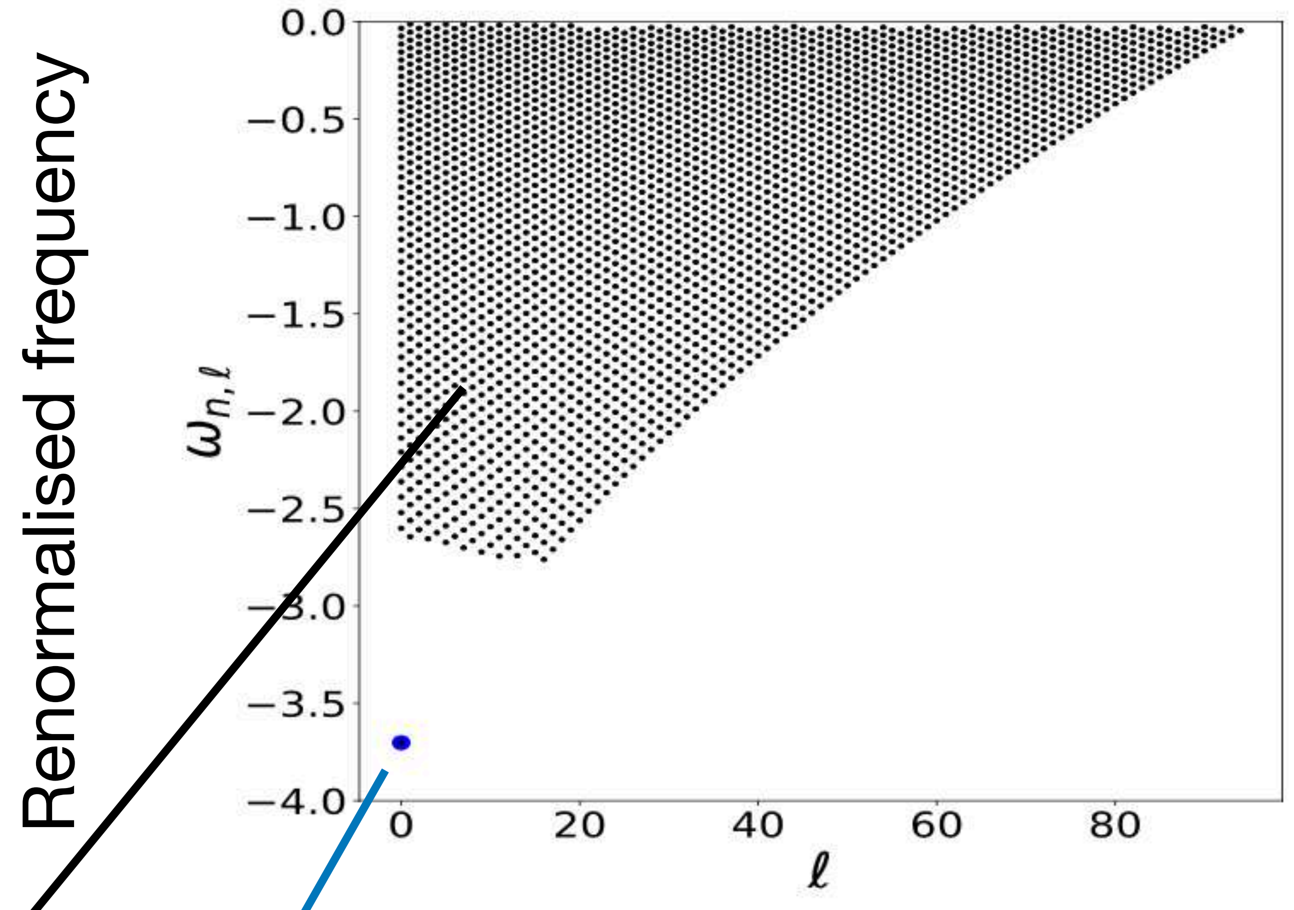

excited halo states

soliton

angular momentum quantum number

Formation of a frequency gap, which prevents resonances and decreases the soliton growth rate.

Growth rate as a function of the soliton mass, for several initial conditions

$$\Gamma_{\mathrm{sol}} = \frac{\dot{M}_0}{M_0}$$

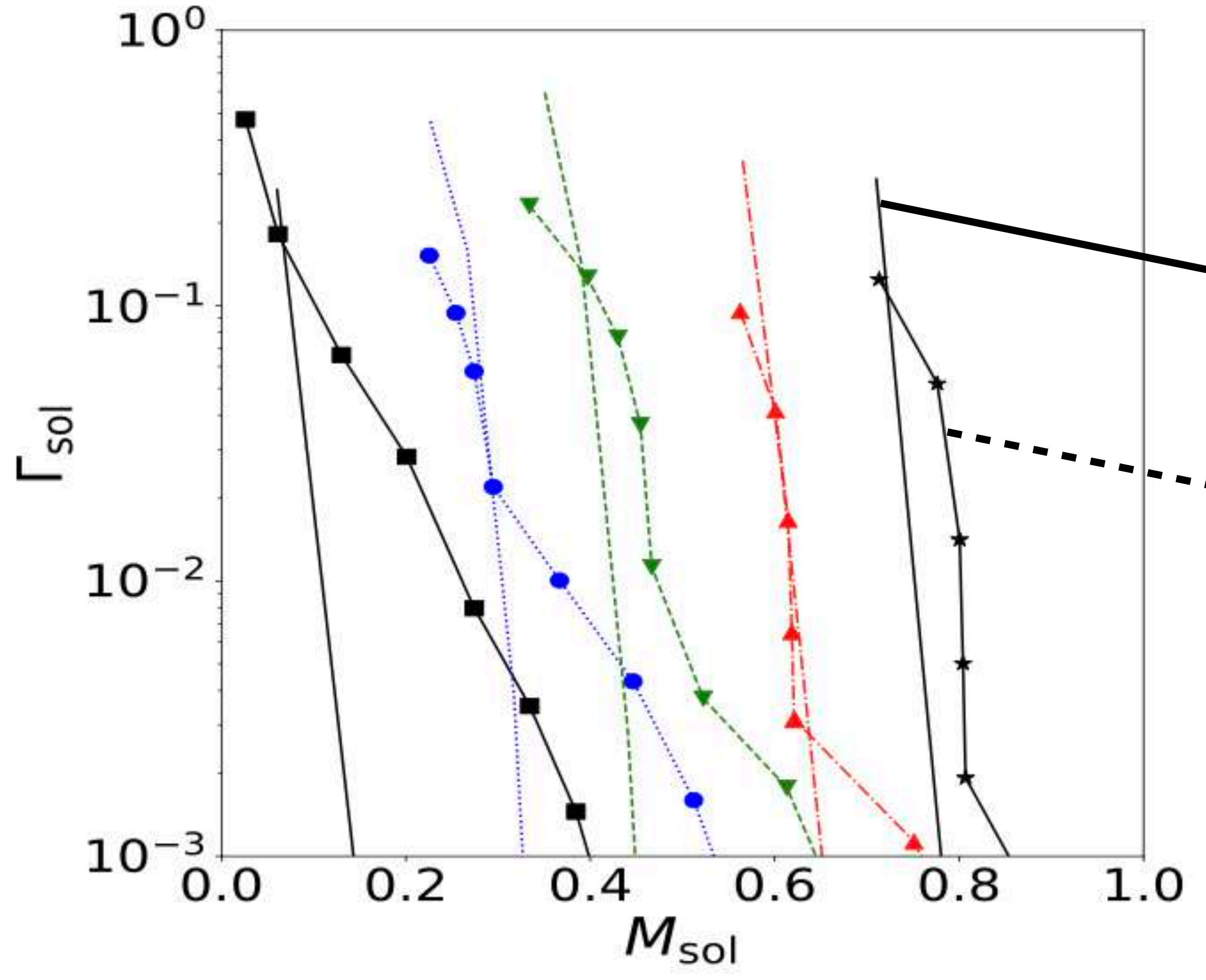

analytical model (kinetic theory)

numerical simulation

With this approximation, we recover
- the positivity of the growth rate
- its initial order of magnitude
- qualitatively its fast falloff with time.

However, we underestimate the growth rate at late times: the low energy modes are probably partly replenished and we should improve the treatment of their occupation numbers.

BH dynamics inside DM solitons
-
Accretion and Dynamical friction

(Schwarzschild BH)

I- RADIAL INFALL ONTO A BH

Again, $V_{\rm I}(\phi) = \frac{\lambda_4}{4}\phi^4.$

quartic repulsive self-interaction

A) Spherically symmetric relativistic and nonlinear system

Classical Bondi problem: steady-state spherical accretion of gas onto a central BH $1 < \gamma < 5/3$ $P \propto \rho^\gamma$

Here: $\gamma = 2$ in the Newtonian regime, and we perform a relativistic analysis:

- metric deviations from Minkowski are large close to the BH horizon

static spherical symmetry: $ds^2 = -f(r)dt^2 + h(r)(dr^2 + r^2 d\vec{\Omega}^2).$ (isotropic coordinates)

* Schwarzschild metric close to the BH: $\frac{r_s}{4} < r < r_{\rm NL}: \; f(r) = \left(\frac{1 - r_s/(4r)}{1 + r_s/(4r)}\right)^2,$ $h(r) = (1 + r_s/(4r))^4,$

* small metric fluctuations and self-gravity far from the BH, in the galactic-scale soliton:

$\Phi \ll 1, \quad f = 1 + 2\Phi, \quad h = 1 - 2\Phi$ $r \gg r_{\rm sg}: \; \nabla^2\Phi = 4\pi\mathcal{G}\rho_\phi,$

- field oscillations are large and the cosine is significantly deformed by the self-interactions: anharmonic oscillations

⇒ nonlinear approach to the K.G. eq.

B) Nonlinear oscillator

nonlinear cubic term due to the self-interactions

Nonlinear Klein-Gordon eq. of motion: $$\frac{\partial^2\phi}{\partial t^2} - \sqrt{\frac{f}{h^3}}\frac{1}{r^2}\frac{\partial}{\partial r}\left[\sqrt{fh}r^2\frac{\partial\phi}{\partial r}\right] + fm^2\phi + f\lambda_4\phi^3 = 0.$$

In the large-mass limit, use a nonlinear local approximation: $\phi = \phi_0(r)\mathrm{cn}[\omega(r)t - \mathbf{K}(r)\beta(r), k(r)],$

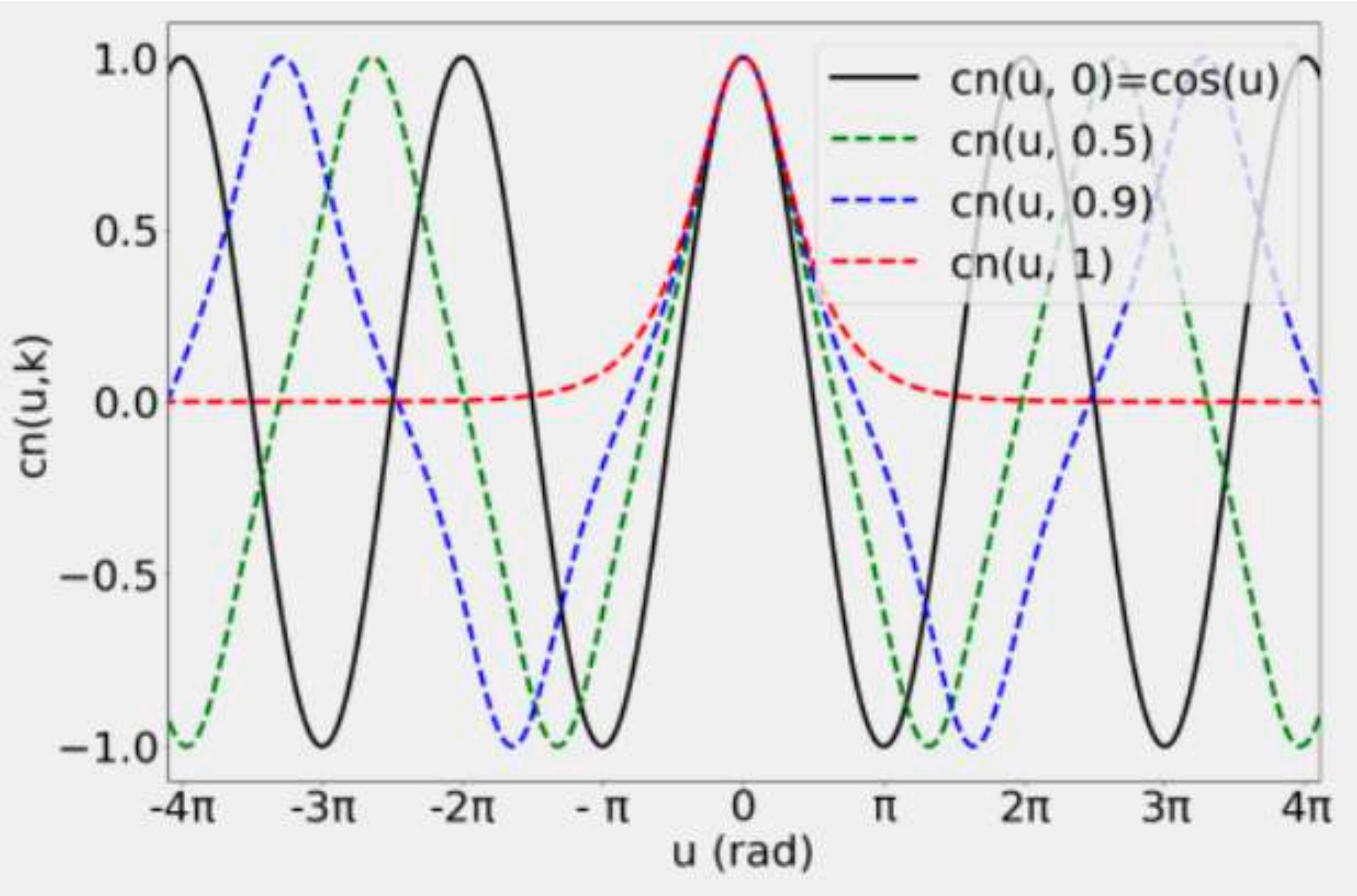

$\mathrm{cn}(u,k)$ is a generalization of the cosine to the nonlinear (cubic) oscillator: $\frac{\partial^2\mathrm{cn}}{\partial u^2} = (2k^2-1)\mathrm{cn} - 2k^2\mathrm{cn}^3,$

(Jacobi elliptic function) $k=0: \quad \mathrm{cn}(u, k=0) = \cos(u)$

$\phi_0(r), \ \omega(r), \ \beta(r), \ \mathbf{K}(r), \ k(r)$ are slow functions of r

$\omega \sim \beta \sim m$ $\quad \nabla_r \ll m$ $\quad 1/m \ll r_s$ Compton wavelength shorter than the Schwarzschild radius

Substituting into the Klein-Gordon eq. determines all parameters $\{\phi_0, \ \omega, \ \beta, \ \mathbf{K}\}$ in terms of $k(r)$ (at leading order)

$k(r)$ is determined by a self-consistency constraint: the mean flux (averaged over the fast oscillations) must be constant over radius: steady state

$\nabla_\mu T^\mu_0 = 0,$ $\quad F = -\sqrt{fh^3}r^2\langle T^r_0\rangle = \sqrt{fh}r^2\phi_0^2\omega\mathbf{K}\beta'\left\langle\left(\frac{\partial\mathrm{cn}}{\partial u}\right)^2\right\rangle,$ is a constant.

C) Critical flux: unique transsonic solution

The behaviour is qualitatively similar to the classical Bondi problem:

- For a given flux $F < F_\star$ there are 2 solutions: a fully subsonic and a fully supersonic solution.
- At the critical flux $F_\star$ these 2 branches join at a critical radius $r_\star$, which allows 2 unique transsonic solutions.
- The boundary conditions select the unique transsonic solution that is subsonic at large radii and supersonic at small radii.

matching to the hydrostatic soliton

free fall at the BH horizon

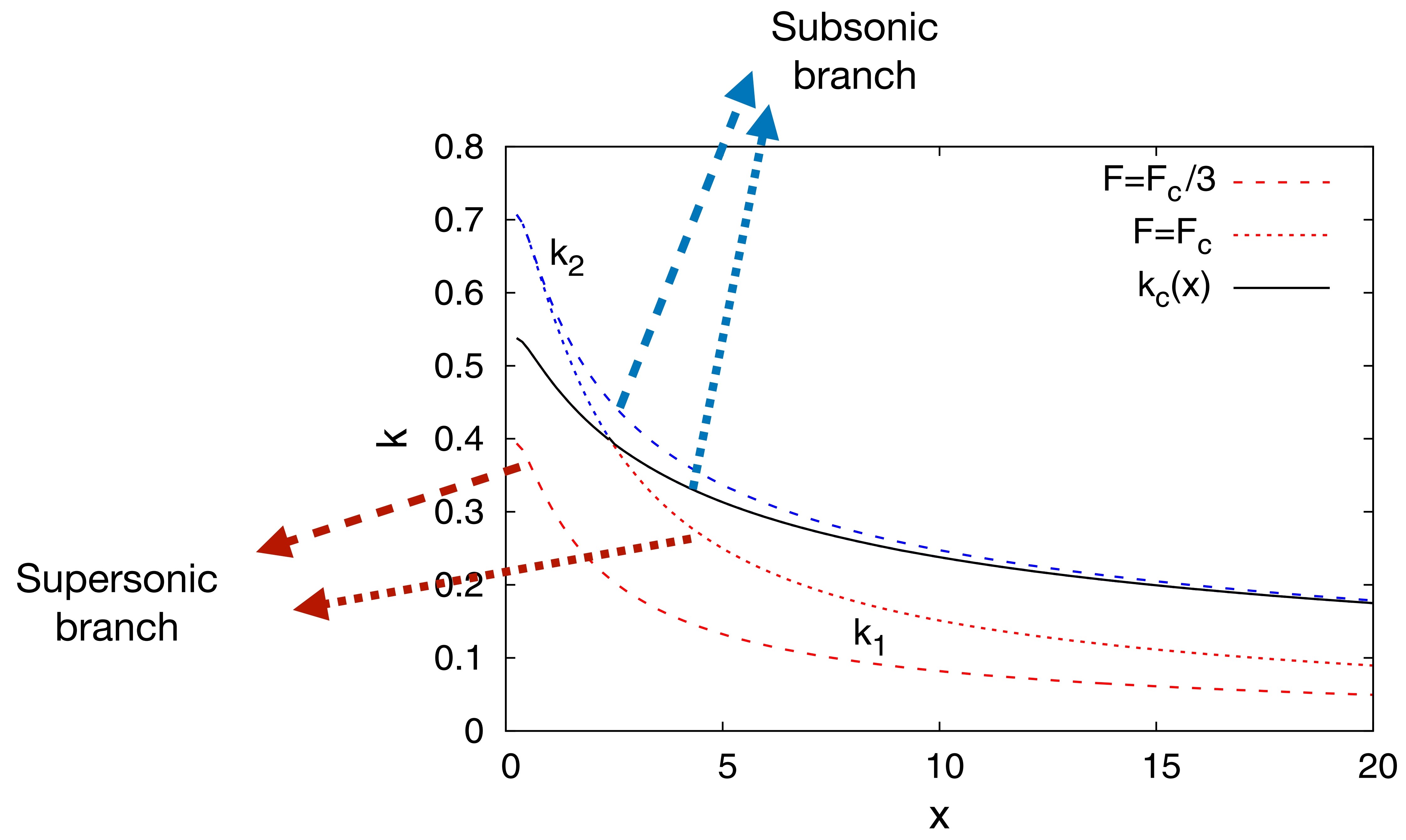

Characteristic density: $\rho_a \equiv \frac{4m^4}{3\lambda_4}$.

Critical flux: $F_c = F_\star F_s$ with $F_\star \sim 0.7$ $F_s = \frac{r_s^2 m^4}{\lambda_4}$

$r \sim r_s: \quad \rho \sim \rho_a, \quad v \sim c$

greater repulsive self-interactions decrease the scalar-field energy density and flux.

- intermediate radii (weak gravity dominated by the BH mass): $r_s \ll r \ll r_{\rm sg}: \ \langle\tilde\rho_\phi\rangle \propto r^{-1}$ and $v_r \propto r^{-1}$.

Impact of the repulsive self-interactions FDM (free-fall): $\rho \propto r^{-3/2}$

- large radii (weak gravity dominated by the scalar-field soliton self-gravity):

$r_{\rm sg} < r < R_s: \ \tilde\rho_\phi \sim \rho_s, \qquad v_r \sim -\frac{\rho_s}{\rho_a}\frac{r_{\rm sg}^2}{r^2}$.

radial scalar-field energy-density profile

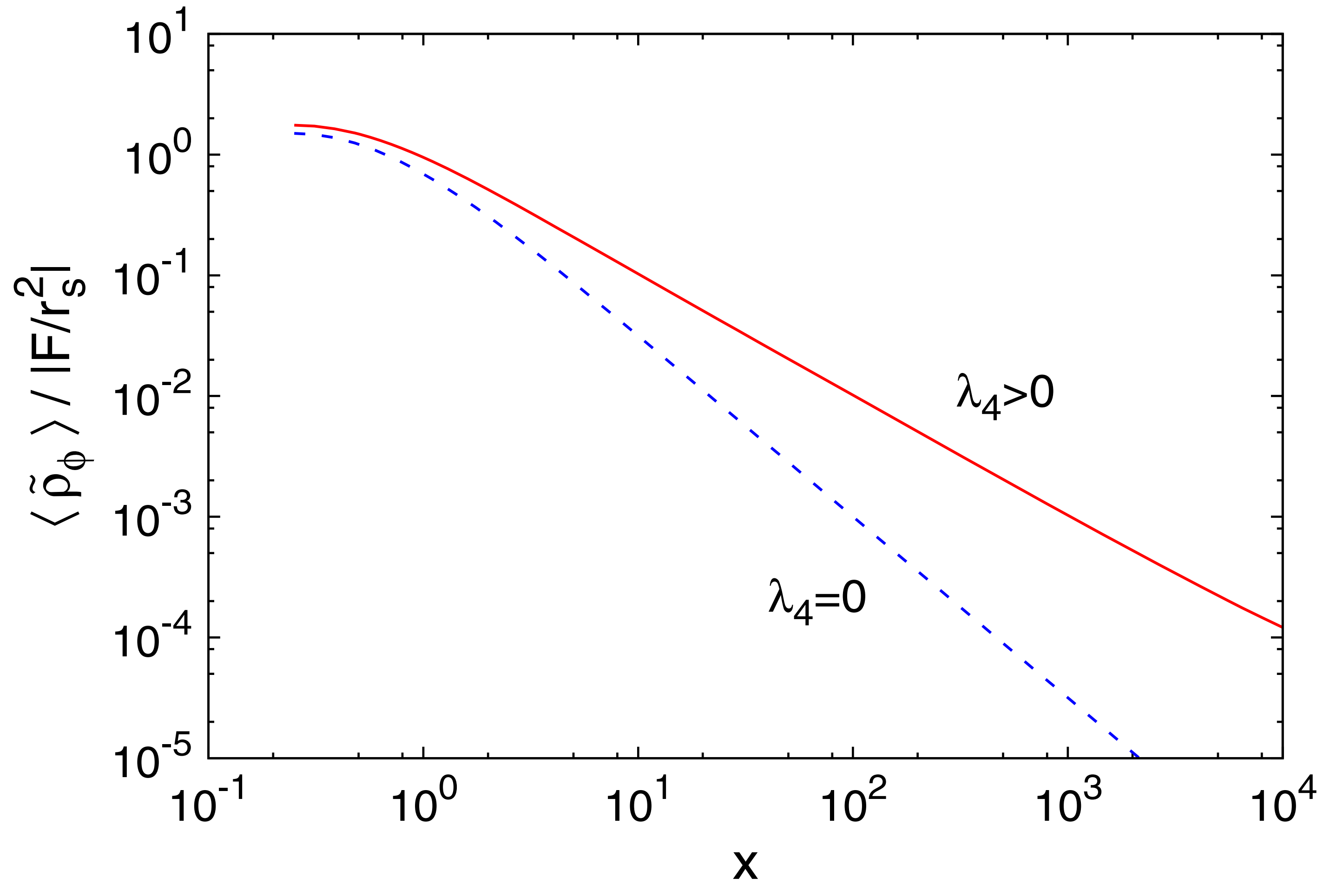

$$\dot M_{\rm Bondi} = \frac{2\pi\rho_0\mathcal{G}^2 M_{\rm BH}^2}{c_s^3}$$

$$\boxed{\dot M_{\rm SFDM} = \frac{12\pi F_\star \rho_0 \mathcal{G}^2 M_{\rm BH}^2}{c_s^2 c}}$$

relativistic, much smaller than Bondi

$r_\star \sim 2.4 r_s$ in the relativistic regime

II- BH MOVING INSIDE A SFDM CLOUD

A) Soliton and BH frames

In the static SFDM cloud (soliton) frame

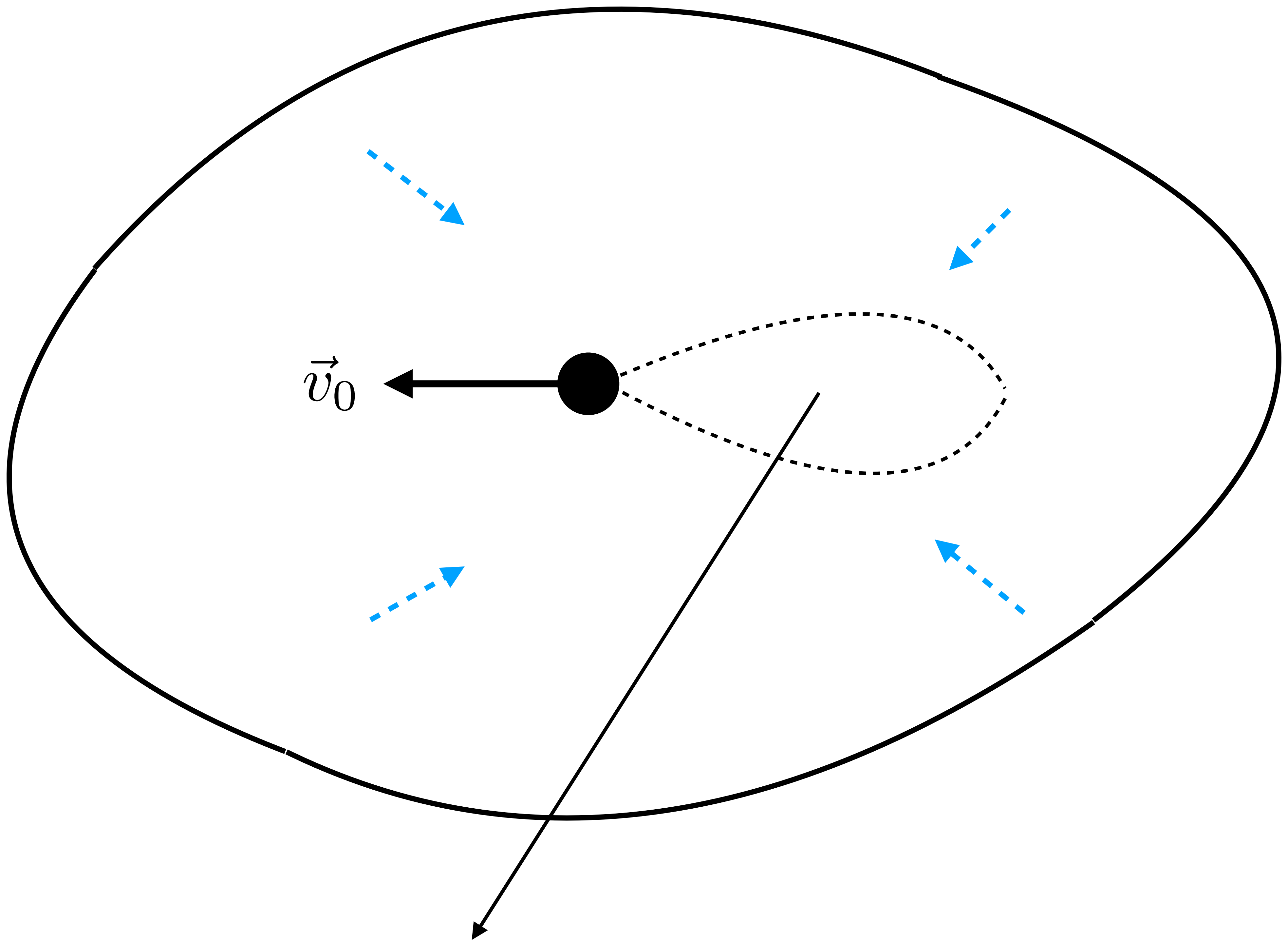

An overdense wake behind the BH, due to the BH gravity.
Slows down the BH.

Dynamical friction Chandrasekhar 1943

In the BH frame (subsonic case)

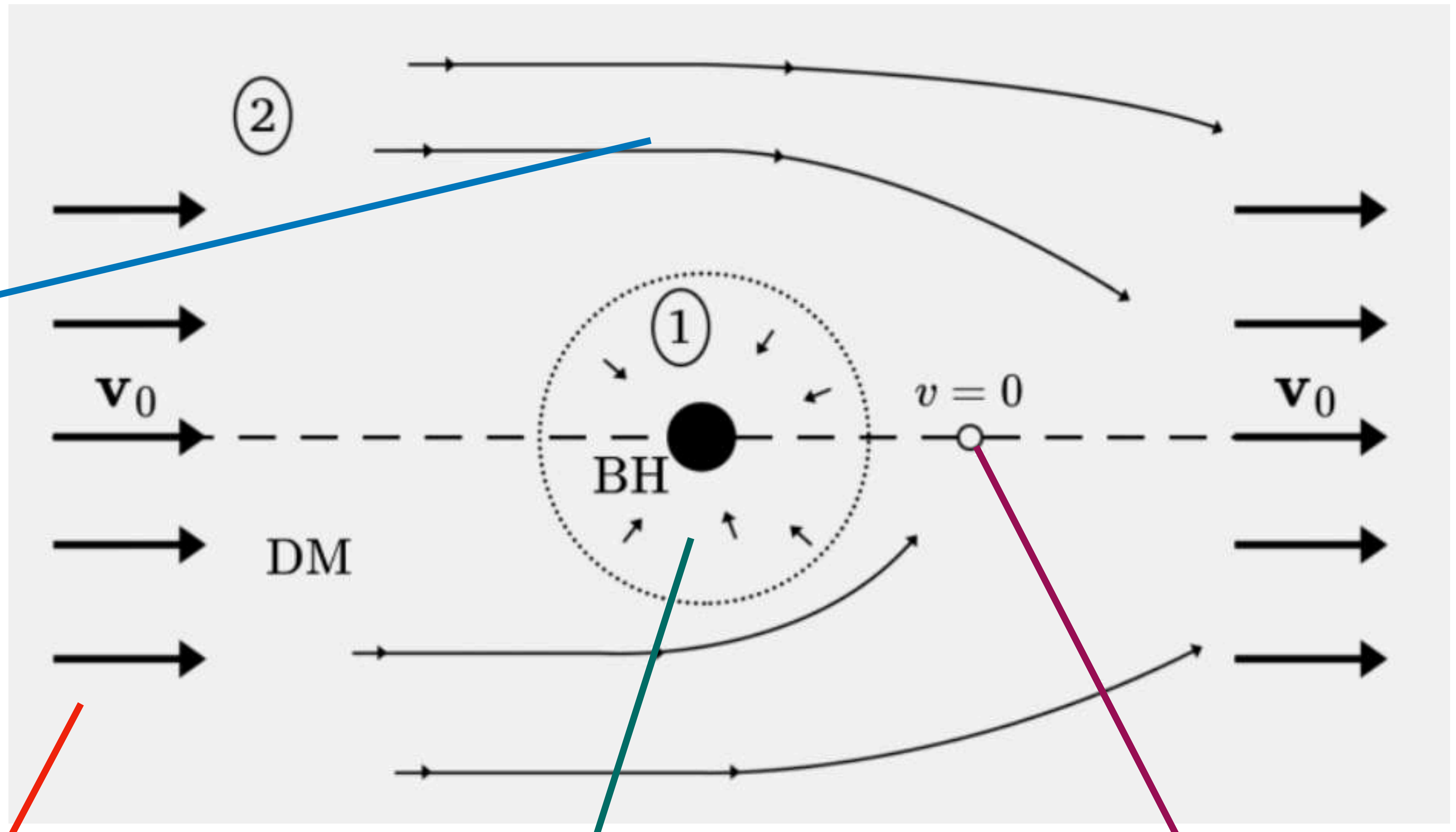

Bending of streamlines
by the BH gravity

Uniform DM fluid velocity at infinity

Radial accretion close
to the BH horizon

Stagnation point
behind the BH

B) Large-distance domain

Far from the BH: hydrodynamical equations of an isentropic gas of effective adiabatic index $\gamma = 2$

Continuity eq. + Euler eq.

$$\hat{\nabla}(\hat{\rho}\vec{v}) = 0$$

Potential flow $\vec{v} = \nabla\beta$

Bernoulli eq.: $$v^2 - \frac{1}{r} + \rho = \text{constant} = v_0^2 + \rho_0$$

BH gravity

effective pressure

Isentropic potential flow eq.: $$\hat{\nabla} \cdot \left[\left(\hat{\rho}_0 + \frac{1}{\hat{r}} + v_0^2 - (\hat{\nabla}\hat{\beta})^2 \right) \hat{\nabla}\hat{\beta} \right] = 0.$$

Steady state, in the BH frame

Conservation of mass and momentum allow us to obtain the mass and momentum flux through any arbitrarily distant surface:

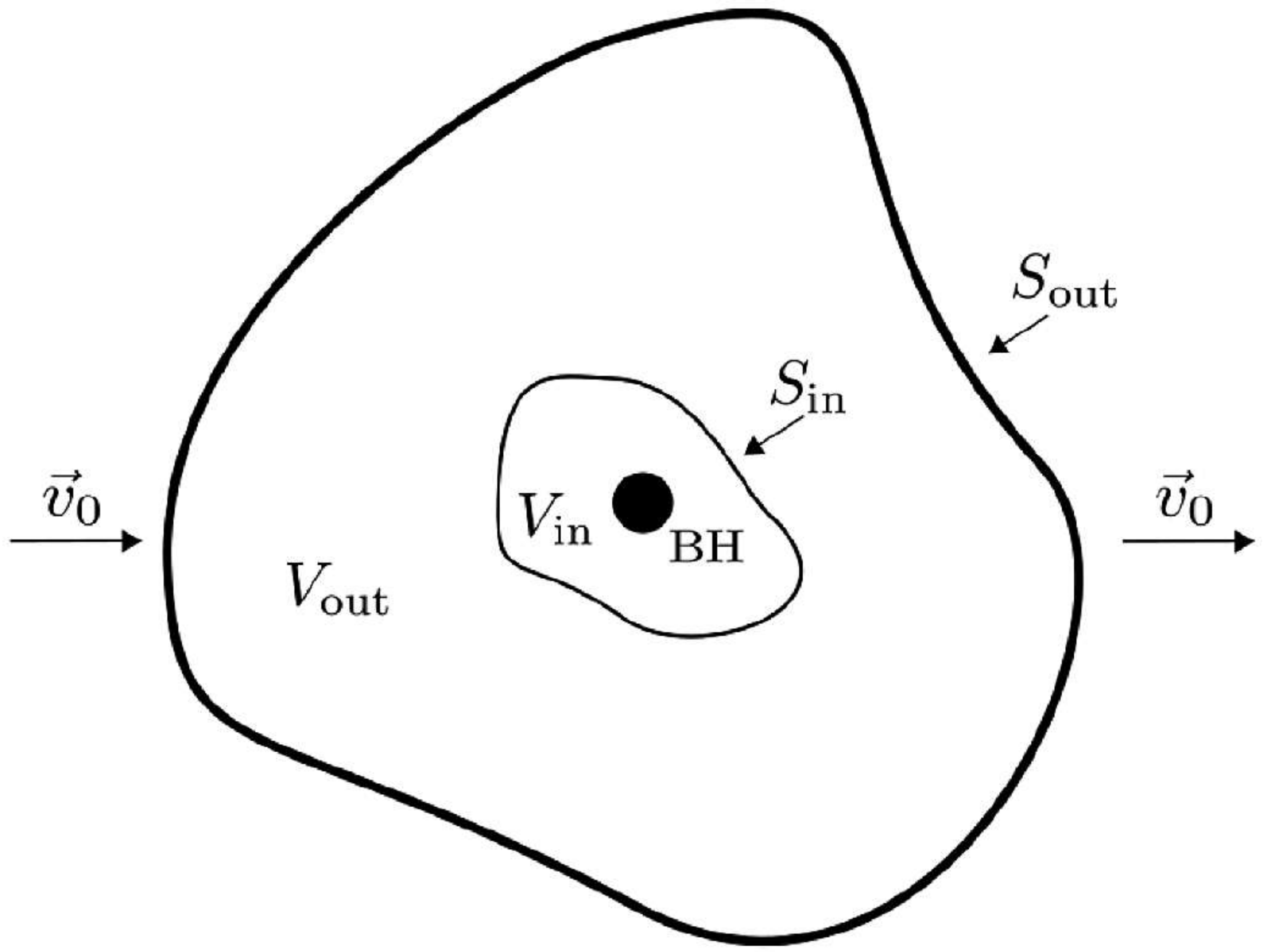

Allows us to obtain analytical results from large-distance expansions

C) Subsonic and supersonic regimes

Velocity potential: $\beta = v_0 r \cos\theta + \delta\beta$

uniform flow perturbation (due to the BH)

Linearize over $\delta\beta$

$$\frac{\partial^2 \delta\beta}{\partial x^2} + \frac{\partial^2 \delta\beta}{\partial y^2} + \left(1 - \frac{v_0^2}{c_{s0}^2}\right) \frac{\partial^2 \delta\beta}{\partial z^2} = \frac{v_0 z}{\rho_0 r^3}$$

$v_0 < c_{s0}$: subsonic BH velocity, elliptic eq., boundary-value problem, smooth

$v_0 > c_{s0}$: hypersonic BH velocity, hyperbolic eq., Cauchy problem, shock

III- SUBSONIC REGIME

Exact analytical results using a large-distance expansion: $\hat{\beta} = \hat{\beta}_{-1} + \hat{\beta}_0 + \hat{\beta}_1 + \ldots, \quad \text{with} \quad \hat{\beta}_n \sim \hat{r}^{-n}$

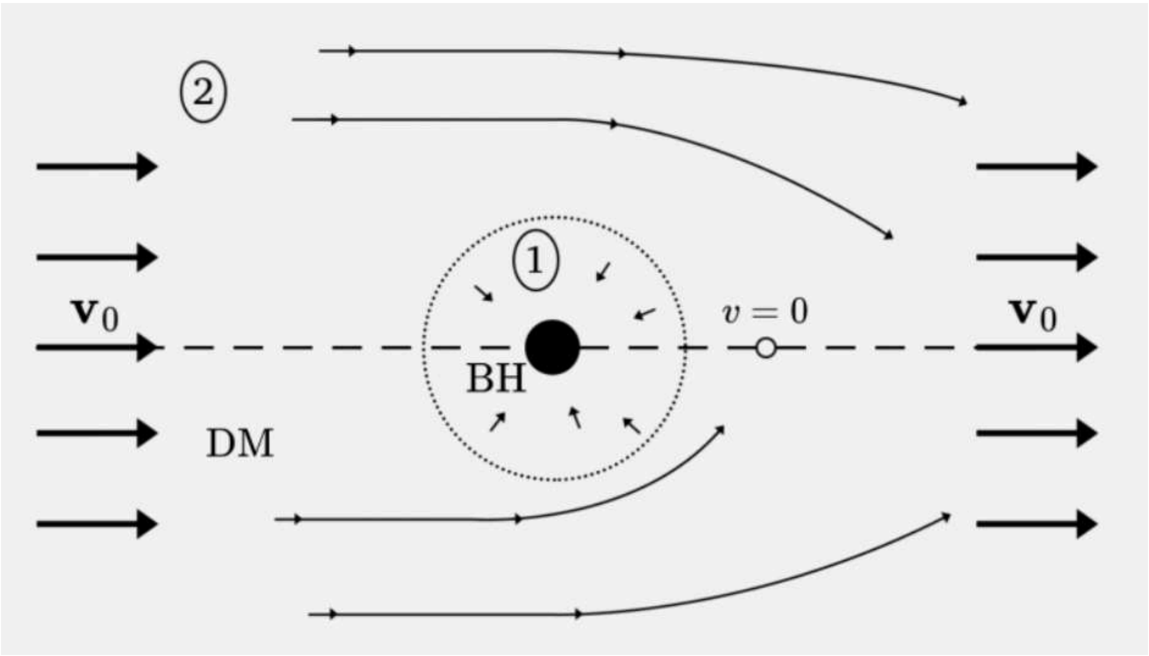

$$\rho_{\rm even} = \rho_0 + \frac{\mathcal{G} M_{\rm BH} \rho_0}{c_s \sqrt{(c_s^2 - v_0^2) r^2 + v_0^2 z^2}} + \ldots, \qquad \rho_{\rm odd} = \frac{4 B \rho_0 \mathcal{G}^2 M_{\rm BH}^2 v_0 c_s z}{[(c_s^2 - v_0^2) r^2 + v_0^2 z^2]^{3/2}} + \ldots$$

1 remaining integration constant B

Velocity field (v)

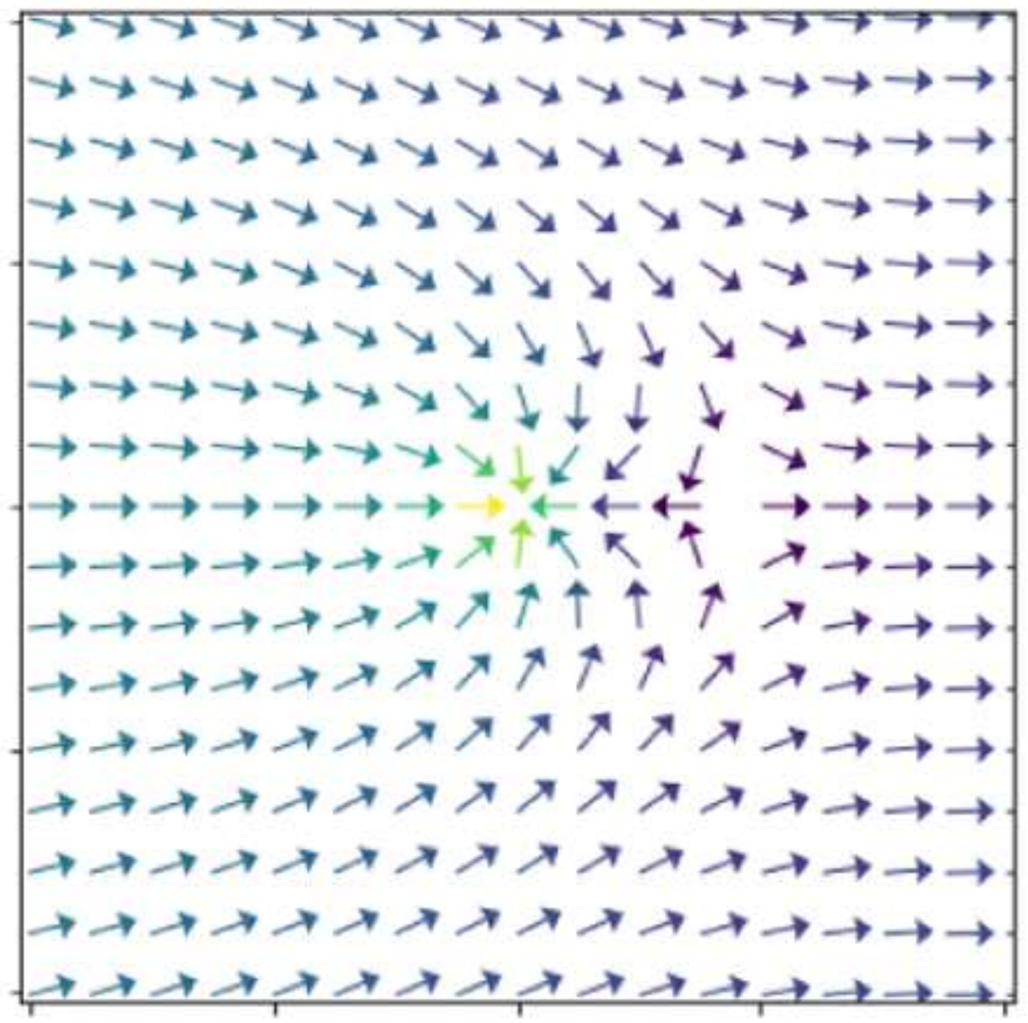

Conservation of mass: B in terms of $\dot{m}_{\rm BH}$

$$F_z = \frac{dp_z}{dt} = \mathcal{G} M_{\rm BH} \int_{V_{\rm out}} d\vec{r} \rho(\vec{r}) \frac{\vec{r} \cdot \vec{e}_z}{r^3} - \int_{\partial V_{\rm in}} d\vec{S} \cdot P \vec{e}_z - \int_{\partial V_{\rm in}} d\vec{S} \cdot \rho \vec{v} v_z .$$

Conservation of momentum: $\boxed{F_z = \frac{dp_z}{dt} = - \int_{S_{\rm out}} \overrightarrow{dS} \cdot \rho \vec{v} v_z - \int_{S_{\rm out}} \overrightarrow{dS} \cdot P \vec{e}_z}$

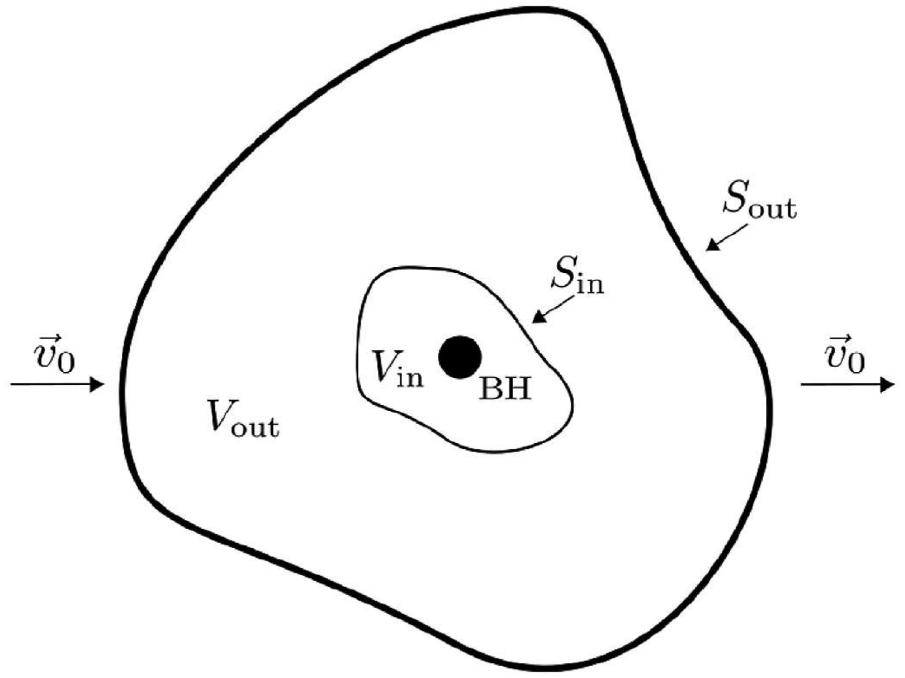

Only accretion drag force, no dynamical friction !

(d'Alembert paradox)

Velocity and Density Fields in Subsonic Regime

(Supersonic Regime Up-Coming!)

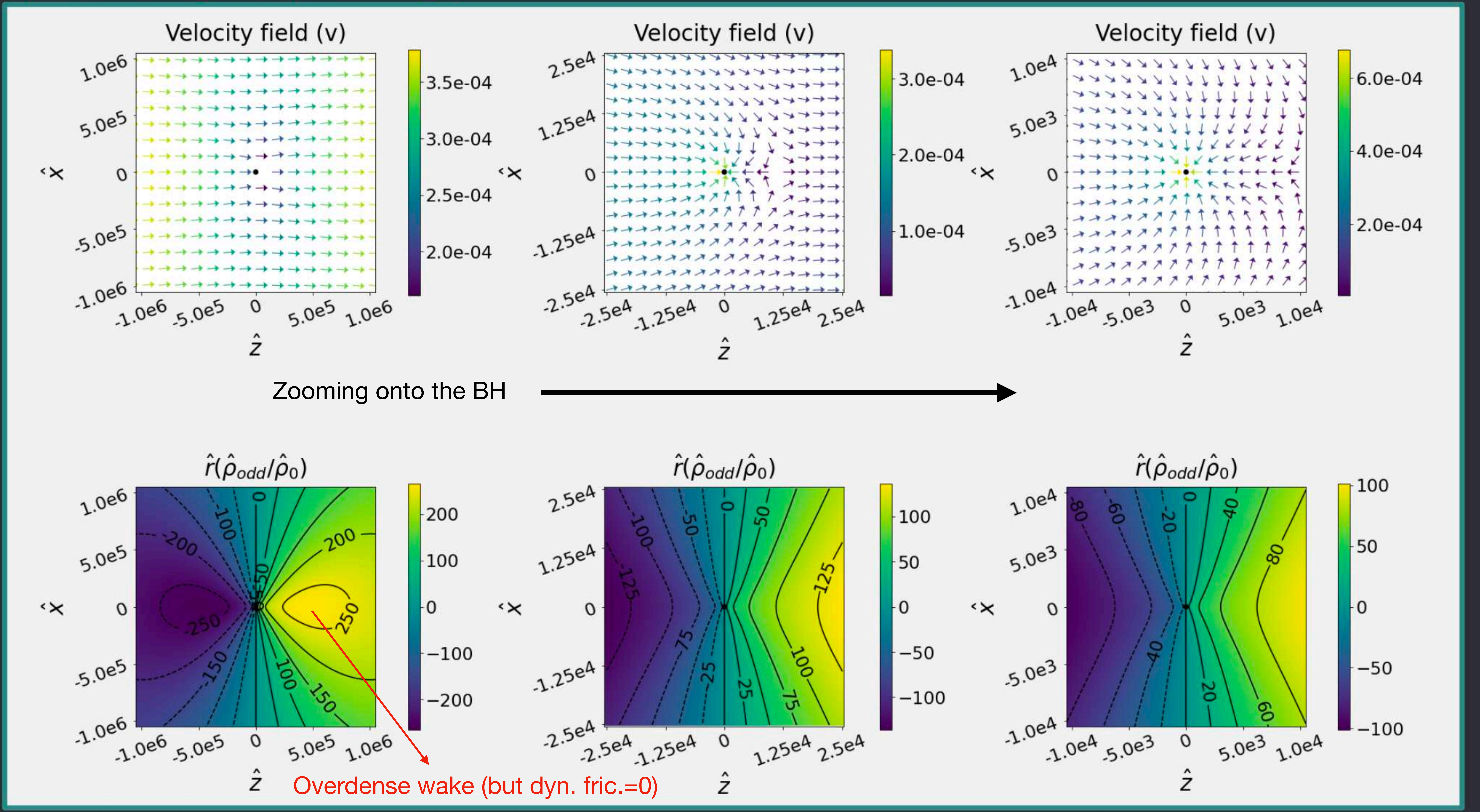

A. Boudon

IV- SUPERSONIC REGIME

A) Moderate Mach number

$$v_0 < \frac{c_{s0}^{2/3}}{(3F_\star)^{1/3}} : \quad \dot{M}_{\rm BH} = \frac{12\pi F_\star \rho_0 \mathcal{G}^2 M_{\rm BH}^2}{c_{s0}^2}$$

Max. radial accretion rate

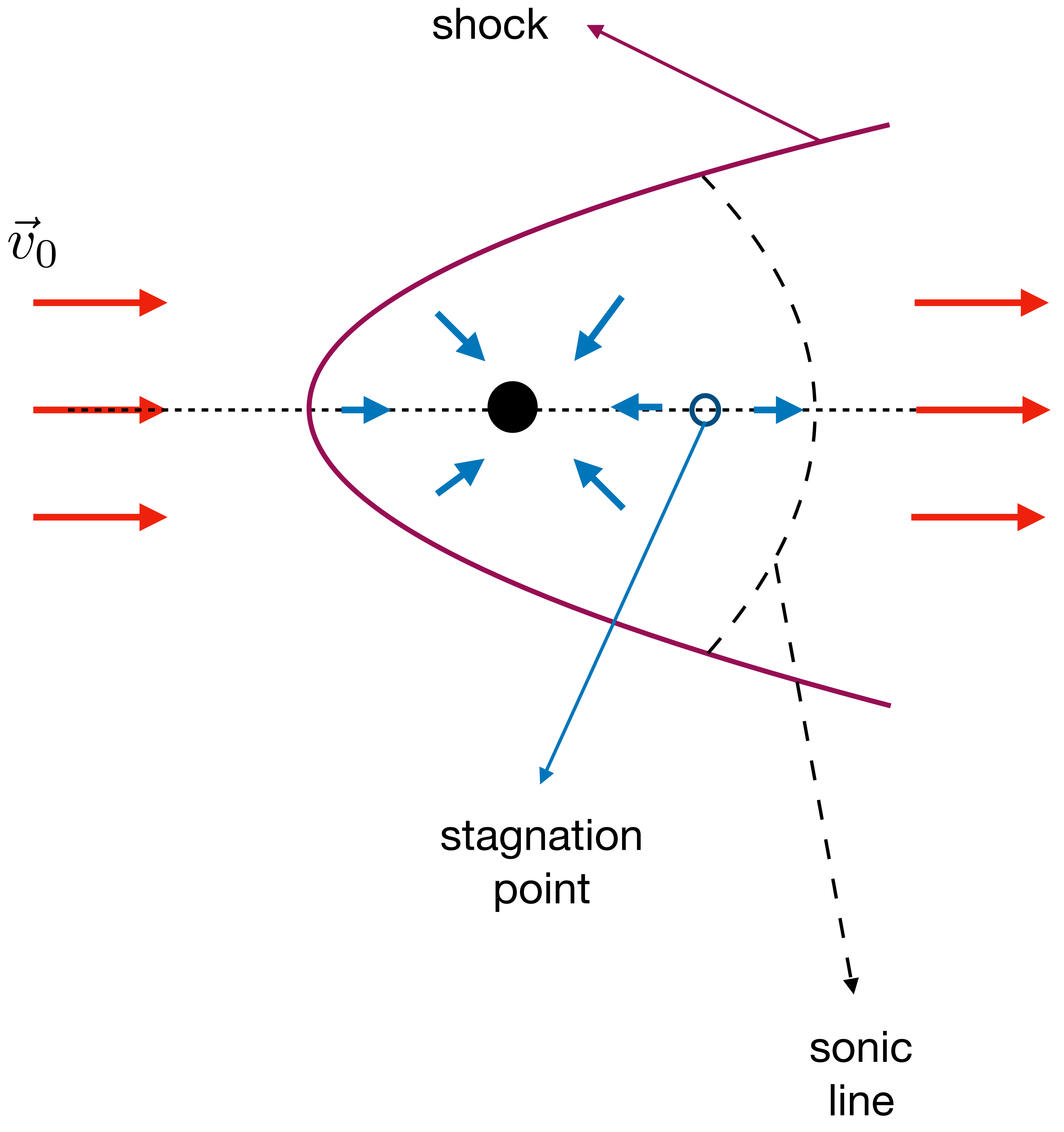

Shock front upstream of the BH, radial accretion close to the BH

3 maps of the Mach number (3 zoom-in onto the BH) and 1 map of the velocity field

AMRVAC simulations

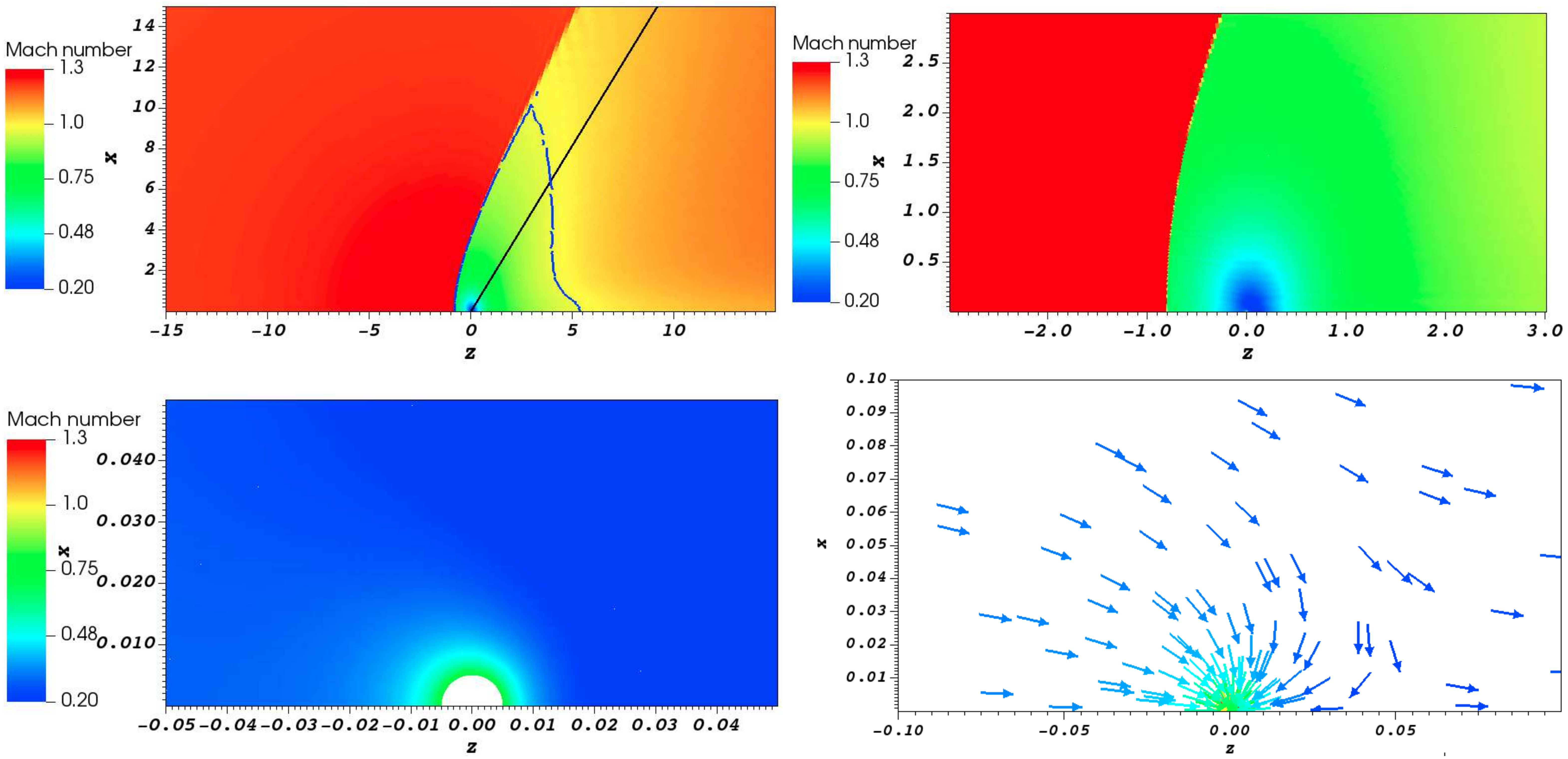

B) High Mach number

$$v_0 > \frac{c_{s0}^{2/3}}{(3F_\star)^{1/3}} : \quad \dot{M}_{\rm BH} = \frac{4\pi\rho_0\mathcal{G}^2M_{\rm BH}^2}{v_0^3} \quad \ll \quad \dot{M}_{\rm radial} = \frac{12\pi F_\star\rho_0\mathcal{G}^2M_{\rm BH}^2}{c_{s0}^2}$$

HL accretion rate

radial accretion rate

Hoyle-Lyttleton accretion mode

Edgar (2004)

Most of the accretion occurs through a narrow accretion column at the rear.

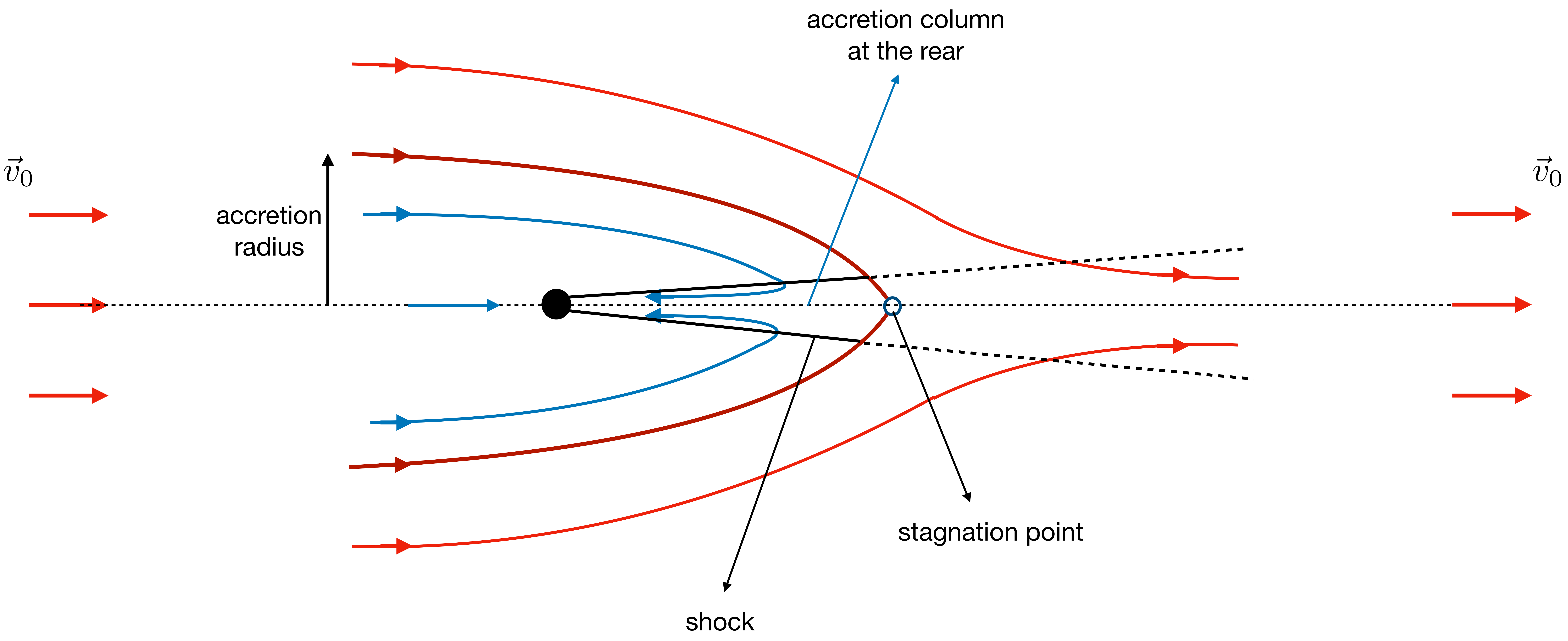

C) Analytical results using large-distance expansions and asymptotic matching

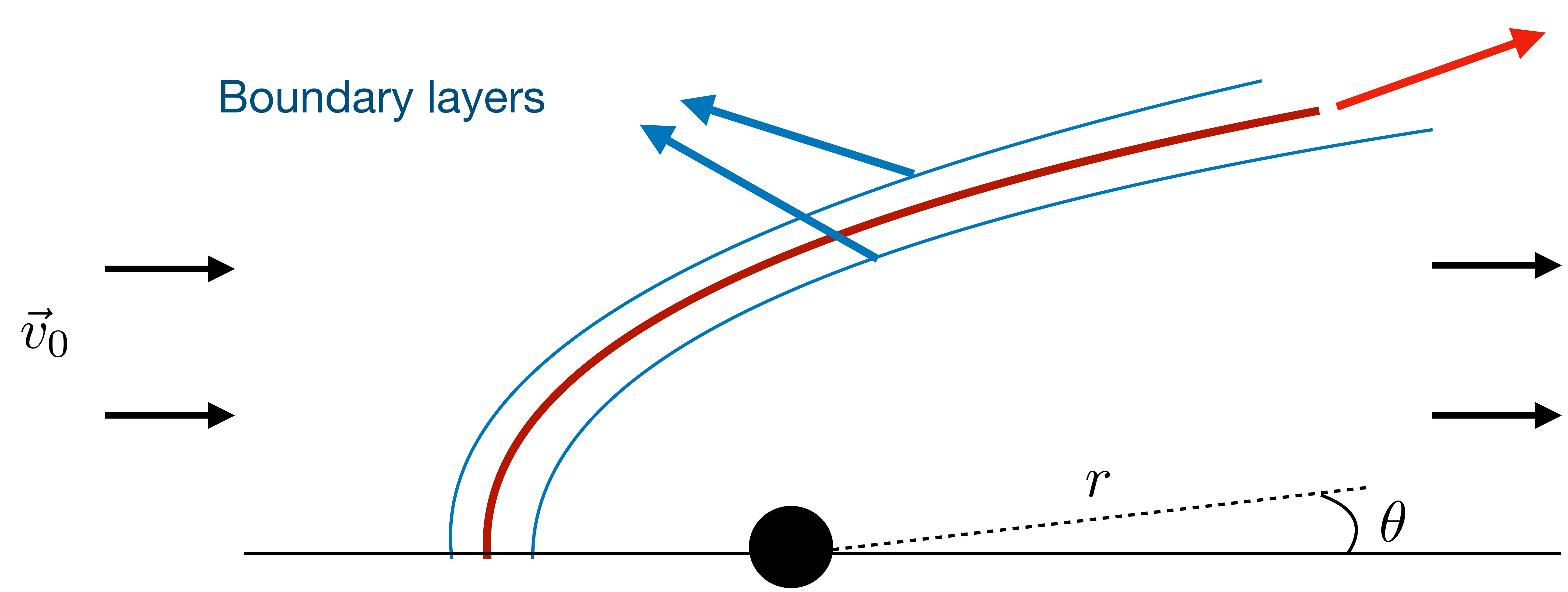

$$u = \cos\theta$$

$$\vec{v} = \hat{\nabla}\hat{\beta}$$

logarithmic terms

In the bulk, upstream: $$\hat{\beta} = v_0 r u + a\ln(r) + f_0(u) + \frac{f_1(u)}{r} + \ldots$$

In the bulk, downstream: $$\hat{\beta} = v_0 r u + a\ln(r) + f_0(u) + \frac{f_1(u) + g_1(u)\ln(r)}{r} + \ldots$$

In the boundary layers: $$\hat{\beta} = v_0 \hat{r} u - \frac{1}{2v_0}\ln[\hat{r}(1-u_c)] + \frac{F_1(U)}{\hat{r}^{1/3}} + \frac{F_2(U)}{\hat{r}^{2/3}} + \frac{F_3(U) + \mathcal{F}_3(U)\ln\hat{r}}{\hat{r}} + \ldots$$

anomalous exponents

$$U = \hat{r}^{2/3}[u - u_s(\hat{r})]$$

D) Dynamical friction

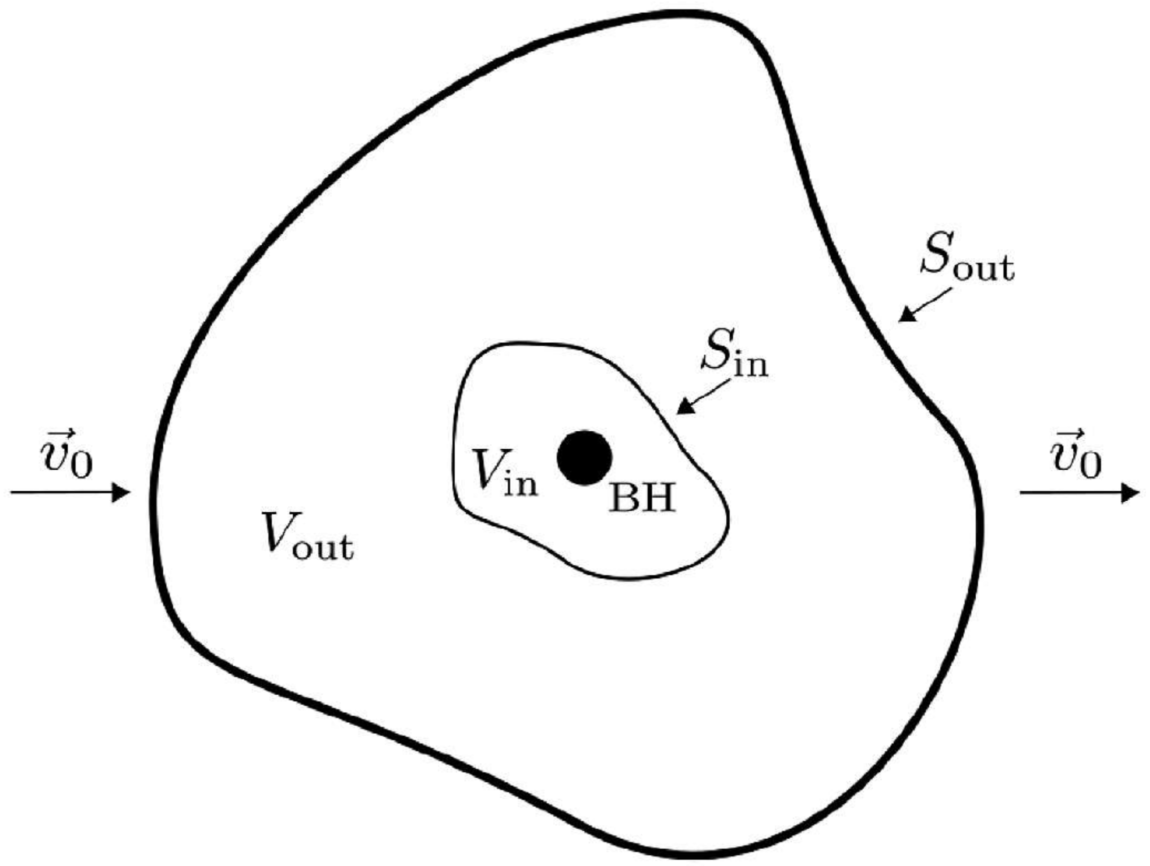

Again, use conservation of mass and momentum:

$$F_z = \dot{M}_{\text{BH}} v_0 + \frac{8\pi\rho_0 \mathcal{G}^2 M_{\text{BH}}^2}{3v_0^2} \ln\left(\frac{r_a}{r_{\text{UV}}}\right)$$

Accretion drag

Dynamical friction

2/3 smaller than Chandrasekhar's expression

UV cutoff greater than b_min and set by the self-interactions:

$$r_{\text{UV}} = 6\sqrt{\frac{2}{e}} \frac{\mathcal{G} m_{\text{BH}}}{c_s^2} \left(\frac{c_s}{v_{\text{BH}}}\right)^{3/2}$$

$$r_{\text{UV}} \simeq \sqrt{\frac{18}{e}} r_{\text{sg}} \mathcal{M}_0^{-3/2} \qquad r_{\text{sg}} = \frac{r_s}{c_{s0}^2}, \quad c_{s0}^2 = \frac{\rho_0}{\rho_a}$$

Gravitational Waves emitted by a BH binary inside a SFDM soliton

I- Additional forces on the BHs due to the dark matter environment

Gravity of the dark matter cloud:

$$m_{\rm BH}\dot{\mathbf{v}}_{\rm BH}|_{\rm halo} = -\frac{4\pi}{3}\mathcal{G}m_{\rm BH}\rho_0(\mathbf{x}-\mathbf{x}_0)$$

Accretion drag:

$$m_{\rm BH}\dot{\mathbf{v}}_{\rm BH}|_{\rm acc} = -\dot{m}_{\rm BH}\mathbf{v}_{\rm BH}$$

Dynamical friction:

$$m_{\rm BH}\dot{\mathbf{v}}_{\rm BH}|_{\rm df} = -\frac{8\pi\mathcal{G}^2 m_{\rm BH}^2\rho_0}{3v_{\rm BH}^3}\ln\left(\frac{r_{\rm IR}}{r_{\rm UV}}\right)\mathbf{v}_{\rm BH}$$

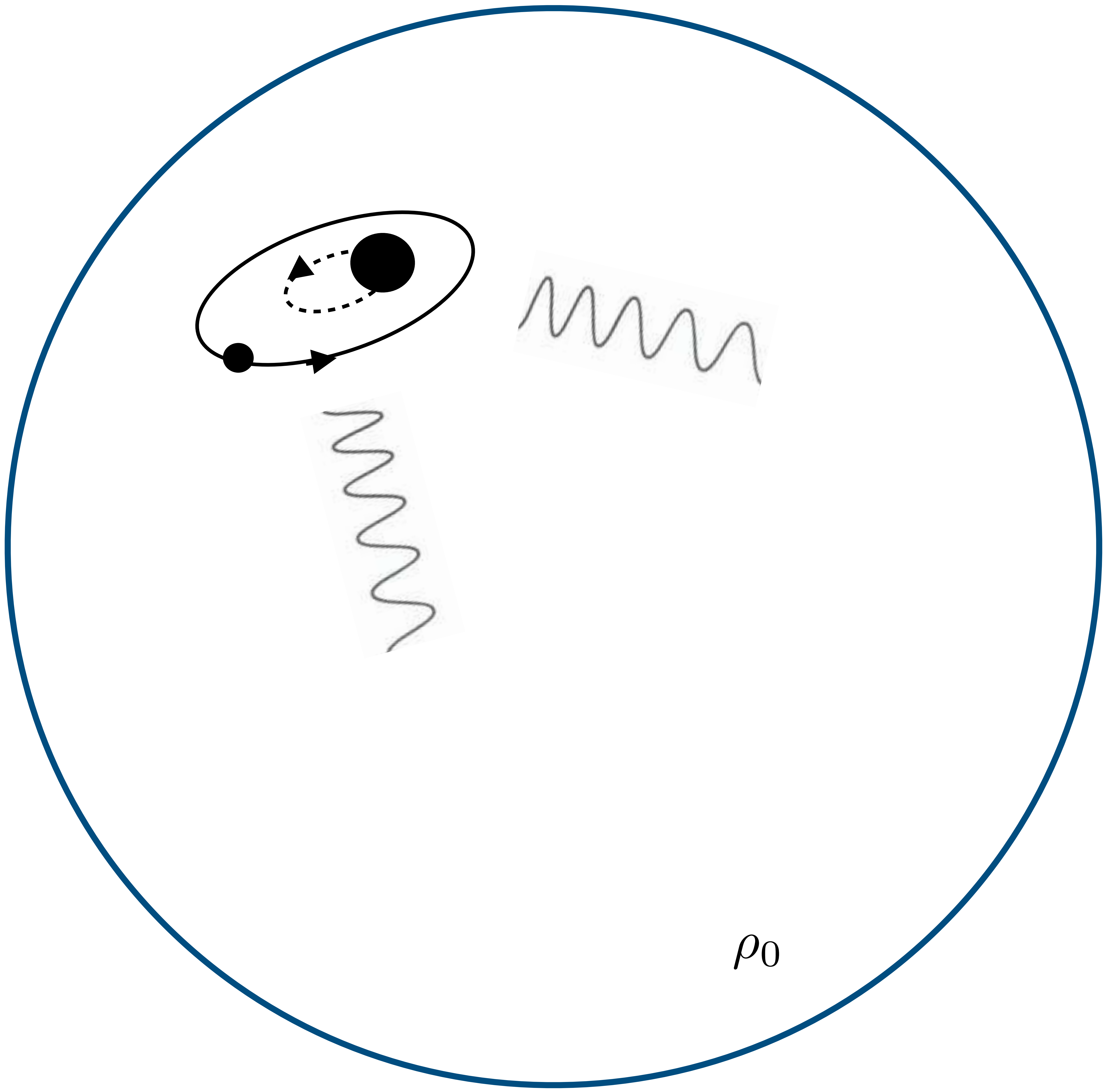

II- Decay of the orbital radius

$$\langle \dot{a} \rangle = \langle \dot{a} \rangle_{\rm acc} + \langle \dot{a} \rangle_{\rm df} + \langle \dot{a} \rangle_{\rm gw}$$

$$\langle \dot{a} \rangle_{\rm gw} = -\frac{64\nu \mathcal{G}^3 m^3}{5c^5 a^3}\left(1 - \frac{4\pi\rho_0 a^3}{3m}\right)$$

Correction due to the halo bulk gravity

$$\langle \dot{a} \rangle_{\rm acc} = -aA_{\rm acc} - a\left(\frac{a}{\mathcal{G}m}\right)^{3/2} B_{\rm acc}$$

Accretion drag

$$\langle \dot{a} \rangle_{\rm df} = -a\left(\frac{a}{\mathcal{G}m}\right)^{3/2}\left[B_{\rm df} + C_{\rm df}\ln\left(\sqrt{\frac{\mathcal{G}m}{a}}\frac{1}{c_s}\right)\right]$$

Dynamical friction

III- Phase of the GW waveform

GW frequency: $$\mathfrak{f} = \frac{1}{\pi}\sqrt{\frac{\mathcal{G}m}{a^3}}\left(1 + \frac{2\pi\rho_0 a^3}{3m}\right)$$

Frequency drift: $$\dot{\mathfrak{f}} = \frac{1}{\pi}\sqrt{\frac{\mathcal{G}m}{a^3}}\left(\frac{\dot{m}}{2m} - \frac{3\dot{a}}{2a}\right) + \mathcal{G}\rho_0\left(\frac{a^3}{\mathcal{G}m}\right)^{1/2}\frac{\dot{a}}{a}$$

Phase: $\Phi(t) = 2\pi \int d\mathfrak{f}\,(\mathfrak{f}/\dot{\mathfrak{f}})$ Time: $t = \int d\mathfrak{f}\,(1/\dot{\mathfrak{f}})$

Fourier transform of the GW signal: $\boxed{\tilde{h}(f) = \mathcal{A}(f)e^{i\Psi(f)}}$

Phase: $$\boxed{\Psi(f) = 2\pi f t_c - \Phi_c - \frac{\pi}{4} + \Psi_{gw} + \Psi_{halo} + \Psi_{acc} + \Psi_{df}}$$

DM corrections

$$\Psi_{gw} = \frac{3}{128}\left(\frac{\pi\mathcal{G}\mathcal{M}f}{c^3}\right)^{-5/3}\left[1 + \frac{20}{9}\left(\frac{743}{336} + \frac{11}{4}\nu\right)\left(\frac{\pi\mathcal{G}mf}{c^3}\right)^{2/3}\right]$$ O + 1 PN

Ψ_{halo} -3 PN

Ψ_{acc} -4.5 / -5.5 PN

Ψ_{df} -5.5 PN

$$\Psi_{\rm halo} = \frac{25\pi}{924}\frac{\rho_0 \mathcal{G}^3\mathcal{M}^2}{c^6}(\pi\mathcal{G}\mathcal{M}f/c^3)^{-11/3}$$

$$\begin{aligned}\Psi_{\rm acc} = &-\frac{25\pi\mathcal{G}^3\mathcal{M}^2\rho_0}{38912c^6}\left(\frac{\pi\mathcal{G}\mathcal{M}f}{c^3}\right)^{-16/3}\sum_{i=1}^{2}\Theta(f>f_{{\rm acc},i})\frac{m_i^3}{\mu^2 m}\left(3+2\frac{m_i^2}{m\mu}\right)\\
&-\frac{75\pi F_\star \nu^{2/5}\mathcal{G}^3\mathcal{M}^2\rho_a}{26624c^6}\left(\frac{\pi\mathcal{G}\mathcal{M}f}{c^3}\right)^{-13/3}\sum_{i=1}^{2}\Theta(f<f_{{\rm acc},i})\left(3+2\frac{m_i^2}{m\mu}\right)\left[1-\left(\frac{f}{f_{{\rm acc},i}}\right)^{13/3}+\frac{13}{19}\left(\frac{f}{f_{{\rm acc},i}}\right)^{16/3}\right]\end{aligned}$$

$$\begin{aligned}\Psi_{\rm df} = &\frac{875\pi\mathcal{G}^3\mathcal{M}^2\rho_0}{11829248c^6}\left(\frac{\pi\mathcal{G}\mathcal{M}f}{c^3}\right)^{-16/3}\sum_{i=1}^{2}\frac{m_i^3}{\mu^2 m}\Theta(f^-_{{\rm df},i}<f^+_{{\rm df},i})\Bigg\{\Theta(f^-_{{\rm df},i}<f<f^+_{{\rm df},i})\left[1+\frac{304}{105}\ln\frac{f}{f^+_{{\rm df},i}}-\frac{361}{105}\left(\frac{f}{f^+_{{\rm df},i}}\right)^{16/3}+\frac{256}{105}\left(\frac{f}{f^+_{{\rm df},i}}\right)^{19/3}\right]\\
&+\Theta(f<f^-_{{\rm df},i})\left[-\frac{361}{105}\left(\frac{f}{f^+_{{\rm df},i}}\right)^{16/3}+\frac{361}{105}\left(\frac{f}{f^-_{{\rm df},i}}\right)^{16/3}+\frac{5776}{315}\left(\frac{f}{f^-_{{\rm df},i}}\right)^{16/3}\ln\frac{f^-_{{\rm df},i}}{f^+_{{\rm df},i}}+\frac{256}{105}\left(\frac{f}{f^+_{{\rm df},i}}\right)^{19/3}-\frac{256}{105}\left(\frac{f}{f^-_{{\rm df},i}}\right)^{19/3}-\frac{4864}{315}\left(\frac{f}{f^-_{{\rm df},i}}\right)^{19/3}\ln\frac{f^-_{{\rm df},i}}{f^+_{{\rm df},i}}\right]\Bigg\}\end{aligned}$$

IV- Fisher matrix analysis

$$\Gamma_{ij} = \frac{(\mathrm{SNR})^2}{\int_{f_{\min}}^{f_{\max}} \frac{df}{S_n(f)} f^{-7/3}} \int_{f_{\min}}^{f_{\max}} \frac{df}{S_n(f)} f^{-7/3} \frac{\partial \Psi}{\partial \theta_i} \frac{\partial \Psi}{\partial \theta_j}$$

Parameters: $\{\theta_i\} = \{t_c, \Phi_c, \ln(m_1), \ln(m_2), \rho_0, \rho_a\}$

ρ_0 halo bulk density

$$\rho_a = \frac{4m^4}{3\lambda_4}$$

V- Region in the parameter space that can be detected

ρ_0 halo bulk density

LISA:

BHL accretion mode

Plane (ρ_0, ρ_a)

$$\rho_a = \frac{4m^4}{3\lambda_4}$$

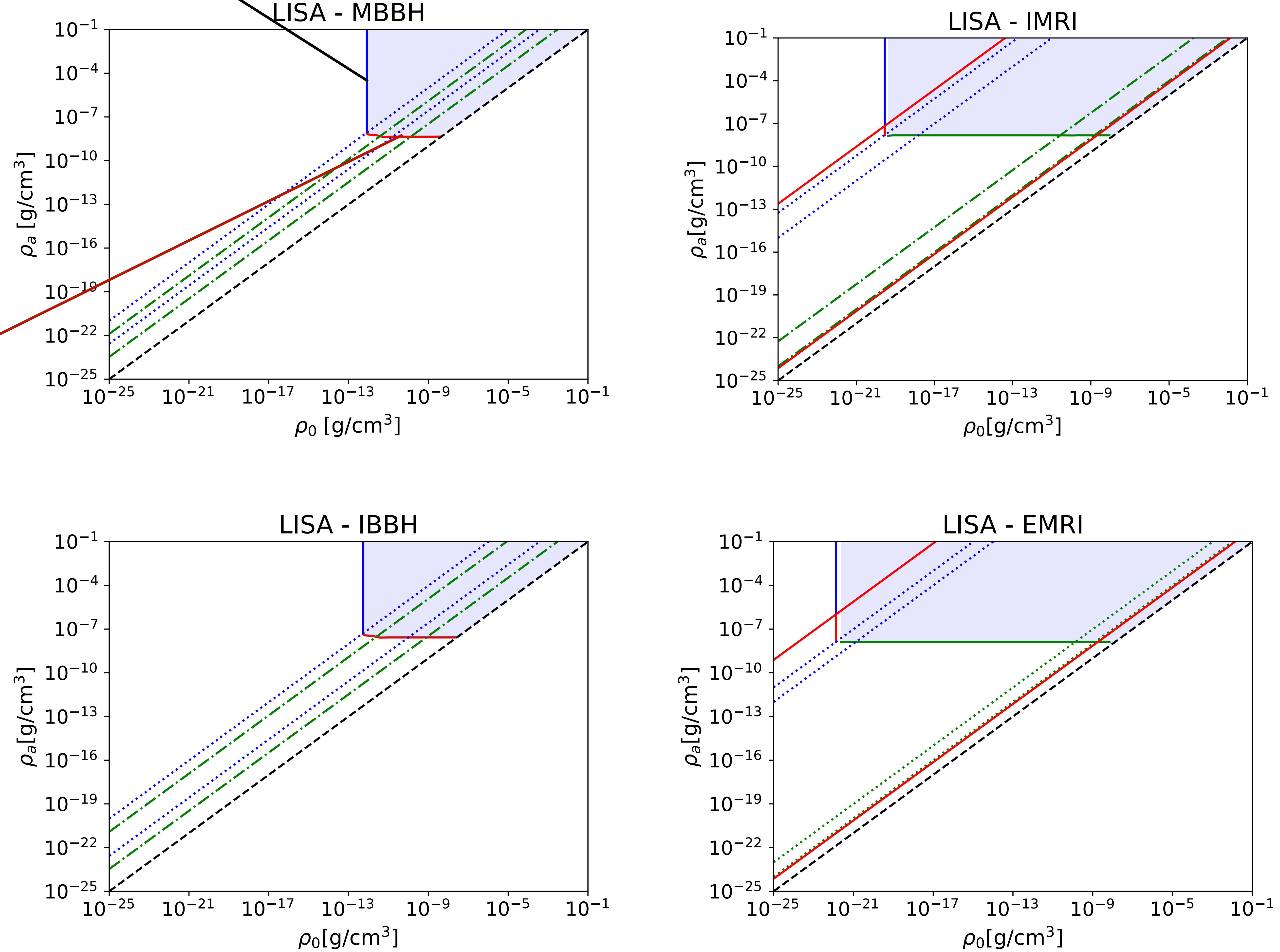

Max. radial accretion mode

$$\frac{\rho_a}{\rho_0} = \frac{c^2}{c_s^2} \geq 1$$

Event \ Properties	m_1 ($M_\odot$)	m_2 ($M_\odot$)	χ_1	χ_2	$\chi_{\rm eff}$
MBBH	10^6	5×10^5	0.9	0.8	0.87
IBBH	10^4	5×10^3	0.3	0.4	0.33
IMRI	10^4	10	0.8	0.5	0.80
EMRI	10^5	10	0.8	0.5	0.80

$$1\ M_\odot/\text{pc}^3 = 6.7 \times 10^{-23}\ \text{g/cm}^3$$

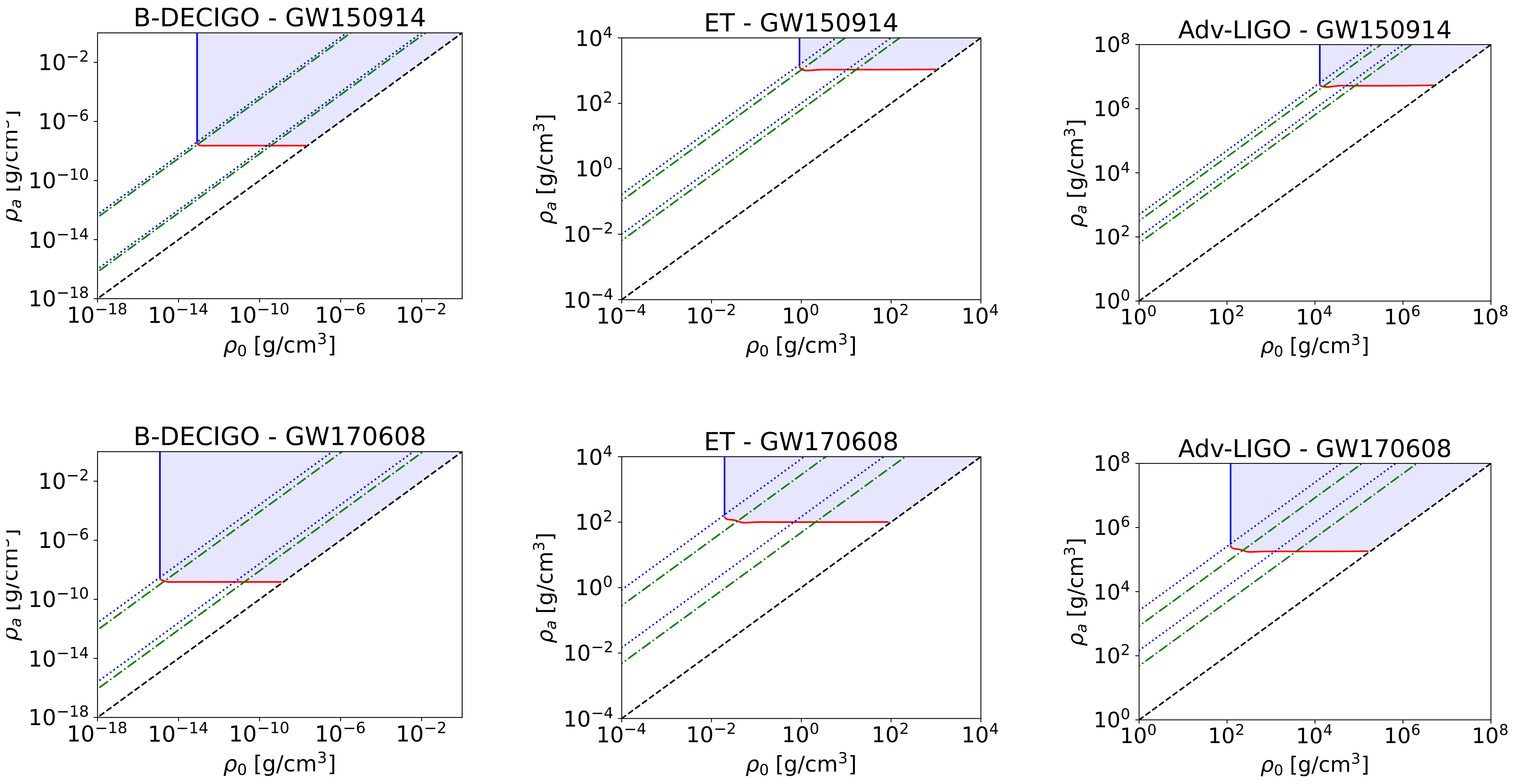

ρ_0 halo bulk density

$$\rho_a = \frac{4m^4}{3\lambda_4}$$

Event \ Detector	LISA	B-DECIGO	ET	Adv-LIGO
MBBH	$\rho_0 > 8 \times 10^{-13}$ g/cm^3 $\rho_a > 5 \times 10^{-9}$ g/cm^3	× ×	× ×	× ×
IBBH	$\rho_0 > 5 \times 10^{-13}$ g/cm^3 $\rho_a > 3 \times 10^{-8}$ g/cm^3	× ×	× ×	× ×
IMRI	$\rho_0 > 3 \times 10^{-20}$ g/cm^3 $\rho_a > 2 \times 10^{-8}$ g/cm^3	× ×	× ×	× ×
EMRI	$\rho_0 > 10^{-22}$ g/cm^3 $\rho_a > 10^{-8}$ g/cm^3	× ×	× ×	× ×
GW150914	× ×	$\rho_0 > 8 \times 10^{-14}$ g/cm^3 $\rho_a > 2 \times 10^{-8}$ g/cm^3	$\rho_0 > 0.9$ g/cm^3 $\rho_a > 10^3$ g/cm^3	$\rho_0 > 10^4$ g/cm^3 $\rho_a > 5 \times 10^6$ g/cm^3
GW170608	× ×	$\rho_0 > 10^{-15}$ g/cm^3 $\rho_a > 2 \times 10^{-9}$ g/cm^3	$\rho_0 > 0.02$ g/cm^3 $\rho_a > 101$ g/cm^3	$\rho_0 > 120$ g/cm^3 $\rho_a > 2 \times 10^5$ g/cm^3

Critical density:

$$\rho_c \sim 10^{-29} \mathrm{g/cm^3} \sim 10^{-7} M_\odot/\mathrm{pc}^3$$

Solar neighborhood:

$$\rho_{\mathrm{DM}} \sim 1\ M_\odot/\mathrm{pc}^3 \sim 7 \times 10^{-23}\ \mathrm{g/cm^3}$$

Baryonic density in thick disks:

$$\rho_{\mathrm{b}} \lesssim 10^{-7} \mathrm{g/cm^3}$$

Plane $(m_{\rm DM}, \lambda_4)$

Models with coupling below this line can be detected

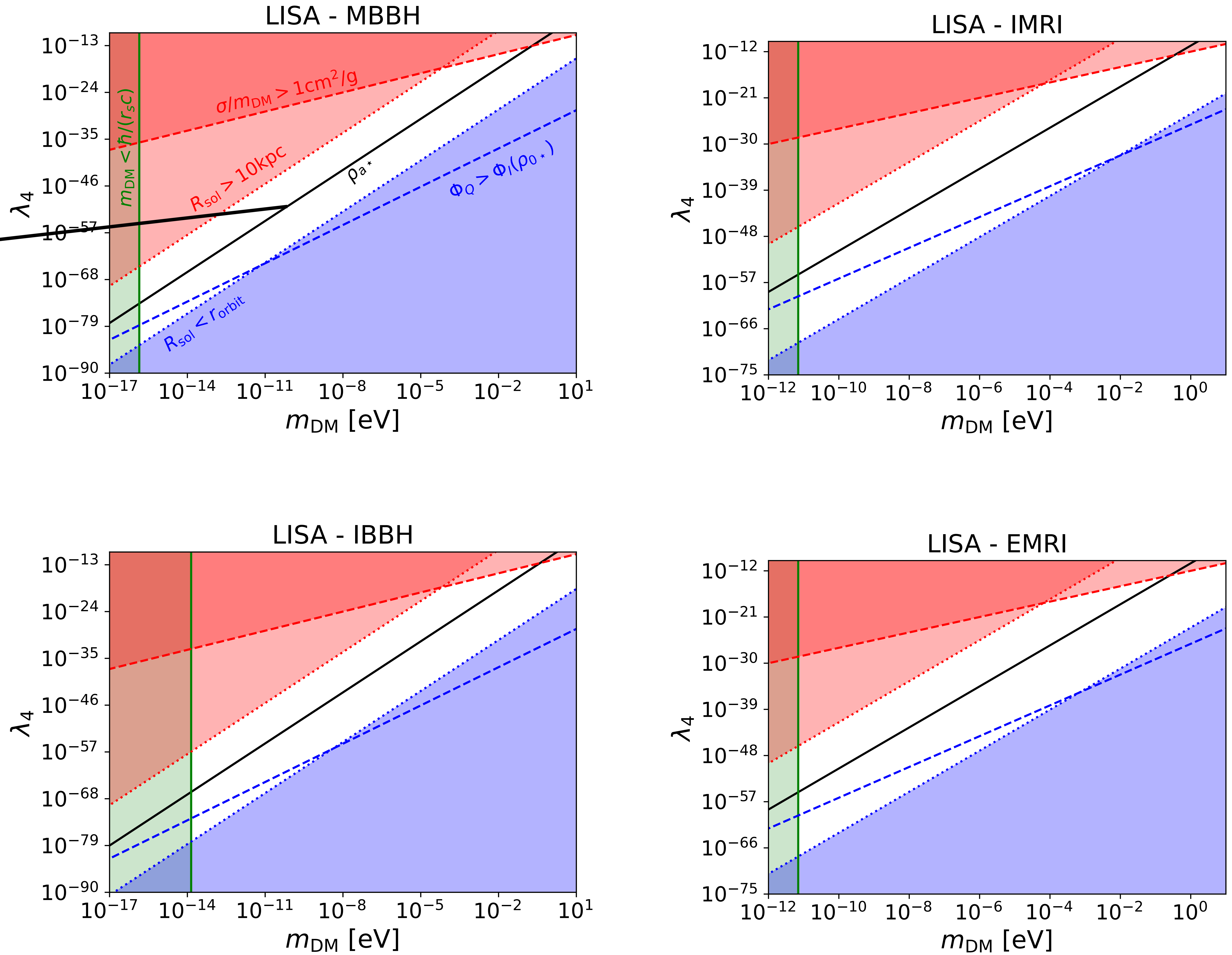

Plane $(m_{\rm DM}, R_{\rm sol})$

$$R_{\rm sol} = \pi\sqrt{\frac{3\lambda_4}{2}\frac{M_{\rm Pl}}{m^2}}$$

$$R_{\rm sol} = \sqrt{\frac{\pi}{4\mathcal{G}\rho_a}}$$

Radius of the scalar cloud (soliton)

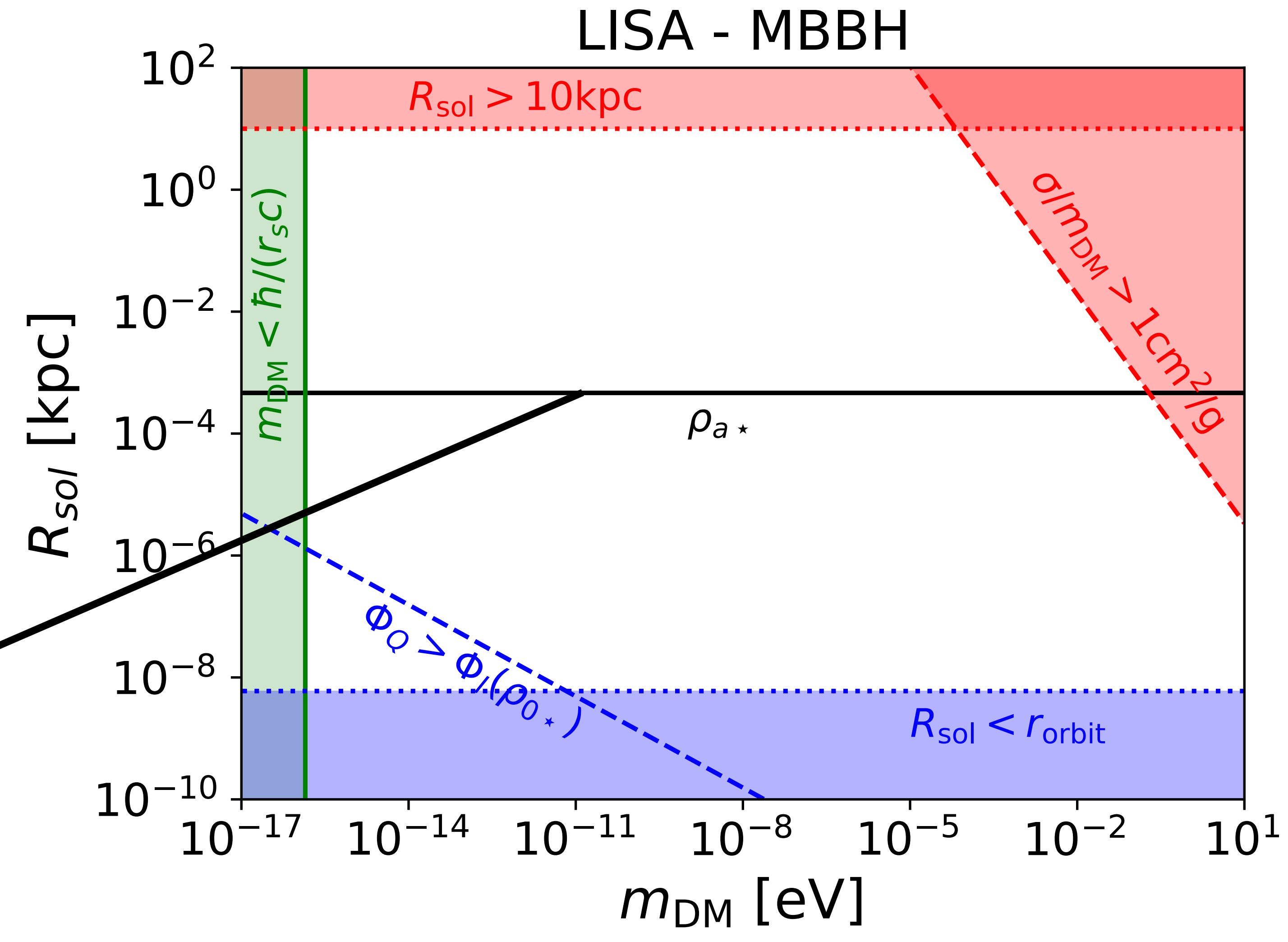

Models with soliton radius below this line can be detected

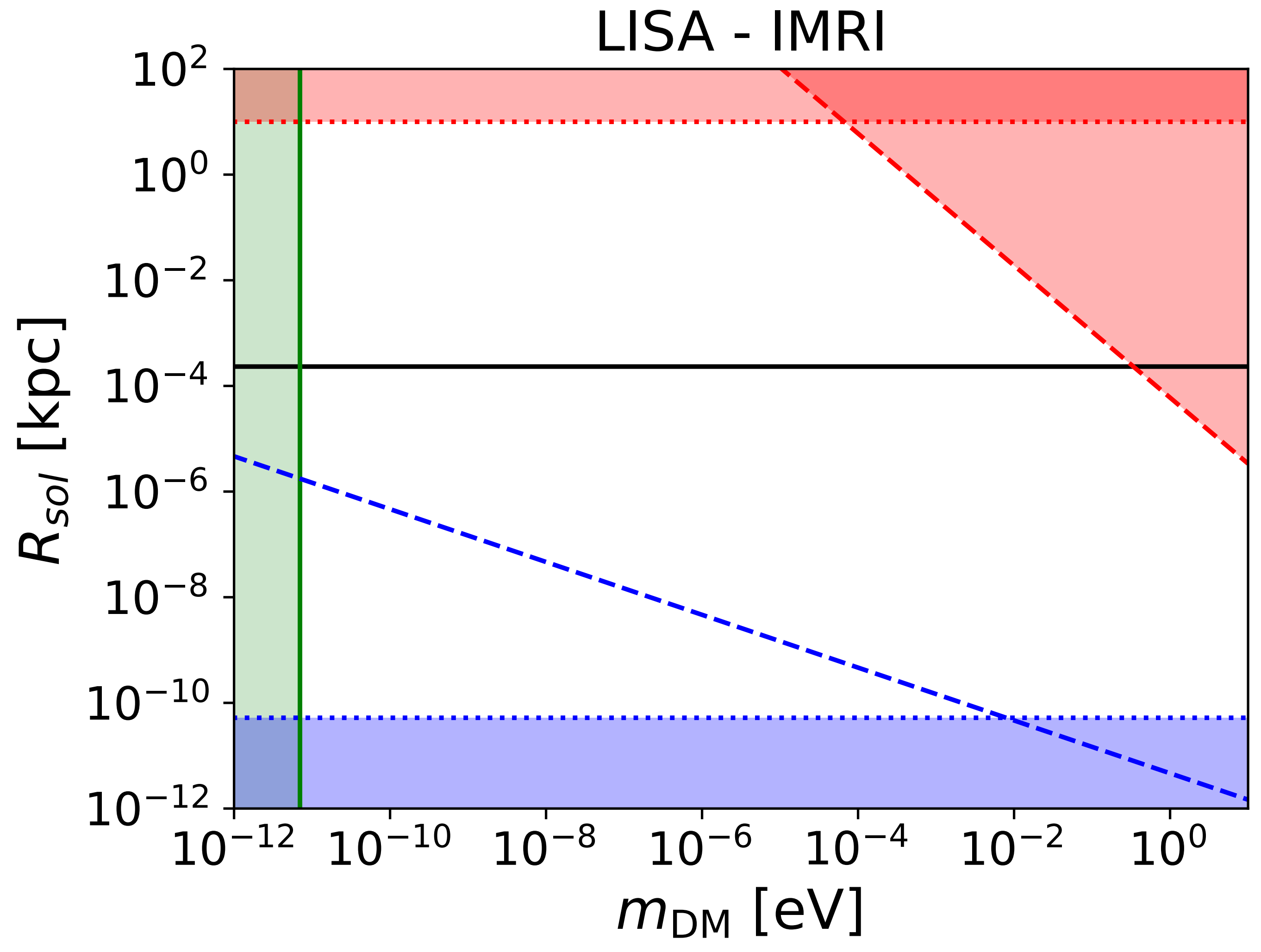

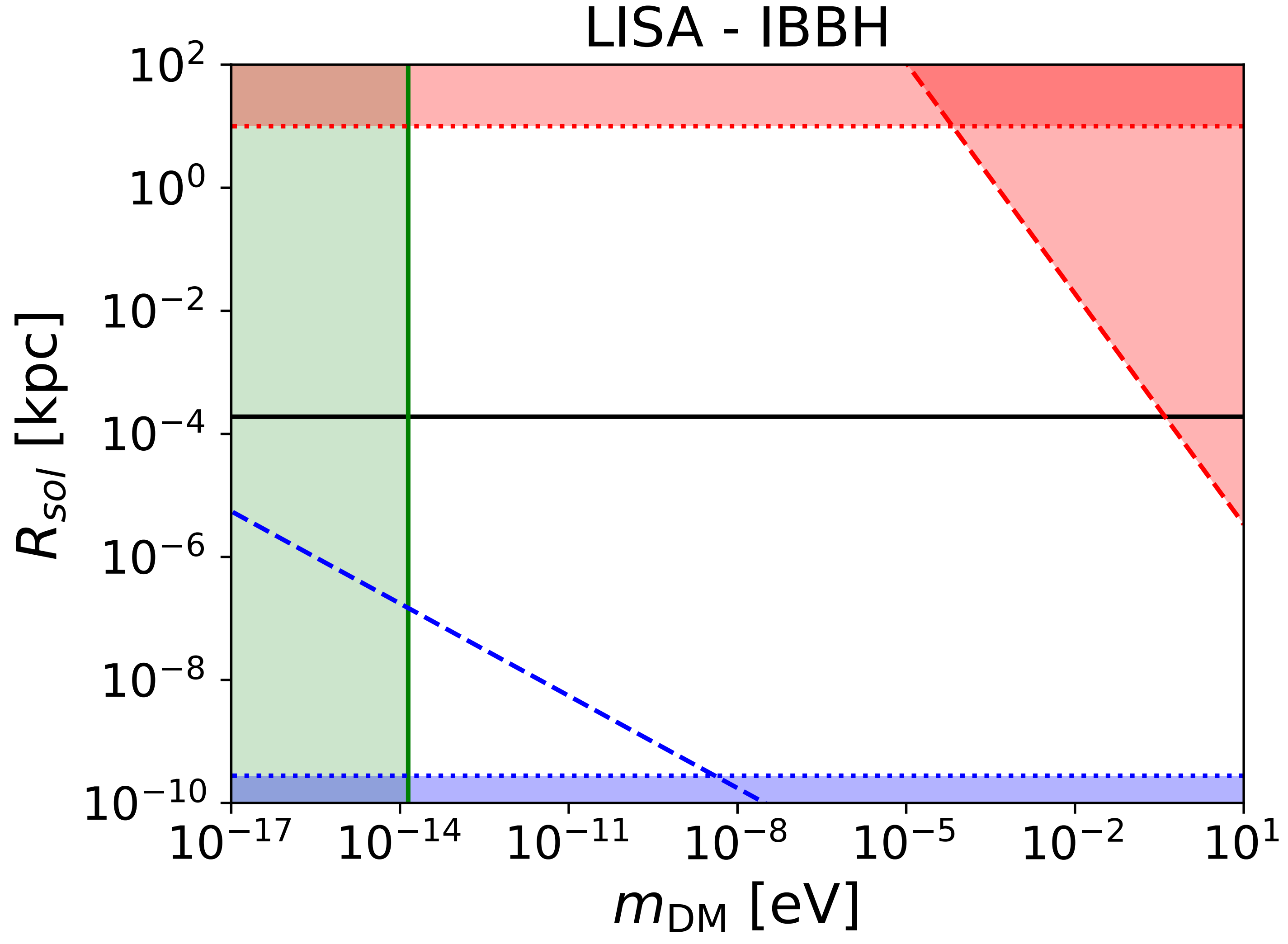

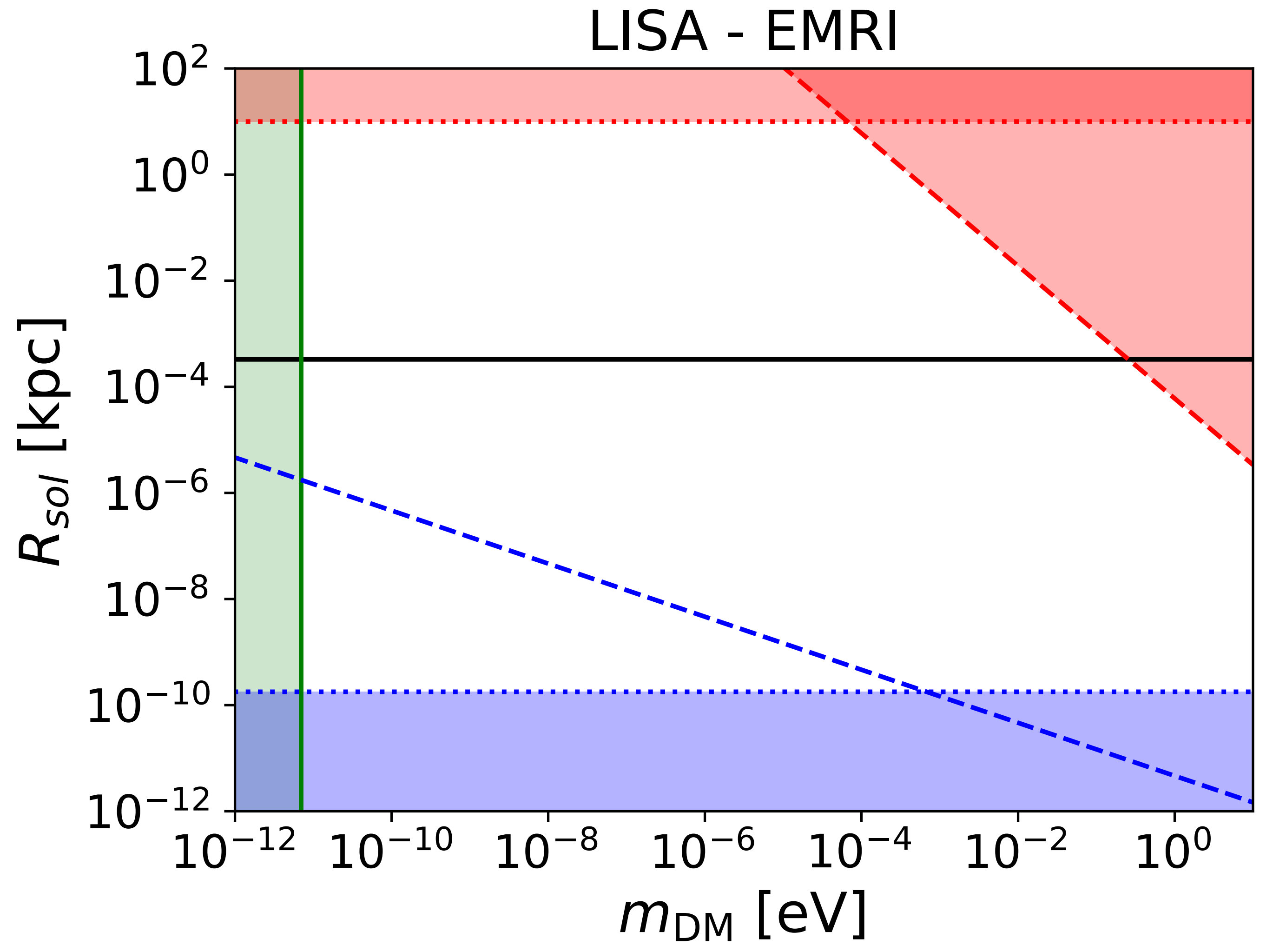

Impact of the time-dependent DM gravitational potential on GW

A) Frequency shift

Khmelnitsky & Rubakov. 2013

(shift of PTA time delays)

fast oscillations

$$\phi(\vec{x},t) = A(\vec{x},t)\cos[mt + \alpha(\vec{x},t)]$$

slow variations on astrophysical scales

The density field has a subleading oscillatory component: $\rho_{DM} = \rho_0 + \rho_{\rm osc}$

$$T_{\mu\nu} = \partial_\mu\phi\,\partial_\nu\phi - \frac{1}{2}g_{\mu\nu}\left((\partial\phi)^2 - m^2\phi^2\right)$$

$$\rho_0 = \frac{1}{2}m^2A^2 \qquad \rho_{\rm osc} \sim (\nabla\phi)^2 \sim k^2\phi^2 \sim \frac{k^2}{m^2}\rho_0 < v^2\rho_0 \qquad \lambda_{\rm dB} = \frac{2\pi}{mv}, \quad k < \frac{2\pi}{\lambda_{\rm dB}}$$

The gravitational potential also has a subleading oscillatory component:

$$\boxed{\Psi_N(\vec{x},t) = \Psi_0(\vec{x}) + \Psi_{\rm osc}(\vec{x})\cos[\omega t + 2\alpha(\vec{x})]}$$

$$\omega = 2m$$

$$\nabla^2\Psi_0 = 4\pi\mathcal{G}\rho_0 \qquad \Psi_{\rm osc} = \pi\frac{\mathcal{G}\rho}{m^2}$$

In the optical approximation, as for the Sachs-Wolfe effect for CMB photons, the gravitational potential along the line of sight leads to a frequency shift of the GW signal:

$$\boxed{\frac{\Delta f}{f} = \Psi_N(\vec{x}_e, t_e) - \Psi_N(\vec{x}, t)}$$

emission reception (negligible)

$$f \gtrsim \omega \qquad \text{whence } m_\phi < \left(\frac{f_{\rm min}}{1 \text{ Hz}}\right) 3 \times 10^{-16} \text{ eV}$$

The integrated Sachs-Wolfe effect is neglected (many oscillations along the l.o.s.): $\lambda = \frac{c}{f} \ll \frac{2\pi}{k}$

B) GW phase shift

GW signal: $h(t) = A(t) \cos[\Phi(t)]$

Phase and time related to the frequency drift: $\Phi = 2\pi \int df \frac{f}{\dot{f}}, \qquad t = \int df \frac{1}{\dot{f}}$

Going to Fourier space: $$\boxed{\tilde{h}(f) = \int dt\, e^{i2\pi f t} h(t) = A(f) e^{i\psi(f)}}$$

Saddle-point approximation: $A(f) \propto f^{-7/6}, \qquad \psi(f) = 2\pi f t_\star - \Phi(t_\star) - \pi/4, \qquad f(t_\star) = f.$

At leading order, the frequency drift is due to the emission of GW:

$$\bar{\psi}(f) = 2\pi f t_c - \Phi_c - \frac{\pi}{4} + \psi_{\rm GW}(f),$$

$$\psi_{\rm GW}(f) = \frac{3}{128}\left(\frac{\pi \mathcal{G}\mathcal{M} f}{c^3}\right)^{-5/3}\left[1 + \left(\frac{3715}{756} + \frac{55\nu}{9}\right)\left(\frac{\pi \mathcal{G} M f}{c^3}\right)^{2/3}\right]$$

$$M = m_1 + m_2, \quad \nu = m_1 m_2/M^2, \quad \mathcal{M} = \nu^{3/5} M$$

The DM gravitational potential gives a correction: $\Delta\psi(f) = 2\pi \int_{\bar{t}_\star}^{t_c} dt \bar{f} \Psi.$

The contribution from the constant part is degenerate with the leading GW contribution: $\Delta\psi_0(f) = \frac{\Psi_0}{16}\left(\frac{\pi \mathcal{G}\mathcal{M} f}{c^3}\right)^{-5/3}$

The contribution from the oscillatory part reads: $\Delta\psi_{\rm osc}(f) = \Psi_{\rm osc} 2\pi \left(\frac{5}{256\pi}\right)^{3/8}\left(\frac{\pi \mathcal{G}\mathcal{M}\omega}{c^3}\right)^{-5/8} {\rm Re}[e^{i(5\pi/16+\theta-\omega t_c)}\gamma(5/8, -iy)]$

$$y = \omega(t_c - \bar{t}_\star) = \frac{m_\phi}{m_\star}, \qquad m_\star = f\frac{128\pi}{5}\left(\frac{\pi \mathcal{G}\mathcal{M} f}{c^3}\right)^{5/3}$$

Low scalar mass, degeneracy with leading GW term

$$m_\phi \ll m_\star: \ \Delta\psi_{\rm osc}(f) = \frac{\Psi_{\rm osc}}{16}\left(\frac{\pi \mathcal{G}\mathcal{M} f}{c^3}\right)^{-5/3}\cos(\omega t_c - \theta)$$

Large scalar mass, degeneracy with constant factor Φ_c

$$m_\phi \gg m_\star: \ \Delta\psi_{\rm osc}(f) = \Psi_{\rm osc}\Gamma(5/8) 2\pi \left(\frac{5}{256\pi}\right)^{3/8}\left(\frac{\pi \mathcal{G}\mathcal{M}\omega}{c^3}\right)^{-5/8}\cos(\omega t_c - \theta - 5\pi/16)$$

Probe scalar masses $m \sim m_\star,$ $\quad m_\star \ll f \ \text{ for } \ (\mathcal{G}\mathcal{M} f/c^3) \ll 1, \quad R_{\rm Sch} \ll \lambda$

C) Comparison with dynamical friction

In many cases (CDM, supersonic motion in fluids or SFDM), the drag force on a BH moving within a medium takes the form of the Chandrasekhar result:

$$m_i \dot{\vec{v}}_i = -\frac{4\pi\mathcal{G}^2 m_i^2 \rho}{v_i^3} \Lambda \vec{v}_i,$$

This gives a correction to the frequency drift and to the GW phase, which is independent of the scalar mass:

$$\Delta\psi_{\rm df} = -\frac{75}{38912} \frac{\pi\mathcal{G}^3\mathcal{M}\rho}{c^6} \left(\frac{\pi\mathcal{G}\mathcal{M}f}{c^3}\right)^{-16/3} \frac{\Lambda(m_1^3+m_2^3)}{\nu^{1/5}\mathcal{M}^3}$$

D) Fisher matrix analysis

$$\Gamma_{ij} = \frac{(\mathrm{SNR})^2}{\int_{f_{\rm min}}^{f_{\rm max}} \frac{df}{S_n(f)} f^{-7/3}} \int_{f_{\rm min}}^{f_{\rm max}} \frac{df}{S_n(f)} f^{-7/3} \frac{\partial\psi}{\partial\theta_i} \frac{\partial\psi}{\partial\theta_j}$$

$$\{\theta_i\} = \{t_c, \Phi_c, \ln(m_1), \ln(m_2), \Psi_{\rm osc}\}$$

E) LISA

Detection thresholds for 1 event (comparison of various binary systems)

DM gravitational potential

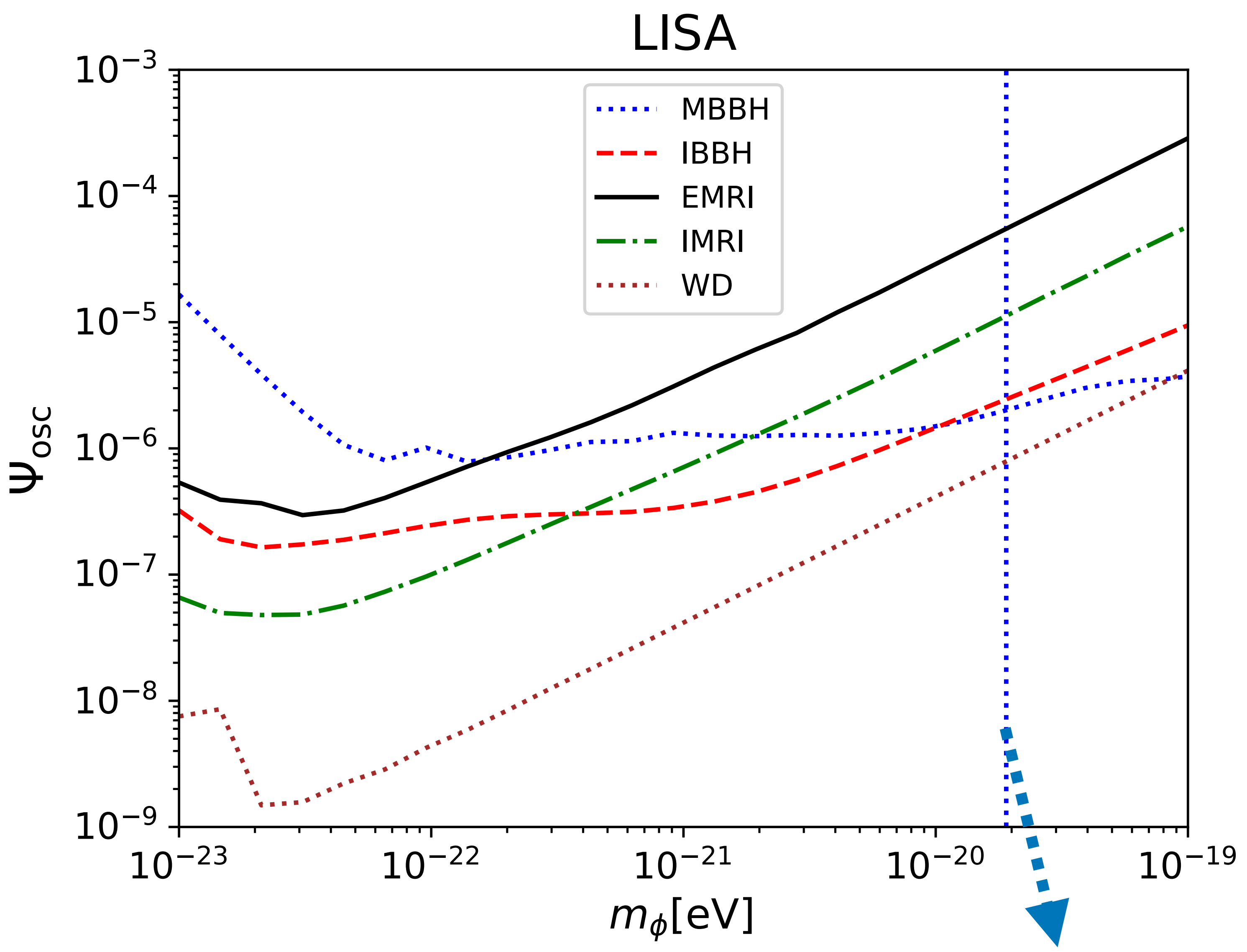

$2m < f_{\rm min}$ for MBBH

DM density

relativistic DM cloud

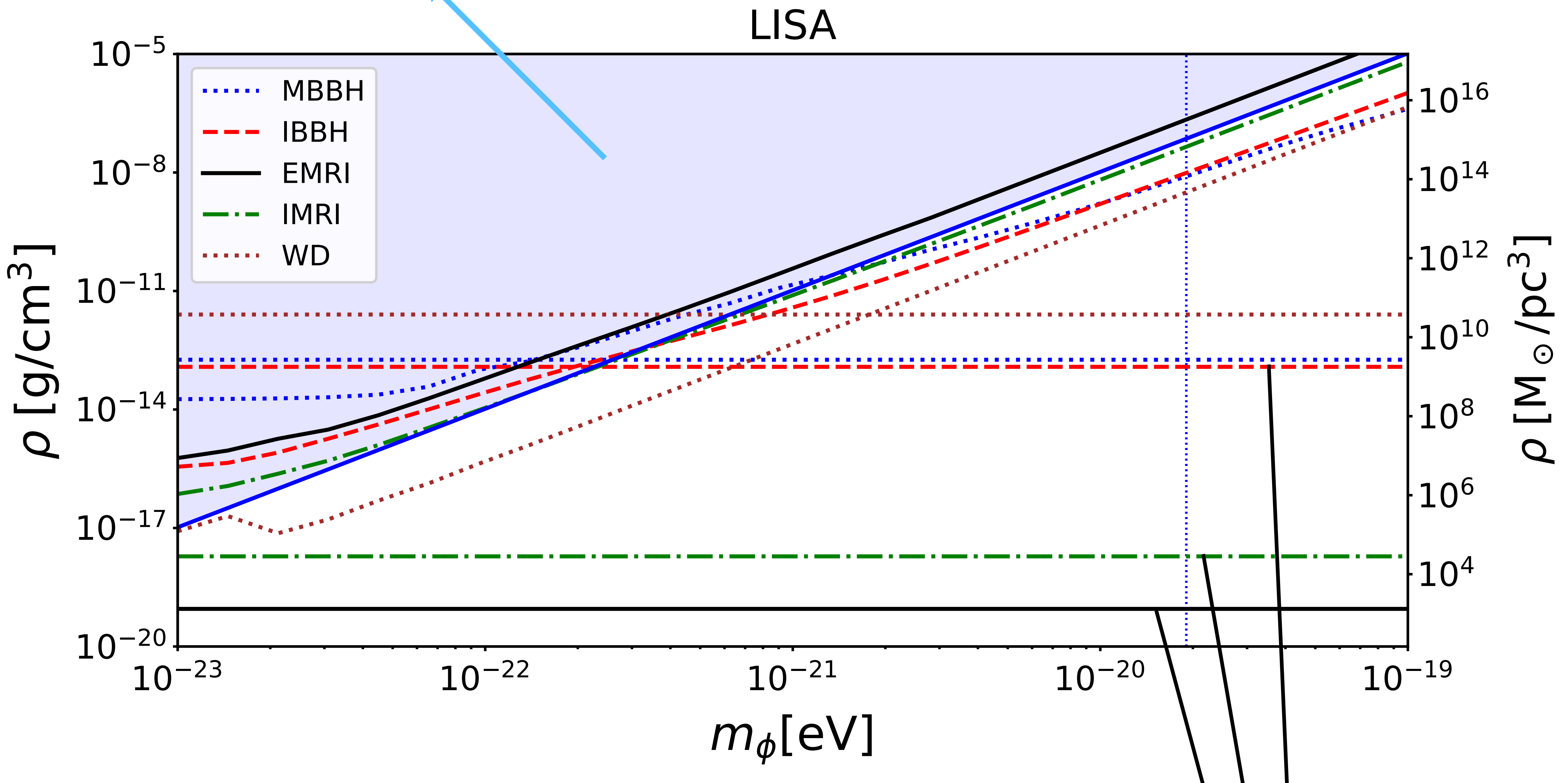

dynamical friction

$$\Delta\psi_{\rm osc}(f) \sim \Psi_{\rm osc} 2\pi \left(\frac{5}{256\pi}\right)^{3/8} \left(\frac{\pi\mathcal{G}\mathcal{M}2m_\phi}{c^3}\right)^{-5/8} \left|\gamma\left(\frac{5}{8}, -i\frac{m_\phi}{m_\star(f)}\right)\right|$$

WD have smaller mass, which improves the detection threshold.

$$\Psi_{\rm osc} = \pi\frac{\mathcal{G}\rho}{m_\phi^2} \qquad \sigma_\rho \propto m^2 \sigma_{\Psi_{\rm osc}}$$

The density threshold increases with the scalar mass.

For $m_\phi \gtrsim 10^{-21}$ eV dynamical friction is more important than the oscillations of the DM potential.

Non-relativistic DM cloud: $$\rho = \frac{M_{\rm cloud}}{R^3} < \frac{M_{\rm cloud}}{\lambda_c^3} = \frac{M_{\rm cloud}}{1M_\odot}\left(\frac{m_\phi}{1 \text{ eV}}\right)^3 10^{45} \text{ g/cm}^3$$

$$\lambda_C = \frac{2\pi}{m_\phi} = \left(\frac{m_\phi}{1 \text{ eV}}\right)^{-1} 4\times 10^{-23} \text{ pc.}$$ Compton wavelength

F) DECIGO

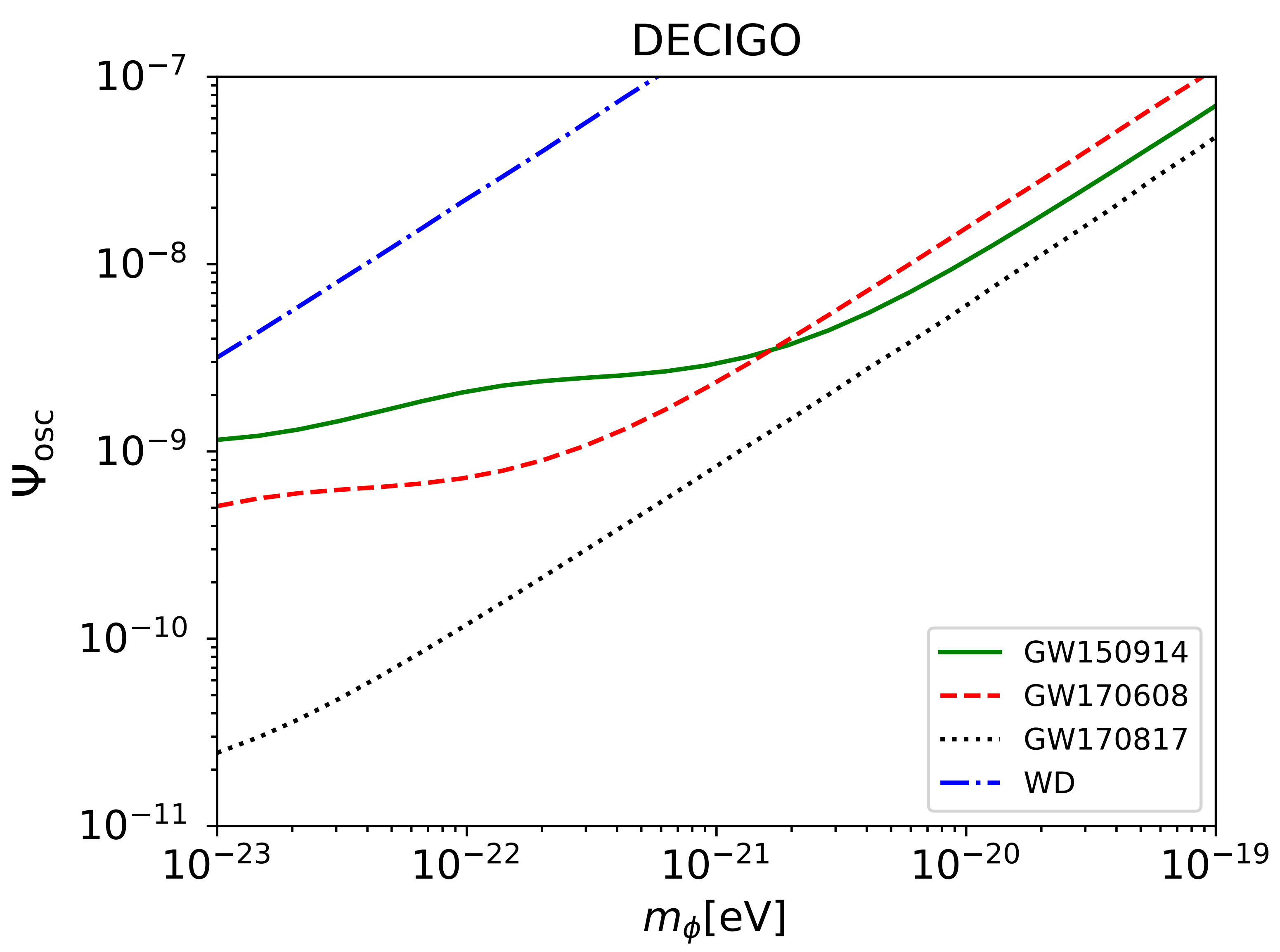

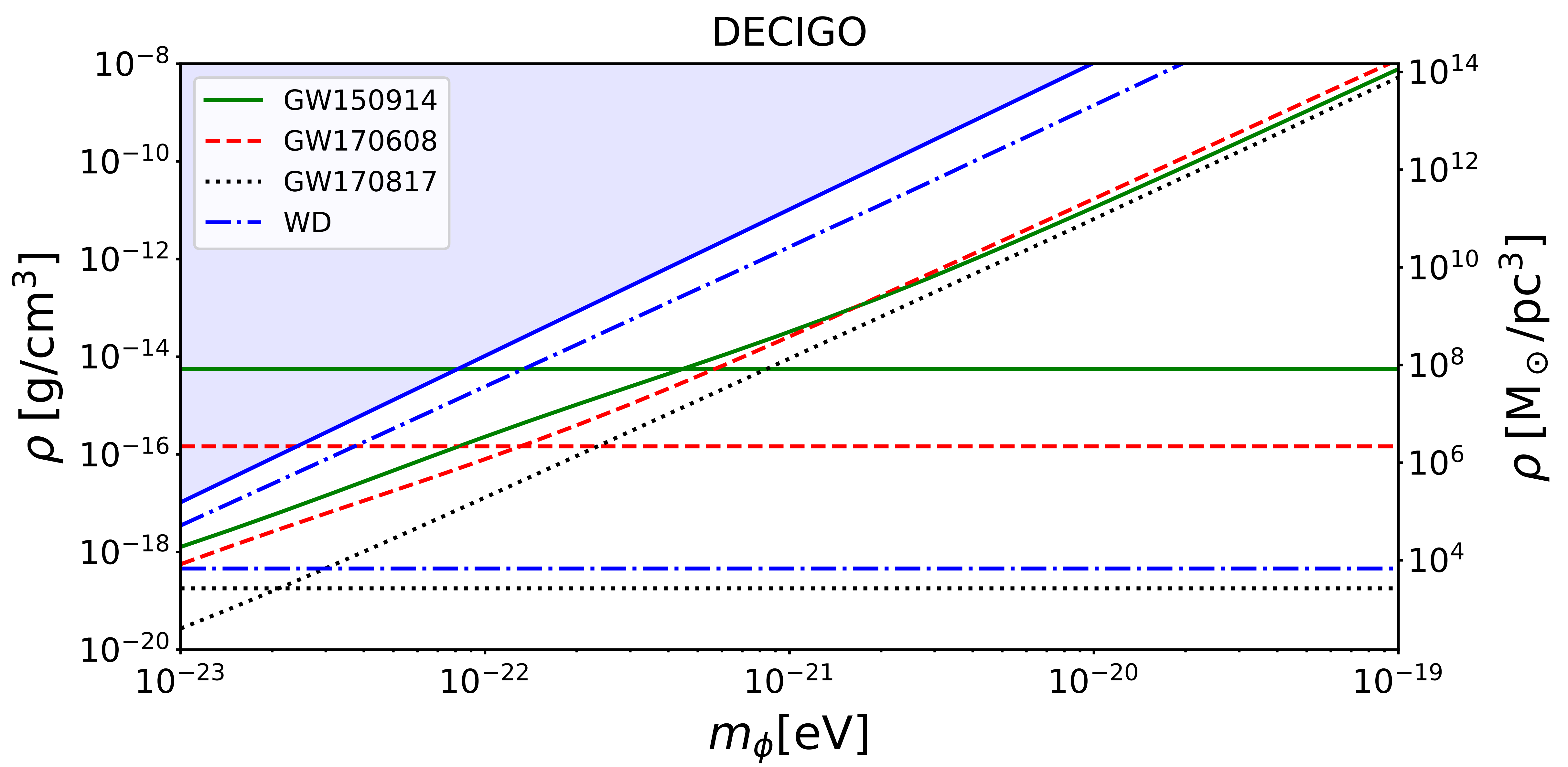

The detection thresholds are of the same order as for LISA, but somewhat better.

G) Conclusion

This probe is unlikely to be competitive with other more direct observations of DM substructures.

For $m_\phi > 10^{-21}$ eV standard effects such as dynamical friction (accretion, gravitational pull) are expected to dominate.

For $m_\phi < 10^{-23}$ eV the clouds that could be detected would have a Compton wavelength greater than 1 pc.

For $m_\phi \sim 10^{-22}$ eV the clouds that could be detected by LISA would have a density that is greater than in the solar neighbourhood by a factor of 10^5 , a mass above $10^5\, M_\odot$ and a radius above $0.4\,\mathrm{pc}$

non-standard formation mechanism at $z \sim 10^4$

→ Except for a small region of the DM parameter space, standard analysis where such an effect is neglected are justified.

CONCLUSIONS

- Scalar dark matter models with self-interactions allow detailed analysis in the large scalar-mass limit
- Hydrodynamical picture in the non-relativistic regime (but does not always hold: mapping can be singular)

- Solitons (flat cores) appear at the center of virialized halos
- They do not seem to converge to a scaling regime $\longrightarrow$ expect a large diversity of profiles
- Transitions between different regimes could take place for some models

- Radial accretion onto a BH similar to Bondi problem, with unique transsonic solution,
but with a much smaller accretion rate, self-regulated by a bottleneck in the relativistic regime

- Such a dark matter environment could be detected by LISA and B-DECIGO, if it contains BH binaries.
- They would see scalar clouds that are smaller than 0.1 pc: difficult to detect by other probes

Other topics: vorticity, gravitational atoms (superradiance),

THANK YOU FOR YOUR ATTENTION !

Parameter space

Hui et al. 2017

Approximate shift symmetry, broken by a periodic term

$$S = \int d^4x \sqrt{-g} \left[\frac{1}{2} F^2 g^{\mu\nu} \partial_\mu a \partial_\nu a - \mu^4 (1 - \cos a) \right]$$

F: axion decay constant

$$a \to a + 2\pi$$

$$\phi = F a$$

$$S = \int d^4x \sqrt{-g} \left[\frac{1}{2} (\partial\phi)^2 - \frac{\mu^4}{2F^2}\phi^2 + \frac{\mu^4}{4! F^4}\phi^4 + \dots \right]$$

$$m = \frac{\mu^2}{F}, \quad \lambda_4 = -\frac{\mu^4}{6F^4}$$

The field starts oscillating when $m \sim H$

$$3M_{\rm Pl}^2 H^2 = T^4, \quad T_{\rm osc} \sim M_{\rm Pl}^{1/2} m^{1/2}$$

At this time the DM density is $\rho_\Phi \sim \mu^4$

$$\phi \sim F, \quad \dot{\phi} \simeq 0$$

Afterwards: $\rho_\phi \propto a^{-3} \propto T^3$

$$\boxed{\Omega_\phi = 5 \times 10^{10} \left(\frac{F}{10^{17}\,\mathrm{GeV}} \right)^2 \left(\frac{m}{1\,\mathrm{eV}} \right)^{1/2}}$$

If: $\Omega_\Phi \simeq 0.3$ then: $F \propto m^{-1/4}$

$$m = 1\,\mathrm{eV}, \quad F = 2.5\times 10^{11}\,\mathrm{GeV}, \quad \mu = 16\,\mathrm{GeV}, \quad \lambda_4 = -3\times 10^{-42}$$

$$m = 10^{-15}\,\mathrm{eV}, \quad F = 1.4\times 10^{15}\,\mathrm{GeV}, \quad \mu = 3.7\times 10^{-5}\,\mathrm{GeV}, \quad \lambda_4 = -9\times 10^{-80}$$

→ Same order of magnitude as the couplings that we consider.

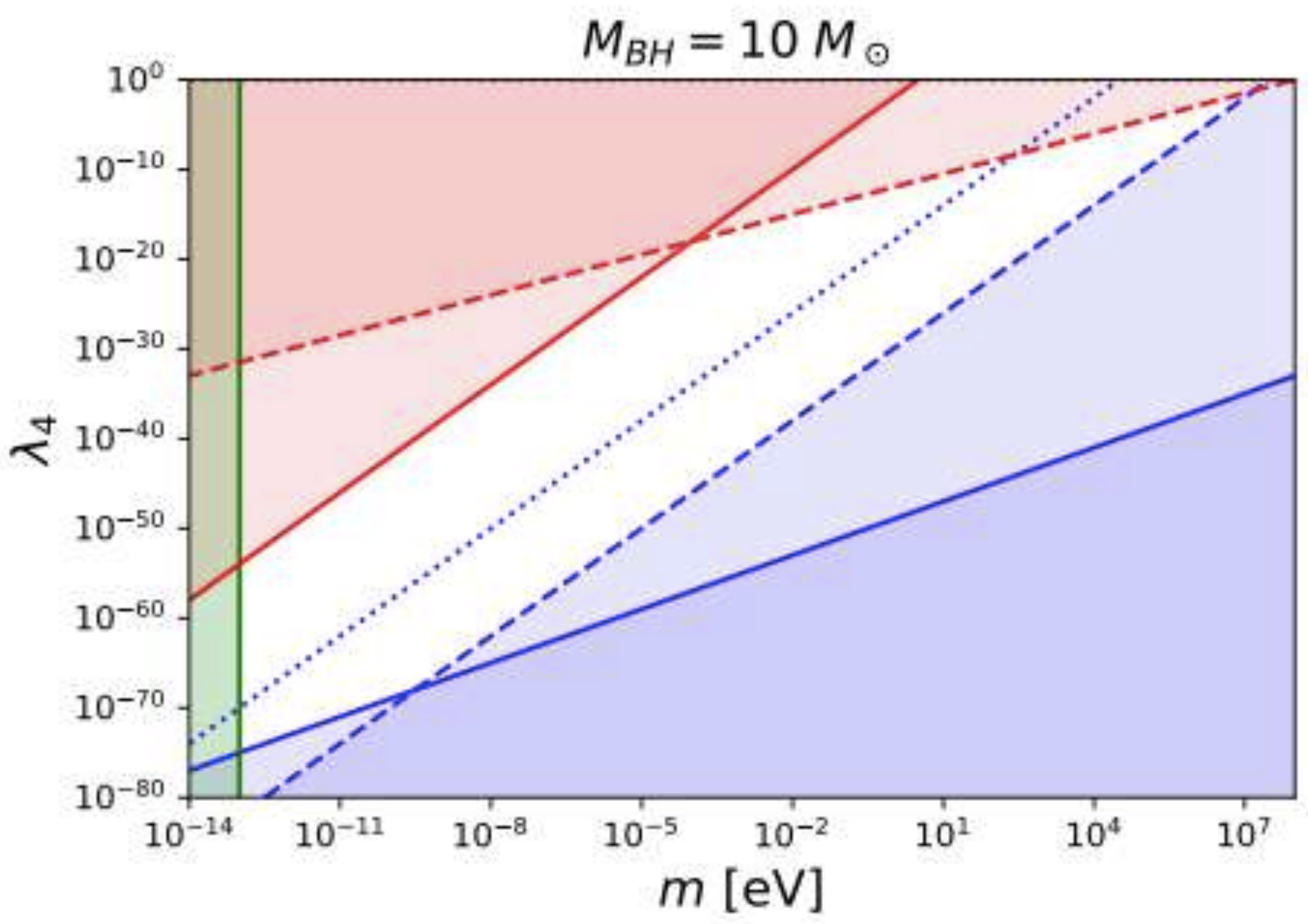

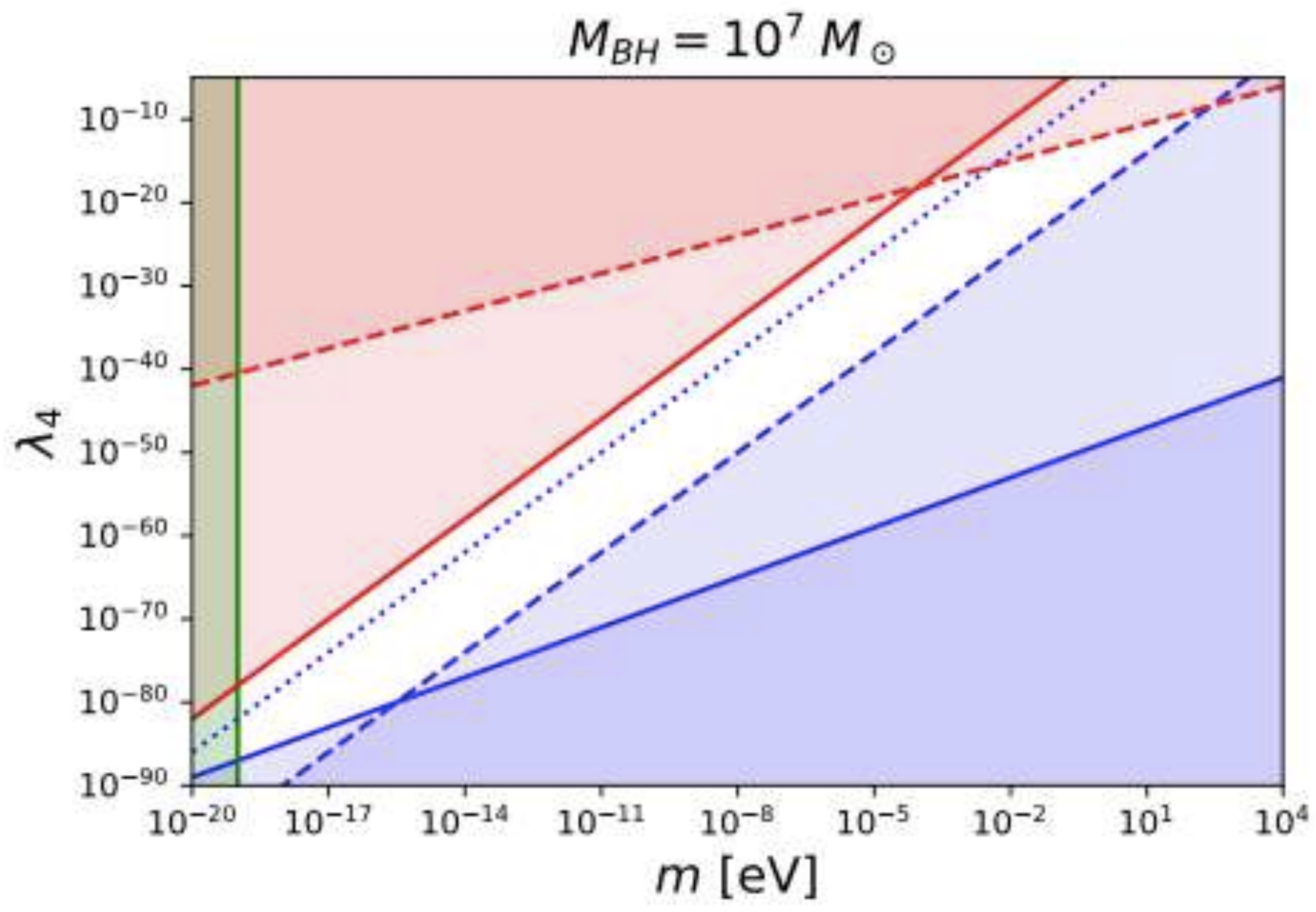

Non-perturbative instanton effects

$$\mu^4 \sim M_{\rm Pl}^2 \Lambda^2 e^{-S}$$

instanton action

$$m = 10^{-15}\,\mathrm{eV}, \quad \Lambda = 10^{18}\,\mathrm{GeV}, \quad S = 208$$

$$m = 1\,\mathrm{eV}, \quad \Lambda = 10^{18}\,\mathrm{GeV}, \quad S = 157$$

Near the BH horizon: $$\phi \sim \frac{m}{\sqrt{\lambda_4}}, \quad \rho_\phi \sim \rho_a \sim \frac{m^4}{\lambda_4}$$

$$\rho_a \sim \mu^4, \quad \phi \sim \frac{m}{\sqrt{\lambda_4}} \sim F$$ $\rightarrow$ OK: perturbative regime down to the BH horizon.